Optimize Your Research

With the Latest Generation of Compact Mass Spectrometer PrismaPro

Your added value

- Optimum adaptability due to modular design
- High performance in spite of compact size
- A variety of interfaces make for simple systems integration
- Networkable through Ethernet
- High measurement speed, stability and high resolution
- Flexible operation thanks to interchangeable analyzers and electronics

Pfeiffer Vacuum GmbH
Germany
T +49 6441 802-0

PFEIFFER VACUUM

Your Success. Our Passion.

www.pfeiffer-vacuum.com

Received: 22 June 2023 | Revised: 10 October 2023 | Accepted: 8 November 2023

DOI: 10.1002/mas.21869

REVIEW ARTICLE

WILEY

Investigations into the characterization, degradation, and applications of biodegradable polymers by mass spectrometry

Paola Rizzarelli | **Melania Leanza** | **Marco Rapisarda**

Consiglio Nazionale delle Ricerche (CNR), Istituto per i Polimeri Compositi e Biomateriali (IPCB), ede Secondaria di Catania, Catania, Italy

Correspondence
Paola Rizzarelli, Consiglio Nazionale delle Ricerche (CNR), Istituto per i Polimeri Compositi e Biomateriali (IPCB), Sede Secondaria di Catania, Via Paolo Gaifami 18, 95126 Catania, Italy.
Email: paola.rizzarelli@cnr.it

Abstract

Biodegradable polymers have been getting more and more attention because of their contribution to the plastic pollution environmental issues and to move towards a circular economy. Nevertheless, biodegradable materials still exhibit various disadvantages restraining a widespread use in the market. Therefore, additional research efforts are required to improve their performance. Mass spectrometry (MS) affords a relevant contribution to optimize biodegradable polymer synthesis, to confirm macromolecular structures, to examine along the time the progress of degradation processes and highlight advantages and drawbacks in the extensive applications. This review aims to provide an overview of the MS investigations carried out to support the synthesis of biodegradable

Abbreviations: 3HB, beta-hydroxybutyric acid methyl ester; A, adipic acid; ADXPS, angle dependent X-ray photoelectron spectroscopy; AHcP, anionic hybrid copolymerization; AMS, accelerator mass spectrometry; ASAP, atmospheric solid analysis probe; AuNPs, gold nanoparticles; B, boron; BCR, biomass carbon ratios; BCY, bis-(ε-caprolactone-4-yl); BNCT, boron neutron capture therapy; BnOH, benzyl alcohol; BS, black soil; BSF, black soldier fly; BSTFA, N,O-bis-trimetilsilil-trifluoroacetamide; CCM, central carbon metabolism; CDCL, oligoCL cyclodextrin derivatives; CDLA, cyclodextrin-oligoLA conjugates; CF, cellulose filler; CID, collision induced dissociation; CL, ε-caprolactone; CS, corn starch; DDS, drug delivery systems; DMA, *N*,*N*-dimethylacrylamide; DMSO, dimethylsulfoxide; DOM, dissolved organic matter; DSC, differential scanning calorimetry; DW, date waste; ESI-MS, electrospray ionization mass spectrometry; FR, furfural; FTIR, fourier transform infrared spectroscopy; FT-ICR-MS, ultrahigh-resolution Fourier transform ion cyclotron resonance mass spectrometry; GC, gas chromatography; Gd, gadolinium; GNO, groundnut oil; GPC, gel permeation chromatography; HB, hydroxyl butyrate; HiC, Humicola insolens; HPLC, High performance liquid chromatography; HS, hard segment; ICP-MS, inductively coupled plasma mass spectrometry; IM-MS, ion mobility-MS; IR, infrared; IRMS, isotope ratio mass spectrometry; LA, L-lactide; LAIF, long-acting injectable formulations; LC, liquid chromatography; MALDI-TOF MS, matrix-assisted laser desorption ionization time of flight mass spectrometry; MM, Molar mass; MPs, microplastics; MRI, magnetic resonance imaging; MRM, multiple reaction monitoring; MS, mass spectrometry; MS/MS, tandem mass spectrometry; MW, molecular weight; MWO, Mealworm; NMR, nuclear magnetic resonance; NPs, nanoparticles; NS, native starch; OPS, oligopeptide segment; PBA, poly(1,4-butylene adipate); PBAT, polybutylene adipate terephthalate; PBSu, poly (butylenesuccinate); PCL, poly(ε-caprolactone); PE, polyethylene; PEG, poly(ethylene glycol); PET, poly(ethylene terephthalate); PHA, polyhydroxyalkanoate; PHB, poly(R-3-hydroxy butyrate); PHBV, poly(R-3-hydroxy butyrate-*co*-R-3-hydroxy valerate); PLA, polylactic acid; PLGA, poly(lactide-*co*-glycolide); PLLA, poly(L-lactide); PPF, pranoprofen; PPG, propylene glycol; PPUU, poly(peptide-urethane-urea); PS, polystyrene; PTX, Paclitaxel; PVL, poly(δ-valerolactone); Py-GC/MS, pyrolysis-gas chromatography-mass spectrometry; P(3HB), poly(3-hydroxybutyrate); ROO, ring opening oligomerization; ROP, ring-opening polymerization; RSM, response surface methodology; sCT, salmon calcitonin; SEC, size-exclusion chromatography; SIMS, secondary ion mass spectrometry; SS, soft segment; SUP, single-use plastic; TBDMS, *N*-methyl-*N*-(t-butyldimethylsilyl) trifluoroacetamide + 1% t-butyl-dimethylchlorosilane; TA, terephthalic acid; TGA, thermogravimetric analysis; Thc-Cut 1, Thermobifida cellulosilytica; TOF-SIMS, time-of-flight secondary ion mass spectrometry; TPGS, α-Tocopheryl polyethylene glycol 1000 succinate; TPS, thermoplastic starch; UHPLC, ultra-HPLC; ULP, ultrashort laser pulses; UV, ultraviolet; WM, Wax Moth; YS, yellow soil; β-CD, β-cyclodextrin.

This review celebrates the career of Professor Chrys Wesdemiotis.

Funding information
PO FESR 2014–2020,
Grant/Award Number: G68I18000700007

polymers, with helpful information on undesirable products or polymerization mechanism, to understand deterioration pathways by the structure of degradation products and to follow drug release and pharmacokinetic. Additionally, it summarizes MS studies addressed on environmental and health issues related to the extensive use of plastic materials, that is, potential migration of additives or microplastics identification and quantification. The paper is focused on the most significant studies relating to synthetic and microbial biodegradable polymers published in the last 15 years, not including agro-polymers such as proteins and polysaccharides.

KEYWORDS
biodegradable polymers, characterization, degradation, drug release, microplastics, polyhydroxyalkanoates

1 | INTRODUCTION

Biodegradable polymers are a whole family of materials with different properties and applications (Mukherjee et al., 2023). They can be derived from agro-sources, be synthesized by microorganisms or monomers, either bio-based or fossil-based (Figure 1). There are two major advantages of biodegradable plastic products compared to the conventional ones: they can save fossil resources by using biomass that renews (in short time) and offer additional means of recovery at the end of lifetime through biodegradability. Consequently, in the last decade, the uses and applications of biodegradable polymers have increased, absolutely conditioned by environmental concerns and consecutive legislative choices.

Even though nowadays there are several commercial biodegradable systems, consistent research activities, and financial supports are still focused in improving their performances by tailoring structural properties to further broaden the application fields. Thus, a good understanding of characterization features and a reliable structural analysis is of noteworthy significance to successfully enhance the properties of this class of polymers. Furthermore, some controversies and doubts have arisen recently about the end-life fate and persistence of biodegradable bioplastics and microplastics (Serrano-Ruiz et al., 2021; Wang et al., 2021; Wei, Bohlén, et al., 2021). Mass spectrometry (MS) has been increasingly involved in biodegradable polymer analysis, thanks to the enhancement of instruments and up-to-date configurations. Among the MS methods, the soft ionization techniques, for example, matrix-assisted laser desorption ionization time of flight MS (MALDI-TOF MS) and electrospray ionization MS (ESI-MS), have been extensively applied in the structural characterization of biodegradable polymers. In recent times, reviews and book chapters on MS in biodegradable polymer analyses

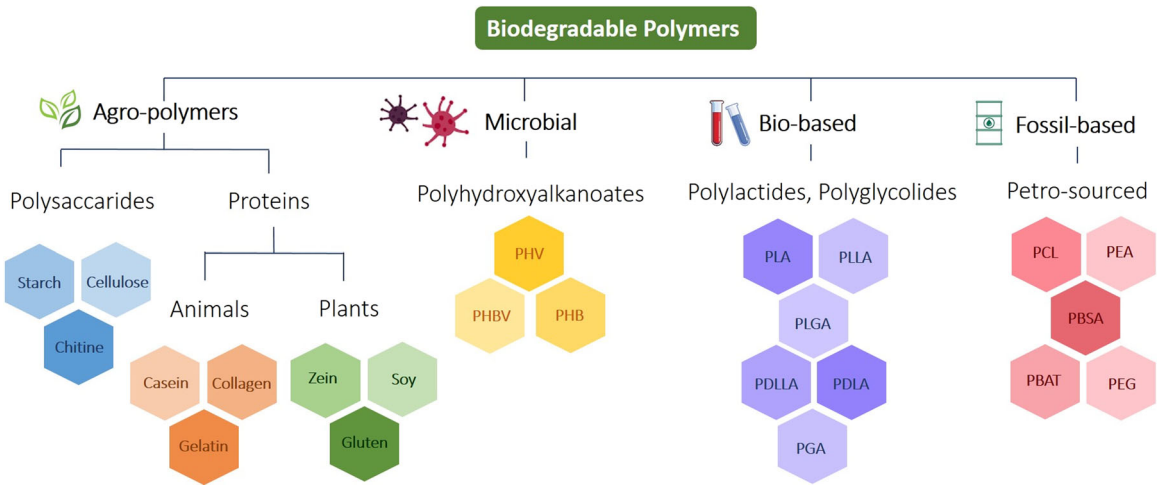

FIGURE 1 Types of biodegradable polymers. [Color figure can be viewed at wileyonlinelibrary.com]

have been published (Kowalczuk, 2016; Kowalczuk & Adamus, 2016; Rizzarelli & Carroccio, 2014, 2015; Rizzarelli & Rapisarda, 2021, 2023; Rizzarelli et al., 2019a, 2020). MS methods, for their high sensitivity, selectivity, and quickness, allow the finest structural details to be revealed still in complex polymer samples. Thus, different strategies, based on or supported by MS techniques, have been applied and developed to help biodegradable polymer analyses, related to the characterization, degradation, and usage challenges.

Whenever single-stage MS has not been able to ascertain the polymer structure, tandem mass spectrometry (MS/MS) provided helpful checking interpretation of MS data and supplementary information (Crecelius et al., 2009; Rizzarelli & Rapisarda, 2021, 2023). It has been used in the characterization, degradation, and applications of traditional and biodegradable polymeric systems. Preliminary fragmentation studies represent the first step for the confident structure assignments of tandem mass spectra (Chendo et al., 2018; Rizzarelli, 2013; Wesdemiotis et al., 2011). Both MALDI and ESI-MS/MS techniques provided valuable structural details on end-groups, copolymer composition and sequence distribution, pharmacokinetic, fate of polymeric excipients, drug delivery systems (DDS) as well as degradation products and mechanisms as very recently reviewed (Rizzarelli & Rapisarda, 2023). Multidimensional MS methodologies, combining MALDI and ESI with TOF mass analysis, MS/MS fragmentation, and/or ion mobility MS (IM-MS), have been successfully employed to give insights on chain-end or in-chain substituents, composition, isobaric and isomeric species, isomeric purity, differentiate linear and cyclic polymers, macromolecular connectivity chain, sequences, and architectures (Charles et al., 2020; Crotty et al., 2016; Wesdemiotis, 2017). On selected biodegradable polymers, the efficiency of new ionic liquid matrices in MALDI (Berthod et al., 2009; Serrano et al., 2011) as well as studies on dissociation modes in MS/MS, to support their characterization (Scionti & Wesdemiotis, 2012), and library-method facilitating the MS data interpretation (Ogaki et al., 2008) have been tested, elucidating their structures, and providing information on fragmentation mechanisms.

Interestingly, inductively coupled plasma mass spectrometry (ICP-MS) was recently employed in biodegradable polymer analysis to check metals due to residual catalyst (Rizzarelli et al., 2019b), correlate their contents with polymer degradation (Dintcheva et al., 2017), in antimicrobial textile nanocomposites or for drug delivery studies (Doumbia et al., 2015; Hsieh et al., 2018; Pathak & Dhar, 2015; Qin et al., 2022; Shi et al., 2015; Wang et al., 2012; Yu et al., 2022).

Furthermore, time-of-flight secondary ion mass spectrometry (TOF-SIMS) has been used recurrently in surface characterization of biodegradable polymers and to verify the changes induced by degradation processes. In particular, it highlighted physiochemical surface interactions between bioresorbable polymers and biological environments (Rizzarelli et al., 2020). In fact, the final performance of a biodegradable material is greatly connected with its surface structure and interfacial features. Moreover, MS methods provided comprehensive information on degradation processes by the detection of polymer end-chain structures derived from primary thermal, thermo, and photo-oxidative decomposition mechanisms. The hydrolytic and enzymatic degradation of biodegradable polymers has been monitored mainly by ESI-MS being interfaced promptly with solution-based separation techniques such as high-performance liquid chromatography (HPLC). Furthermore, HPLC-ESI, pyrolysis-gas chromatography/mass spectrometry (Py-GC/MS) and ultrahigh-resolution Fourier transform ion cyclotron resonance mass spectrometry (FT-ICR-MS), with an ESI ion source, have been employed in studies concerning environmental and human health issues, particularly migration of additives and microplastics analysis (Okoffo et al., 2022; Phothisarattana & Harnkarnsujarit, 2022; Savva et al., 2023; Sun et al., 2022; Wang et al., 2022). Whereas investigations on biomass carbon ratios on biodegradable materials have been carried out by accelerator mass spectrometry (AMS) (Flores et al., 2009; Funabashi et al., 2010; Tachibana et al., 2009).

Accordingly, the current review aims to outline an overview of the studies focused on biodegradable polymers in which MS provided helpful information on the synthesis, unexpected side reactions, or polymerization mechanism. Additionally, it summarizes studies addressed using MS on degradation processes, drug release and pharmacokinetic, and the potential environmental impact related to an extensive use of biodegradable plastic materials. The paper is focused on the most significant studies relating to synthetic (bio- and fossil-based) and microbial biodegradable polymers, mainly polyesters (Figure 2). Studies on agro-polymers are not included in this review. GC-MS analysis has been broadly used in PHA samples, previously treated by solvolysis and derivatization to reduce the molecular weight and improve volatilization. LC-MS has been applied in the analysis of the monomeric composion of microbial PHAs, a challenging task for the wide chemical variety of monomers and limited numbers of analytical standards. Both MALDI and ESI have been exstensively employed to get structural information of microbial and synthetic biodegradable polymers. However, molar mass

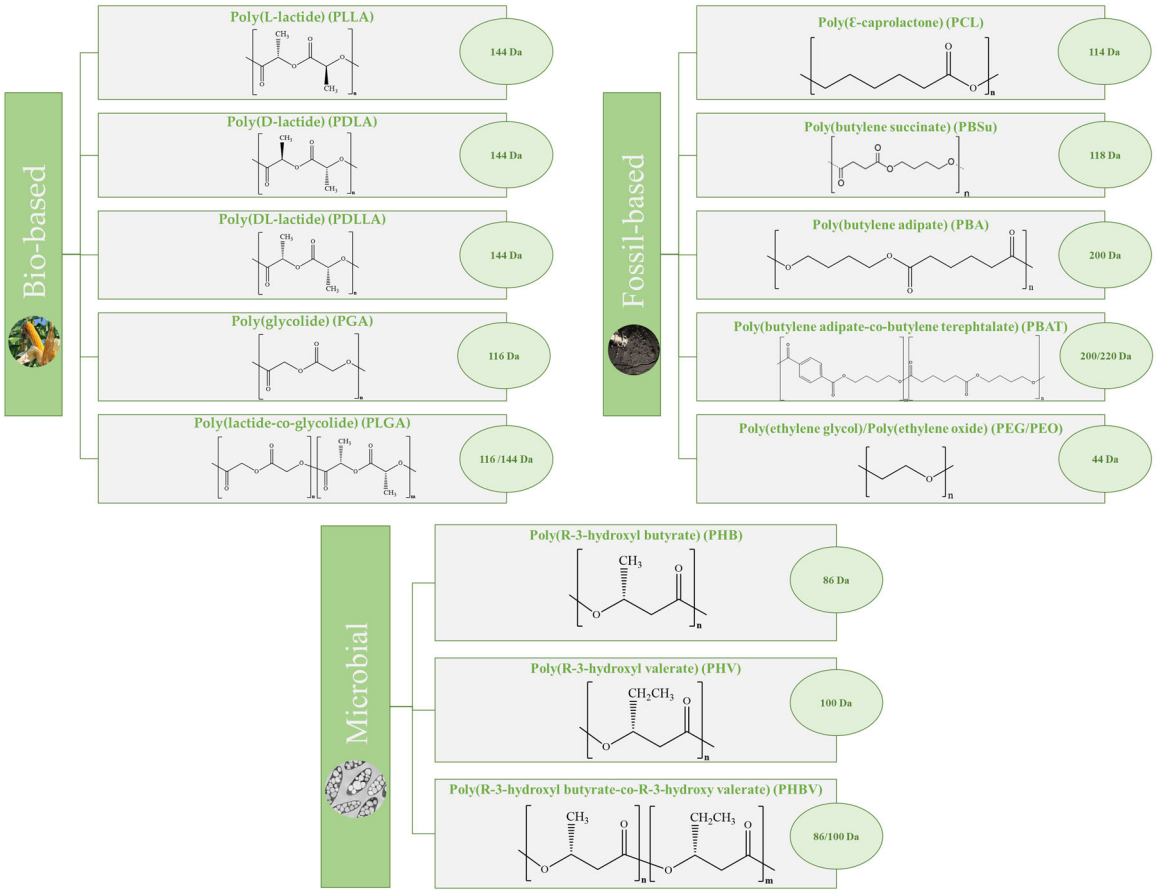

FIGURE 2 Source, name, abbreviations, structure, and molecular weight of the repetitive units, of representative synthetic and microbial biodegradable polymers studied by mass spectrometry. [Color figure can be viewed at wileyonlinelibrary.com]

estimates were reliable only in the case of samples with narrow molar mass distributions. An in-depth outline of the MS methods used to study microbial and synthetic biodegradable polymers and the kind of information obtained will be provided. Challenges and successful strategies will be highlighted. The ultimate goal is to be helpful in the choice of the MS technique in future studies. A right selection is essential to be successful in the consistency and usefulness of the data acquired, further extending the fields of application of MS in the development of biodegradable polymers and supporting resolution of controversies with human and environmental health drawbacks.

2 | CHARACTERIZATION OF BIODEGRADABLE POLYMERS BY MS

The structural characterization is the first stage in the analysis of a polymeric sample. Several MS techniques, combined with other analytical methods or by themselves, are fruitfully used for the structural characterization of polymers, including the biodegradable ones (Crotty et al., 2016; Gerislioglu et al., 2018; Rizzarelli & Carroccio, 2014; Sato et al., 2020; Wesdemiotis et al., 2023). Checking the structure, ascertaining the successful synthesis, detecting unexpected species from side reactions, and so forth involve the selection of appropriate analytical approaches. This is important to detect species in trace amounts with critical health-related implications being a guarantee of safety, efficacy, and quality. Therefore, MS techniques for their high sensitivity, selectivity, and speediness are a valued support for the characterization of biodegradable polymer providing exhaustive structural details even in complex matrices. MS analysis, especially by MALDI and ESI-MS, have been established helpful in the identification of end groups or contaminants, in the validation of functionalization of polymer–drug coniugates systems, to understand the polymerization mechanism, or else to investigate the surface and the distribution of constituents or drugs in polymeric samples. Certainly, the choice of a matrix tailored for a particular kind of polymer sample, of the solvent and polymer/matrix mixture deposition on the sample plate,

of cationization reagents, of the matrix/polymer/cationizing agent mixing ratios, as well as presence of salts, sample concentration, instrument settings, and so forth play a crucial role for the successful characterization of the sample. These MS methods cannot be used for analysis of polymer samples that are insoluble or poorly soluble in organic solvents. Considerable efforts have been devoted to the development of new "solvent-free" MALDI sample preparation methods. The method consists in immersing the polymer sample in liquid nitrogen, followed by addition of powdered matrix. The resulting mixture is finely ground in a rotating-ball mill. The "solvent-free" methodology has not been applied to biodegradable polymers in the last 15 years. High dispersity mass samples with high molecular weight can be analysed with more difficulties by MALDI and ESI-MS. ESI-MS spectra can be complicated by multicharged ions. In MALDI analysis, the lower molecular weight ions are detected with decreasing intensity. However, valuable information has been deduced assuming the spectrum representative of the whole of biodegradable sample (Rizzarelli & Carroccio, 2014). Additionally, MALDI-MS can potentially supply quantitative information necessary for determination of the average molecular masses and molecular mass distribution of a polymer or of relative amounts of different components in a polymer mixture. Nevertheless, molar mass estimates are reliable only in the case of samples with a narrow molar mass distribution, whereas, for polymer samples with high dispersity, the results are far from the actual expected values. The inaccurate determination of molar masses in high mass dispersity samples by MALDI-TOF MS is reasonably due to mass discrimination effects and decreasing detection response at higher masses. In fact, lighter molecules are preferentially desorbed and ionized in the MALDI process, suppressing the desorption and ionization of higher mass molecules, and the detector response is not constant. An accepted method for molar mass determination by MALDI, in high mass dispersity polymer samples, consists of the analytical fractionation by size exclusion chromatography (SEC) followed by MALDI analysis of each narrow-distributed fraction, procedure first described in the analysis of synthetic polymers by Montaudo et al. SEC/MALDI TOF off-line coupling involves the collection of sample fractions through an analytical SEC. The so-obtained narrowly distributed fractions are analyzed by MALDI-MS for the determination of their average molecular weight. This allows calibration of the SEC curve against absolute molecular weight, to be further applied to compute trustworthy molecular weight parameters of unfractionated high dispersity samples (Montaudo et al., 2006). In the last 15 years, the off-line SEC/MALDI method has been applied to a limited number of studies concerning the structural characterization and the MM determination of synthetic biodegradable copolyesters (Fouquet et al., 2020). On the contrary, tandem MS has supported numerous studies being, in several case, crucial to define exactly structures of end group, architectures, and sequence distributions (Rizzarelli & Rapisarda, 2023). All these structural features are essential in the development of biodegradable polymers also for the interconnection with the biodegradability required at the end of their lifetime.

2.1 | Structure investigation

Whatever the type of polymeric material, the inspection of molecular issues and structures is the first step in its development. MS can provide primary information, confirming the mass of the repeating units, establishing the nature of end groups, monomer composition, average molar masses, and so forth. In the past, a variety of biodegradable polymers has been characterized by MS. MS has been used to confirm the successful preparation of monomers and the presence of impurities (Blanquer et al., 2010; Ezati et al., 2022; Liu et al., 2008; Raase et al., 2015; Santra et al., 2020) as well as the structures of polymer and copolymer samples (Bakkali-Hassani et al., 2022; Dria et al., 2012; Feng & Tong, 2017; Fischer et al., 2015; Impallomeni et al., 2013; Landim et al., 2019; Liu et al., 2009; Lochee et al., 2010; Loriot et al., 2016; Saito et al., 2019; Shen et al., 2019; Sobczak, 2012; Takizawa et al., 2008; Ten Breteler et al., 2013; Zhu et al., 2011; Żółtowska et al., 2015), the composition and sequence distributions (Impallomeni et al., 2011, 2015; Rizzarelli & Puglisi, 2008; Rizzarelli et al., 2022), or just the end groups, particularly useful in multi-step synthetic procedure (Impallomeni et al., 2013; Kolmas et al., 2014; Oledzka et al., 2011; Rizzarelli et al., 2015; Tang et al., 2011; Theerasilp et al., 2018; Zhang et al., 2008), and in commercial sample (Rizzarelli et al., 2019b), or else extensively in checking the structure of microbial polyhydroxyalkanoates (PHAs) produced by usual or cheap feeding (Ali & Jamil, 2014; Allen et al., 2010; Bhati et al., 2010; Biernacki et al., 2017; Elain et al., 2015; El-Kadi et al., 2021; Ge et al., 2016; Hagagy et al., 2022; Hamdy et al., 2022; Impallomeni et al., 2011, 2018; Jyoti et al., 2021; Mahato et al., 2021; Mostafa et al., 2020; Salazar et al., 2014; Sriyapai et al., 2022) or by carbon waste sources (Alsafadi et al., 2020; Arshad et al., 2017; Astolfi et al., 2020; Ekere et al., 2022; Johnston et al., 2017, 2018, 2019; Ojha & Das, 2018; Radecka et al., 2016; Sriramani et al., 2022; Susithra et al., 2021),

otherwise to quantify the yield production of PHAs inside microorganisms (Liang et al., 2022). Soft ionization techniques have been exploited to check the polymerization mechanism (Chen et al., 2020; Gorrasi et al., 2016; Gümüştaş et al., 2022; He et al., 2020; Yang et al., 2022) or confirm the effective backbone functionalization (Cicogna et al., 2014) or else the structure of polymer-conjugates (Bansal et al., 2020; Blaj et al., 2021; Den Berghe et al., 2011; Impallomeni et al., 2021; Kwiecień et al., 2012, 2015; Maksymiak et al., 2013; Parwe et al., 2014; Peptu et al., 2018, 2022; Pignatello et al., 2013, 2015; Scherger et al., 2021; Yu et al., 2008) and bioconjugates, hybrid materials with biomolecules covalently bonded to synthetic polymers (Ke et al., 2017; Pedrón et al., 2010; Pelosi et al., 2021; Talelli & Vicent, 2014; Yi et al., 2008). Some studies have been addressed to the challenging identification of branched structures (Fischer et al., 2015; Peptu et al., 2012; Shiravand et al., 2016). MALDI (Shiravand et al., 2016), SEC/MALDI TOF off-line coupling (Fischer et al., 2015), and LC-tandem MS (LC-MS/MS) (Peptu et al., 2012) were used in successful approaches.

MS spectra interpretation of copolymers can be complicated for the higher number of signals and the support of additional techniques and/or MS/MS is in some cases essential. Both ESI-MS/MS (Adamus, 2009; Duale et al., 2021; Fouquet et al., 2020; Johnston et al., 2017, 2018; Kwiecień et al., 2015, 2016; Maksymiak et al., 2016; Prian et al., 2019; Sallam et al., 2017; Wei et al., 2014) and MALDI-MS/MS (Ashby et al., 2017; Sallam et al., 2017; Weidner et al., 2009), with collision-induced dissociation (CID) as the most frequently used fragmentation mode, have supported the characterization of biodegradable copolymers. Furthermore, surface analyses in biodegradabe polymer systems have been carried out almost exclusively by secondary ion mass spectrometry (SIMS) (Bege et al., 2012; Casettari et al., 2011; Chen, Dong, et al., 2010; Du et al., 2018; Lee et al., 2008; Mohiti-Asli et al., 2014; Ugur et al., 2020; Van Royen et al., 2011; Zorn et al., 2022).

2.1.1 | Identification of microbial PHAs by MS

PHAs represent a very important family of biodegradable polymers. They can accumulate in microbial cells with very high molecular weight (MW) or be synthesized in laboratory. Numerous studies have been supported by MS to verify their structures and establish the composition. Relevant information about the influence of carbon source and/or pH, temperature, etc. on the PHA structures were obtained, mainly combining MS with chromatographic separation techniques, LC as well as GC. GC-MS has been extensively adopted on PHA samples previously treated by solvolysis and derivatization. MS studies frequently applied complementary structural analyses by Fourier transform infrared spectroscopy (FTIR) and/or nuclear magnetic resonance (NMR) (Allen et al., 2010; Arshad et al., 2017; Bhati et al., 2010; Biernacki et al., 2017; El-Kadi et al., 2021; Hamdy et al., 2022; Jyoti et al., 2021; Mostafa et al., 2020; Ojha & Das, 2018; Sriramani et al., 2022; Sriyapai et al., 2022; Susithra et al., 2021). A response surface methodology (RSM) was used to examine the combined outcomes of glucose and peptone concentration as well as pH on microbial PHA production. All variables had a substantial effect on PHA production either individually or in the interaction with each other. The chemical composition of the polymer extracted from *Bacillus cereus* SH-02 was checked by ^{1}H NMR, ^{13}C NMR, and GC-MS analysis. Functional groups and surface morphological features were analyzed by FTIR. Both NMR and MS spectra exhibited data that confirmed a poly(R-3-hydroxy butyrate) (PHB) polymer sample, with MW detection for methyl 3-hydroxybutyric acid by MS (Hamdy et al., 2022). A similar RSM approach was used by Ojha and Das in the optimization of PHA production using yeast strain isolated from natural sources. Again, the structure characterization of the extracted PHA was performed by FTIR, GC-MS, and NMR. GC-MS analysis was carried out after methanolysis of the extracted sample. However, NMR revealed that the biopolymer was a poly(3-hydroxybutyrate-co-3-hydroxyvalerate) (PHBV) (Ojha & Das, 2018). Srisawat et al. evaluated the use of 13 engineered nanogel particles to increase PHA accumulation in the marine photosynthetic bacterium *Rhodovulum sulfidophilum* under photoautotrophic culture. The anionic nanogel particles significantly enhanced PHA accumulation in *R. sulfidophilum* up to 157-fold using $NaHCO_3$ as the sole carbon source. The PHA content was determined using a GC-MS instrument. By performing ^{13}C tracer experiments and GC-MS analysis, they confirmed that HCO^{3-} was assimilated throughout the central carbon metabolism. Indeed, the GC-MS mass fragmentation pattern of extracted PHA from the *R. sulfidophilum* culture containing nanogel particles established the incorporation of $[^{13}C]NaHCO_3$ into PHA accumulated in *R. sulfidophilum* (Srisawat et al., 2022). El-Kadi et al. used inexpensive and available alternative carbon sources (whey, sugar beet molasses, and date molasses) to obtain PHB from *Bacillus paramycoides*, *Azotobacter salinestris*, and *Brevundimonas naejangsanensis*. They investigated the chemical structure by FTIR and GC-MS/MS. GC-MS after extraction was carried out after derivatization by

N,O-bis-trimetilsilil-trifluoroacetamide (BSTFA) reagent. Infrared (IR) of the produced PHB from *B. paramycoides* and *A. salinestris* showed similar bands, which confirmed the presence of PHB; however, *B. naejangsanensis* showed weak bands, indicating lower PHB concentration. The obtained information on chemical composition showed that the GC-MS signals of the PHB extracted were due to 2,4-ditert-butylphenol for *B. paramycoides* and isopropyl ester of 2-butenoic acid for both *A. salinestris* and *B. naejangsanensis* (El-Kadi et al., 2021). Jyoti et al. checked the ability of *Ralstonia solanacearum*, a phytopathogen, to accumulate PHB granules. Fluorescence microscopy, GC-MS, and ^{1}H NMR were used to confirm the bacterial accumulation of biodegradable poly (3-hydroxybutyrate) (P(3HB)) by glucose and ^{13}C glucose feeding. In particular, fluorescence microscopy was employed for the vision of P(3HB) granules within the bacterial cells. *R. solanacearum* cells were grown in P (3HB) production media, collected, and highlighted by nile red, a lipophilic fluorescent dye. The presence of fluorescent dots in the cells showed the accumulation of typical P(3HB) granules (Figure 3A). GC-MS on *N*-methyl-*N*-(t-butyldimethylsilyl) trifluoroacetamide + 1% t-butyl-dimethylchlorosilane (TBDMS) derivatized cell hydrolysate confirmed the nature of P(3HB). In fact, 3-hydroxybutyric acid, the monomer of P(3HB), with 2TBDMS was eluted at 13.9 min, and diagnostic mass fragments were detected in the mass spectra (Figure 3B). The metabolite identification was further confirmed using standards and the NIST library (National Institute of Standards and Technology) (Figure 3C) (Jyoti et al., 2021).

GC-MS on methanolyzed PHA and FTIR were used to analyze the content and monomer composition of PHAs synthesized by cheap edible oils as a carbon source. Different edible oils, such as groundnut oil (GNO), mustard oil, sesame oil, and soybean oil were tested on PHA production from *Pseudomonas aeruginosa* EO1. FTIR spectra showed strong typical bands for the PHA polymer. GC-MS highlighted the presence of PHA copolymers. In particular, PHA extracted from *P. aeruginosa* EO1 using GNO contained beta-hydroxybutyric acid methyl ester (3HB) (7.41%), methyl 3-hydroxytetradecanoate (7.26%), and hexadecanoic acid, methyl ester (5.03%) (Mahato et al., 2021). ^{1}H NMR and GC-MS analyses were used to check the structure of PHAs extracted from *Paraburkholderia* sp. PFN29, by comparing to standard PHB and PHBV, the most common PHAs (Sriyapai et al., 2022). On seeking alternative sources for bacterial production of PHA, Allen et al. evaluated the potential of the seed oil from *Jatropha curcas* plant, since it is nonedible, widely available, and can be cheaply produced. The microbial PHA was fully characterized by GC-MS, ESI-TOF-MS, gel permeation chromatography (GPC), and ^{1}H and ^{13}C NMR. In the GC-MS spectra only the methyl 3-hydroxybutanoate monomeric unit was identified. Instead, ESI-TOF-MS showed that the PHA was a copolymer, detecting peaks due to HB/HV copolymer chain. ESI data were confirmed by ^{1}H and ^{13}C NMR analysis (Allen et al., 2010). To determine the type of PHA mainly produced by two new isolate *Halolamina* species, FTIR, LC-MS, and LC-MS/MS analyses were carried out. LC-MS/MS analysis with ESI source displayed peaks, at retention times of 5.2, 7.3, and 8.1 min, which disclosed the occurrence of PHB, acetoacetyl-CoA, and PHB synthase, its synthetic products. The FTIR spectra showed sharp peaks at around 1628.98 and 1629.28 cm^{-1}, which confirmed the presence of the carbonyl group (C=O) on amides and related to proteins, typical of PHB (Hagagy et al., 2022). Ge et al. used a LC-MS for the determination of monomeric composition in bacterial PHAs isolated from *Pseudomonas* cultivated on different carbon sources. LC-MS was performed by an ESI source and on PHAs samples after hydrolysis. Besides C6, C8, C10, C12, C14, and C16, the hydrolized PHAs were also composed of three unknown PHA monomers whose molecular masses were determined by ESI-MS in negative ion mode. Based on the molecular masses, it was suggested the presence of PHA monounsaturated monomers: 3-hydroxydodecenoicacid, 3-hydroxytetradecenoicacid, and 3-hydroxyhexadecenoi cacid. Nonetheless, due to the lack of analytical standards, the chemical structures were further checked by off-line LC-NMR. The study highlighted how much is challenging the analysis of monomeric composition in microbial PHAs for the wide chemical variety of monomers and lack of analytical standards (Ge et al., 2016).

In accordance with the circular economy approach, several recent papers have been addressed in microbial PHAs produced by waste-by-product (Astolfi et al., 2020; Sriramani et al., 2022; Susithra et al., 2021). GC-MS on pretreated samples (Arshad et al., 2017; Sriramani et al., 2022; Susithra et al., 2021), ESI-MS and MS/MS (Ekere et al., 2022; Johnston et al., 2017, 2018; Johnston et al., 2019; Radecka et al., 2016), ICP-MS (Astolfi et al., 2020), isotope ratio mass spectrometry (IRMS) (Alsafadi et al., 2020) have been successfully used to check the structure or elemental composition of the microbial PHAs. ^{1}H NMR and GC-MS techniques were adopted to confirm the PHB biosynthesis, using an alkali-pretreated spent mushroom substrate of sugarcane bagasse as a novel lignocellulosic carbon source, by a *Bacillus tequilensis* PSR-2 isolate. GC-MS was performed after a process of methanolysis. GC-MS and NMR, with

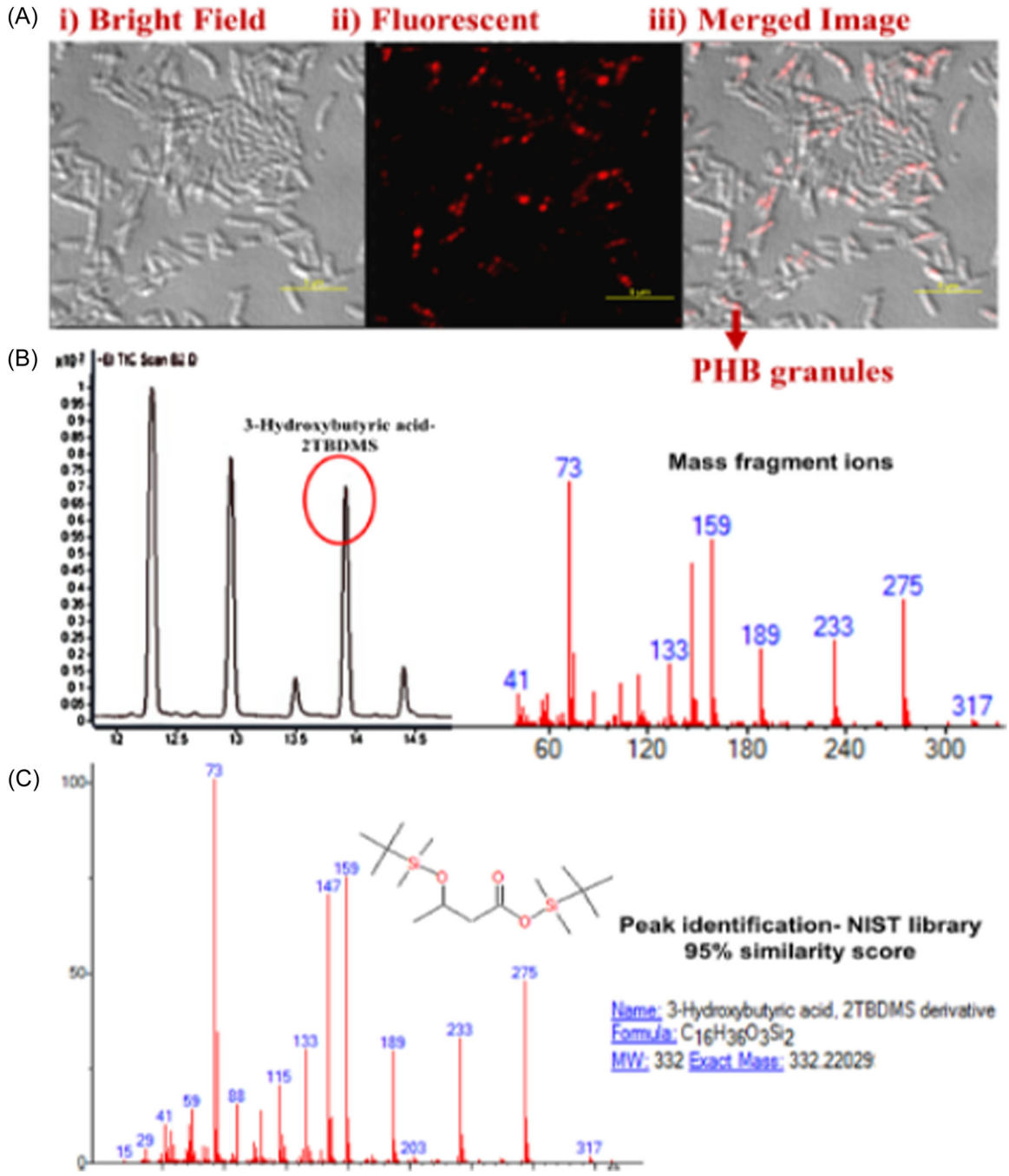

FIGURE 3 Analysis of P(3HB) or its monomer 3-HB in *Ralstonia solanacearum*. (A) Confocal image of *R. solanacearum* highlighting the P(3HB) granules (stained red with nile red) when excited at 560 nm. The figure represents the bright field image (i) of bacterial cells, red fluorescent dots of P(3HB) granules (ii), and the merged image (iii) having bacterial cells with P(3HB) granules. (B) Total ion chromatogram of TBDMS derivatized cell hydrolysate of *R. solanacearum* obtained by GC-MS highlighting the 3HB-2TBDMS peak and mass fragments. (C) Identification of 3HB peak to the NIST library resulted in 95% similarity to the database. Reprinted with permission from Jyoti et al. (2021), copyright 2021 (American Chemical Society). [Color figure can be viewed at wileyonlinelibrary.com]

further support of FTIR, ascertained the PHB structure (Susithra et al., 2021). PHAs produced with organic waste as the feedstock may provide contaminants that could move from bio-waste to the polymer granules. Potential contaminants include inorganic elements, such as heavy metals. Therefore, Astolfi et al. evaluated the total content of particular elements in numerous PHA samples produced from different origins and methods. Two kinds of feedstocks were included: a mixture of organic fraction of municipal solid waste and biological sludge from urban wastewater treatment and fruit waste. The contents of 40 elements were quantified by ICP-MS.

The elemental content of PHA was usually low and ranged from ppb to a few ppm, excluding alkaline and alkaline earth metals. Predictably, the feedstock nature influenced the contaminant levels. In fact, the PHA from fruit waste showed a lower elemental content than PHA originated from the mixture of the organic fraction of municipal waste and sludge from wastewater treatment. The crop-derived commercial PHA sample showed lower concentrations of heavy metals than the waste-based PHA ones. The PHA extraction process affected the contents of contaminants as well, with acid-based extraction resulting in lower heavy metal contents than extraction with either hypochlorite or chloroform. Additionally, several experiments were carried out to check the migration of elements from the PHA samples under different conditions (storage times, temperatures, and pH). ICP-MS data showed that the level of elemental migration from all the PHA samples were below the migration limits reported in EU Commission Regulation on plastic materials and items "intended to come into contact with food under frozen and refrigerated conditions" (Astolfi et al., 2020). Alsafadi et al. explored the use of date waste (DW) biomass as feedstock to obtain PHA by the halophilic archaeon *Haloferax mediterranei*. ^{1}H NMR showed the chemical structure of the biopolymer identified as PHBV with 18.0 mol% of 3-hydroxyvalerate. IRMS analysis of carbon isotopes, usually employed to distinguish between polymers based on their origin (plant- and petroleum-derived plastics), was carried out as a new method to highlight an eventual discrimination by the microorganism towards either of the two carbon isotopes (^{13}C and ^{12}C) in the biosynthesis of PHBV from DW. The isotopic ratio $^{13}C/^{12}C$ ($\delta\ ^{13}C$) for PHBV was found to be –19.1‰, which indicated that *H. mediterranei* preferentially had broken lighter bonds and uses the light atoms for the biosynthesis of PHBV (Alsafadi et al., 2020). Several recent studies have been focused on microbial PHA, synthesized using waste as a carbon source, and carried out by NMR and ESI-MS/MS to determine the molecular structures (Ekere et al., 2022; Johnston et al., 2017, 2018, 2019; Radecka et al., 2016). Waste polyethylene (PE) via nonoxygenated PE wax (Johnston et al., 2017), waste polystyrene (PS) fragments attained using oxidative degradation (Johnston et al., 2018) low-density PE from Tetra Pak® waste (Ekere et al., 2022), oxidized polypropylene (Johnston et al., 2019) and oxidized PE wax (Radecka et al., 2016) were tested as feedstocks for PHA production. In all these studies, ESI-MS supported by MS/MS fragmentation analysis was highly informative providing detailed structural characterization on end groups and co-monomeric unit structures and compositions.

2.1.2 | MS structure analysis of biodegradable synthetic polymers

Different structure investigations have been carried out in synthetic biodegradable polymers by MS, with analytical methodologies developed ad hoc. Bakkali-Hassani et al. developed a strategy for the synthesis of well-defined, curable biodegradable polymer precursors. They used a controlled way via continuous flow ring-opening polymerization (ROP)/postmodification reactions of ϵ-caprolactone (CL) and L-lactide (LA). Polymer architectures were established by ^{1}H NMR, ESI-MS, and SEC. The presence of allylic chain-end groups grafted on the aromatic core molecule was evidenced for both structures by ESI-MS analysis of low molar mass (MM) star polylactic acid (PLA), and linear poly(ε-caprolactone) (PCL). A single population corresponding to sodium adducts of PLA or PCL, with a peak-to-peak mass difference ($\Delta m/z$) of respectively 144.04 (LA) and 114.04 (CL), corresponding to the mass of the two repetitive units, were indeed unambiguously observed. In the case of PCL sample, another population was observed in the low MM region due to nongrafted allylic-ended PCL species, not detected by ^{1}H NMR. Then, the precursors were employed to prepare networks and polymerized high internal phase emulsions via an emulsion templating strategy using photo-initiated thiol-ene click reaction (Bakkali-Hassani et al., 2022).

In the literature, diverse investigations have applied MS analyses to ascertain the structure of biodegradable polymers prepared by ROP of lactones evaluating the influence of the catalyst and the initiator (Duale et al., 2018, 2021; Maksymiak et al., 2016). Duale et al. studied by NMR and MS the molecular structure of low MW poly(δ-valerolactone) (PVL) synthesized via bulk-ROP of δ-valerolactone with boric acid ($B(OH)_3$) as a catalyst and benzyl alcohol (BnOH) as an initiator. They fully characterized the homopolymer sample by MALDI, ESI, and ESI-MS/MS, both in positive and negative ion mode. In ESI-MS spectra two series of ions related to PVL chains terminated by benzyl ester and hydroxyl end groups and with carboxyl and hydroxyl end groups were detected (Figure 4). Furthermore, less abundant ions due to cyclic PVL oligomers were identified. The structure of PVL oligomers were further confirmed by ESI-MS^n by using CID and comparing spectra acquired in positive and negative ion modes. Finally, MALDI-TOF MS proved that the PVL samples were constituted by two types of linear PVL oligomers with different end groups and a small amount of cyclic oligomers, not visible at higher molar masses (Duale et al., 2018).

MS analysis has been helpfully used in the characterization of synthetic biodegradable homo and copolymers

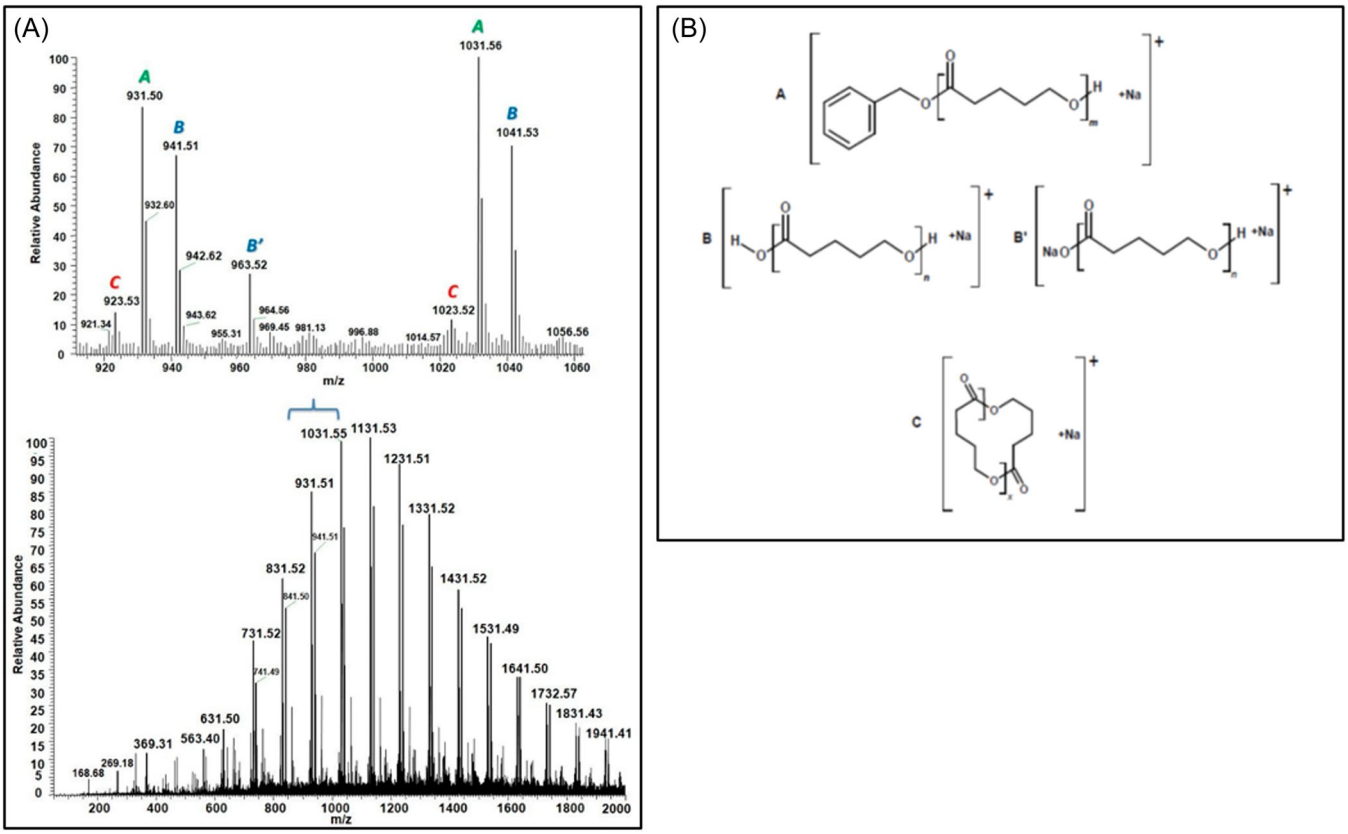

FIGURE 4 (A) Electrospray ionization-mass spectrometry spectrum (ESI-MS) (positive-ion mode) of poly(δ-valerolactone) (PVL) oligomers and the spectral expansion in the range *m/z* 910–1050. (B) The structures of the ions observed in ESI-MS of PVL. Adapted and reprinted with permission from Duale et al. (2018), copyright 2018 (American Chemical Society). [Color figure can be viewed at wileyonlinelibrary.com]

as well. Chemosynthesis of hydroxyl butyrate (HB) copolymers has been adopted to improve the applications of PHB, limited by its brittleness and thermal decomposition temperature near to the melting point. Copolymers based on HB, 1,4-butanediol, and adipic acid (A) were synthetized by microwave-assisted transesterification of the homopolymers PHB and poly(1,4-butylene adipate) (PBA) in solution. A detailed characterization of the copolyesters was carried out by GPC, differential scanning calorimetry (DSC), wide-angle X-ray diffraction, ^{1}H and ^{13}C NMR, and MALDI-TOF. Random and microblock copolymers were obtained changing the experimental conditions, such as the composition of the starting mixture as well as the amount of catalyst (4-toluenesulfonic acid). NMR provided information on the average block length while MALDI-TOF mass spectra confirmed the microstructure and allowed to ascertain the nature of the end groups (Impallomeni et al., 2013). The average number molecular weight (Mn) and the degree of polymerization of triblock copolymers were assessed by ^{1}H NMR and MALDI-TOF and compared. The triblock copolymers, synthesized by ROP, were based on poly(ethylene glycol) (PEG) and PCL-bearing benzyl carboxylate on the α-carbon of caprolactone. Mass discrimination effects were observed. However, a decrease in detection response at higher masses is well known in MALDI analysis due to the preferential desorption and ionization processes in lighter molecules in comparison with higher MM molecules. Anyway, the data of molecular weight and degree of polymerization acquired by MALDI-TOF were comparable to the ^{1}H NMR results (Table 1) (Safaei Nikouei & Lavasanifar, 2011).

An MS analytical protocol was used for a detailed structural characterization of (co)oligoesters functionalized with antioxidants for cosmetic purposes. The bioactive compounds were covalently linked as pendent groups along the backbone via anionic ring-opening copolymerization of β-substituted β-lactone containing the p-anisic moiety (p-AA-CH_2-PL) with β-butyrolactone. Biodegradable samples were synthesized via anionic ROO of p-methoxybenzoyloxymethylpropiolactone initiated by p-anisic acid sodium salt. The homo- and (co) oligoesters were characterized by SEC, ^{1}H NMR, ESI-MS,

TABLE 1 Characteristic of synthesized triblock copolymers.

Polymer	Percent of reduction[a]	Theoretical *Mw* (g mol^{-1})	*Mn*[b]	*Mn*[c]	Degree of polymerization[b]		Degree of polymerization[c]	
					CCL block	BCL block	CCL block	BCL block
PBCL-PEG-PBCL	0	4428	3683	3435	N/A	9.0	N/A	8
PCBCL-PEG-PCBCL	27	4136	3506	3503	1.9	7.1	2	7
PCBCL-PEG-PCBCL	50	3887	3206	–	4.3	4.4	4	–
PCBCL-PEG-PCBCL	75	3618	3303	–	8.0	2.0	8	–
PCCL-PEG-PCCL	100	3350	2367	2240	5.8	N/A	5	N/A

Note: Reprinted with permission from Safaei Nikouei & Lavasanifar (2011), copyright 2011 (Elsevier). N/A, not applicable.

[a]The number shown indicates the percent of debenzylation (reduction of benzyloxy carboxylate to carboxyl group) in each block copolymer determined by ^{1}H NMR spectroscopy.

[b]Number average molecular weight measured by ^{1}H NMR.

[c]Number average molecular weight measured by MALDI-TOF.

and MS/MS. Three series of singly charged ions were detected in the ESI spectrum: the series A and B were assigned to sodium cationized $[(\text{p-AA-CH}_2\text{-HP})_m/\text{HB}_n + \text{Na}]^+$ (co)oligoester chains bearing p-anisic acid and carboxylic end groups and containing one or two (p-AA-CH_2-HP) comonomer units; the less abundant ions were due to sodium cationized oligo(3-HB) terminated by p-anisate and COOH end groups. Thus, MS showed that the (co)oligoester contained up to three bioactive p-anisic moieties along the oligomer chains. ESI-MS/MS analysis was carried out on the precursor ion at *m/z* 819 assigned to the sodium adduct of $[\text{p-AA-(p-AA-CH}_2\text{-HP})_2/\text{HB}_2 + \text{Na}^+]$ terminated by p-anisate and carboxyl end groups. The detection of some product ions (*m/z* 667, 733, and 583) let the authors establishing the fragmentation pathway and confirmed a random breakage of ester bonds along the oligomer chain and ester bonds between the chain and the bioactive pendant group (Maksymiak et al., 2016).

MS methods have been also applied in the characterization of biodegradable polymer blends (Barrère et al., 2014; Rizzarelli et al., 2016). IM-MS combined with an atmospheric solid analysis probe (ASAP) was employed for the analysis of polymer blends (PLA-polybutylene succinate (PBSu) and PLA-PE) prepared mixing PLA with PBSu or PE. Barrère et al. first studied the ASAP-MS spectra of the single polymeric components. In the ASAP-MS spectrum of PBSu an unexpected series was detected and attributed to the presence of trace impurity, whose structure was assigned to adipic acid thanks to MS/MS analysis. Additionally, both PLA and PBSu ASAP spectra showed an ion series due to cyclic oligomers previously found by Py-GC/MS with chemical ionization. ASAP-IM-MS spectra of PLA-PBSu also showed the presence of additive in PLA. The ASAP-MS spectrum of a PLA-PE blend highlighted only one series of ions related to PLA cyclic oligomers. The lack of PE ions in the spectrum was attributed to a huge difference in ionization efficiency between PLA and PE. Nevertheless, from the 2D plot (i.e., drift-time vs. *m/z* plot) of PLA-PE blend, PE mass spectrum was extracted and it was very similar to that of PE alone (Barrère et al., 2014).

LC-ESI MS and NMR were used in the characterization of synthetic end-capped and intramolecular azo-functional oligocaprolactones with interesting potential applications. The azofunctional oligomers (DC) were synthesized by ring-opening oligomerization of CL initiated by the OH groups of the azo dye. Chromatographic separation and MS/MS, performed on an ESI ion trap instrument, highlighted that the reaction product was a mixture of two fractions: an end-capped azo functional oligoCL (α-DC), with a single CL arm oligomer, and one of intramolecular azo functional

oligoCL (β-DC), with two CL arms. The analytical approach allowed discriminating between α-DC and β-DC, establishing that the former constituted a minor component (Peptu et al., 2012).

2.2 | MS investigations on polymer conjugates and bioconjugates

Biodegradable polymers are employed in different kind of biomedical devices, that is, implants, scaffolds, and DDS. One remarkable way to enhance drug delivery ability and reduce systemic toxicity is to use polymer–drug conjugates. MS, particularly MALDI and ESI, has been applied in the analysis of polymer conjugates and to confirm the success of the synthetic method, in some cases comparable to a polymer end group modification (Den Berghe et al., 2011; Impallomeni et al., 2021; Lis-Cieplak et al., 2020; Maksymiak et al., 2013; Parwe et al., 2014; Scherger et al., 2021; Steinbach & Wurm, 2016; Yu et al., 2008). MALDI-TOF MS was used for the structural characterization of pranoprofen (PPF) conjugated to PCL via microwave-assisted transesterification, catalyzed by p-toluenesulfonic acid. PPF is an efficient nonsteroidal anti-inflammatory drug employed mostly in ophthalmology. NMR, MALDI-MS, and GPC gave proof of the covalent link between PPF and PCL. MALDI-TOF mass spectra highlighted a multimodal mass distribution, different from the typical unimodal bell-shaped mass distribution of polydisperse polymers. The several bell-shaped mass distributions were repeated at regular *m/z* values, multiples of the first distribution at lower *m/z*. This phenomenon was related to the synthetic route used and observed in GPC curves as well (Impallomeni et al., 2021). ESI-MS, MALDI-MS, NMR, and MS/MS have been emploied in the structural characterization of cyclodextrin-oligoester and polyester derivatives (Blaj et al., 2021; Lis-Cieplak et al., 2020; Peptu et al., 2018; Peptu et al., 2022) as well as pesticide (Kwiecień et al., 2012, 2015) and lipoic acid (Maksymiak et al., 2013) oligo(3-hydroxybutyrate) conjugates. Lis-Cieplak et al. prepared polymer-drug conjugates based on nontoxic β-cyclodextrin (β-CD) and biocompatible and biodegradable polymers. They used β-CD as the initiator in bulk in the ROP of CL, D,L-, and L,L-lactide (LA and LLA), changing molar ratios and temperatures (100°C and 140°C). The structures of the synthesized β-CD-polymer conjugates were clarified by ^{1}H NMR and solid-state carbon-13 cross-polarization/magic angle spinning NMR. MALDI-TOF MS confirmed the successful incorporation of β-CD molecule into the polymer chain. Moreover, it highlighted different end groups in β-CD-PCL and β-CD-PLA samples prepared at the two diverse temperatures. In MALDI spectra of β-CD-PLA, two populations of chains were detected, due to even and odd numbers of LA repeating units, with mass differences of 72 Da. The two series of peaks were explained by the transesterification reaction, well-know in the polymerization of LA (Lis-Cieplak et al., 2020). Peptu's group carried out different studies on biodegradable CD-polyester conjugates by MALDI, MALDI-MS/MS, and ESI-MS/MS (Blaj et al., 2021; Peptu et al., 2018, 2022). Soft ionization MS techniques were used in the structural and the architecture analysis of CD-oligoPLA to distinguish if the monomer units were attached as single or multiple chains. The NMR showed that CD-LA products were randomly esterified cyclodextrin with LA oligomers with an average of 3 lactate units per chain. Whereas, MALDI-MS analysis highlighted that the CD was substituted with an average of 15.6 lactate units per CD molecule corresponding, on average, to 5.2 oligolactide arms per CD molecule. MS/MS studies by both ESI quadrupole time-of-flight and MALDI-TOF allowed correlating the size of the LA chains bonded to the CD with the observed fragmentation patterns. Additionally, ESI CID MS/MS supported the structure of the CD-LA that was reflected in the observed fragmentation patterns. MS/MS data proved that CD-LA derivatives underwent cleavages of bonds at the level of both oligosaccharide and PLA structures (Figure 5) (Peptu et al., 2018).

Blaj et al. studied the synthesis of cyclodextrin-oligoLA conjugates (CDLA) by an optimized MALDI-MS method to establish the reaction kinetics. MALDI-MS was used to estimate Mn changes during the synthesis for a better understanding of the chemical process. The MALDI-MS data were determined assuming that the LA monomer was transformed only in the CDLA product. They were compared with ^{1}H NMR results for the DL-Lactide conversion rate, which confirmed the reaction kinetics deduced by MALDI-MS, highlighting a high degree of agreement. The MS analysis allowed monitoring the CDLA products throughout the ring opening oligomerization (ROO) reaction. In addition, they got information about degradation products formed during the synthesis procedure and the balance between polymerization and depolymerization processes. MALDI-MS detected changes in MW and secondary products, related to different solvents and temperatures, whose structure was established by MS/MS analysis. The authors showed by MS and MS/MS that the employed solvents (dimethylformamide or *N*-methyl-2-pyrrolidone) interfered with the synthesis process. They suggested that the undesirable reaction proceeded through the cleavage of the amide bonds, leading to amines, which played the

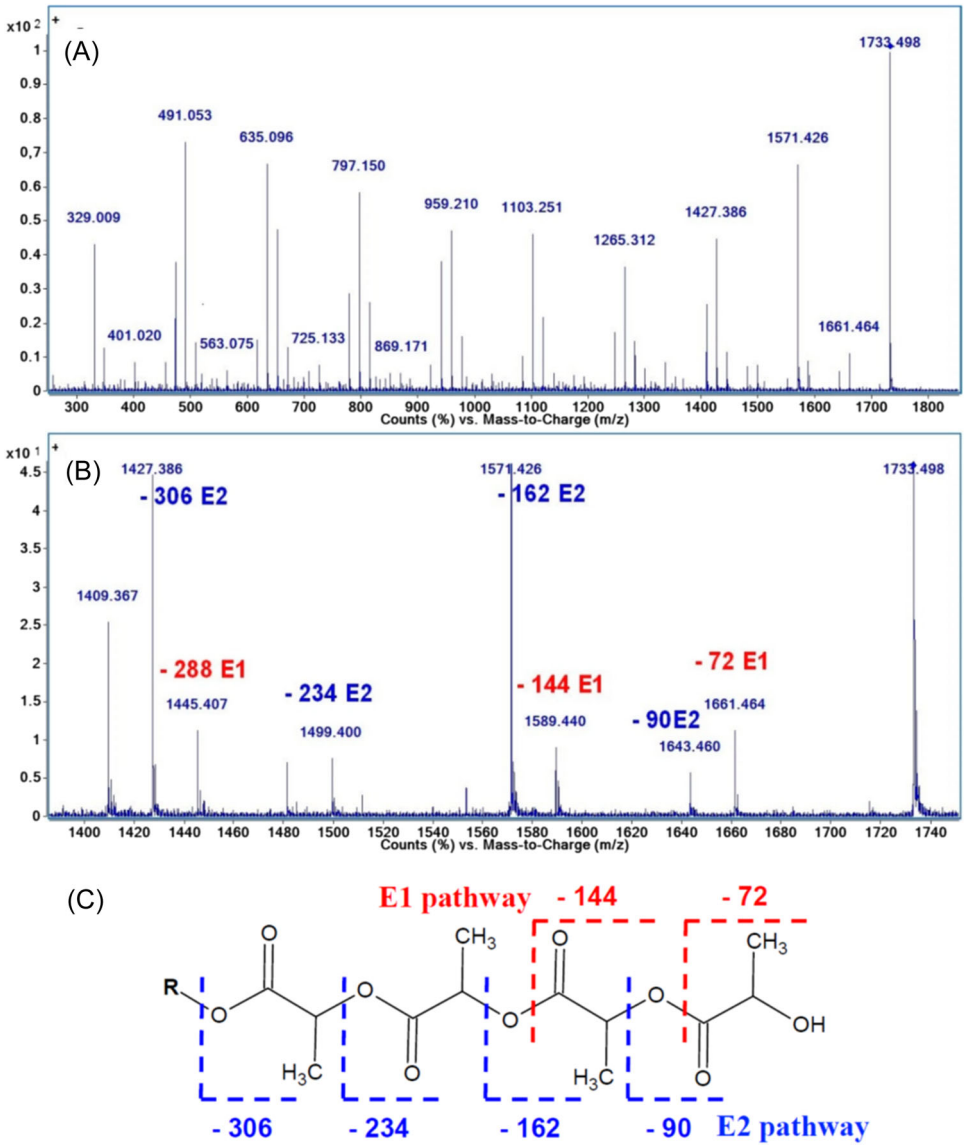

FIGURE 5 Collision-induced dissociation-mass spectrometry (MS/MS) spectrum of $[CD\text{-}LA_4 + Na]^+$ precursor ions: (A) full spectrum, (B) enlarged region between *m/z* 1400–1740, (C) fragmentation of the ester bonds at the level of the oligolactides chains attached to the CD–E pathway. Adapted and reprinted with permission from Peptu et al. (2018), copyright 2018 (MDPI). [Color figure can be viewed at wileyonlinelibrary.com]

role of nucleophile activators in the OH-initiated ROP of LA (Blaj et al., 2021). In a similar way, Peptu et al. explored the solution ROO of CL in the presence of β-CD obtaining highly water-soluble oligoCL cyclodextrin derivatives (CDCL). Oligomerization kinetics, performed by the MALDI-MS optimized method, revealed that monomer conversion occured in two stages: first, the monomer was fast attached to the secondary OH groups of the β-cyclodextrin and then, the monomer conversion proceeded slowly with addition to the primary OH groups. Again, the MALDI results were in outstanding agreement with the reaction kinetics determined via NMR spectroscopy. Moreover, MALDI-MS and MS/MS fragmentation experiments revealed secondary reactions with chemical modification of the CDCL involving the solvent used (Peptu et al., 2022).

In bioconjugates, biomolecules are linked by covalent bonds to a synthetic polymer, among which PEG is the most used. PEGylation is called the covalent connection of PEG with other molecules, and it is principally employed with therapeutic peptide and protein drugs. PEGylated drugs and similar bioconjugates are hardly prepared with high pureness. MS, particularly supported by separation techniques and MS/MS, has provided helpful structural characterization (Alalwiat et al., 2017; Ke et al., 2017; Pedrón et al., 2010; Sallam et al., 2018;

Talelli & Vicent, 2014; Wesdemiotis et al., 2011; Yi et al., 2008). By combining soft ionization methods (i.e., MALDI or ESI) with IM-MS and MS/MS fragmentation, creating a multidimensional technique, relevant understandings into the composition, structure, and architecture of bioconjugates have been provided. Sallam et al. showed the utility of combining MALDI, ESI, MS/MS, and IM-MS experiments for the full characterization of the primary structure and architecture of a polyether dendron conjugated with two different bioactive peptides (Sallam et al., 2018). Furthermore, the MS/MS and IM-MS/MS techniques were employed by Alawiat et al. in the determination of the sequence, derivatization site, and conformation of two alanine-rich peptides (AQK18 and GpAQK18, Gp: Lpropargylglycine) and their PEG conjugates. The sequence and conformation of AQK18 and GpAQK18 polypeptides and their conjugates with PEG were showed by MALDI-MS, ESI-MS, and MS/MS fragmentation, wheras shape-specific dispersion by IM-MS. Both MALDI and ESI-MS/MS analyses established that the PEG chain was attached to the C-terminus of the peptides. Remarkably, the IM-MS experiments showed the existence of random coil and helical conformers in both the peptides and bioconjugates. Moreover, the IM-MS data suggested that the helical structure was stabilized by PEG connection at the C-terminus (Alalwiat et al., 2017).

2.3 | Insights on polymerization mechanisms

MS has been also used in the elucidation of polymerization mechanisms and to check undesired side reactions (Chen et al., 2020; Gorrasi et al., 2016; Gümüştaş et al., 2022; He et al., 2020; Yang et al., 2022). Yang et al. investigated an anionic hybrid copolymerization (AHcP) of cyclic and vinyl monomers as a strategy to synthesize biodegradable heteropolymers. However, in AHcP transesterification between comonomeric units often occurs, complicating the reaction mechanism. Thus the Authors studied the AHcP of *N*,*N*-dimethylacrylamide (DMA) with CL, excluding the transesterification between DMA and CL units since DMA does not have ester group. NMR and MALDI-TOF revealed that DMA and CL units were randomly distributed into the polymer chains and were helpful to confirm the AHcP mechanism (Yang et al., 2022). To predict initiator efficiency before any experiments by means of computational chemistry methods, Gümüştaş et al. carried out a theoretical and experimental studies to investigate the effect of the initiator metal on the coordination–insertion mechanism of PVL. PVL sample was synthesized by ROP, using tin(II) acetate ($SnAcet_2$), lead(II) acetate trihydrate ($PbAcet_2{\cdot}3H_2O$), and cadmium(II) acetate dihydrate ($CdAcet_2{\cdot}2H_2O$) complexes as initiators without any co-initiator. The polymer samples were analyzed by FTIR, ^{1}H NMR, GPC, thermogravimetric analysis (TGA), and DSC. ^{1}H NMR, ^{13}C NMR, and MALDI-TOF/TOF MS analyses were particularly useful to establish the end groups and initiator residue. The occurrence of cadmium isotope distribution in the peaks of the MALDI spectrum supported the conclusion that cadmium metal was connected to the polymer chains. Considering all the data, it was settled that the complexes used behaved as initiators (Gümüştaş et al., 2022). MALDI-TOF and ^{1}H NMR were used to test a new class of catalysts, based on natural amino acids and tin ($Sn(AA)_2$), and establishing the polymerization mechanism, using a BnOH initiator, in PLA, PCL, and poly(trimethylene carbonate) synthesis. The experimental data showed that $Sn(AA)_2$ catalysts were suitable for the synthesis of moderate and high-MW PLLA. The backbone structure and end groups of low-molar-mass polymers determined by MALDI-TOF and NMR displayed that the polymerization proceeded via a traditional coordination-insertion mechanism in which the LA monomer was introduced into the tin-oxygen bond with optional acyloxygen bond scission (He et al., 2020). Chen et al. proposed a new reaction pathway for the catalytic ROP reaction, different to the three-step coordination–insertion mechanism reported in the literature. They studied a biocompatible coordination network, $\{[Zn_4(\mu_4\text{–}O)(tzmb)_3]\ 0.5H_2O\}_n$ (CZU-1), that showed high catalytic efficiency in the solvent-free ROP of cyclic esters (L-LA and CL). Density functional theory calculations, in situ diffuse reflectance FTIR spectroscopy, and MALDI-TOF MS confirmed the new polymerization mechanism. Both experimental and computational data showed that the guest water in CZU-1 played an essential role in the activation of the coordination network producing μ_4-OH Brønsted and Zn-OH Lewis acid centers, with a synergistic effect on the ROP (Chen et al., 2020).

2.4 | Surface analysis by MS

The properties and analysis of surface in biodegradable systems can be significant since degradation processes start and happen when the surface is in contact with biological or aqueous media. Surface analysis in biodegradable polymers has been mostly carried out by TOF-SIMS. TOF-SIMS is a useful surface analysis technique that has provided valuable

information on different type of biodegradable polymeric systems, including stents, microparticles, nanofibrous scaffolds, and so forth (Bege et al., 2012; Casettari et al., 2011; Chen, Dong, et al., 2010; Du et al., 2018; Lee et al., 2008; Mohiti-Asli et al., 2014; Ugur et al., 2020; Van Royen et al., 2011; Zorn et al., 2022). It proved, also with the support of images and depth profile analysis, the presence and uniformity of layers such as silver ion release polymeric system applied as a coating to PLA nanofibrous scaffolds (Mohiti-Asli et al., 2014) or poly(ethylene carbonate), and Paclitaxel sprayed on drug-eluting stents (Bege et al., 2012). The static-SIMS method was successfully used to characterize the surface functionalization of electrospun nanofibers. It provided both qualitative and quantitative information on the molecular composition of the external monolayer of single nanofibres. The detailed interpretation of the spectra permitted to get full diagnostic data on all the surface components even if the PCL fibre matrix and the additive used were structurally very similar. Ion imaging on individual nanofibres showed the homogeneous distribution of the additive on the surface. Although the quantification of the surface groups is challenged by the availability of calibration standards, Van Royen et al. built up a calibration curve and quantified a relevant additive enrichment on the PCL fibre surface (Van Royen et al., 2011). Linear segmented biodegradable poly(peptide-urethane-urea) (PPUU) block copolymers were synthesized, and their surface compositions were characterized by angle-dependent X-ray photoelectron spectroscopy (ADXPS) and TOF-SIMS. Three types of segments were present in PPUU block copolymers: the soft segment (SS), due to PCL-diol; the hard one (HS), constituted by lysine diisocyanate with a hydrazine chain extender; and an oligopeptide segment (OPS), containing three amino acids (proline, hydroxyproline, and glycine), included to provide controllable biodegradation properties. The characterization of the surface composition of biomaterials is essential since biodegradation processes generally start at the interface between biomaterial and living tissue. ADXPS and TOF-SIMS experimental data showed that the surfaces of all block copolymers were enriched with the PCL SS, the most hydrophobic segment. However, the TOF-SIMS results showed that all three segments were present in the outer ≈2 nm of the PPUU samples. Because of the HS and OPS structures mirror natural peptides, their presence on the surface was suggested to improve the biocompatibility and lead to enzymatic degradation products potentially removable from the body by normal metabolic pathways (Zorn et al., 2022).

Ugur et al. used TOF-SIMS to support their investigation on microparticle formulations based on poly (lactide-co-glycolide) (PLGA) and a triblock copolymer PLGA-poloxamer-PLGA obtained via an emulsion-based process. They explored the influence of a surfactant on the properties of the microparticles and stabilized the emulsion by either poly(vinyl alcohol), as a surfactant, or propylene glycol (PPG), as an organic solvent. Four different kinds of microparticles were prepared by combining the two polymers with the two types of stabilizers. Additionally, they studied the influence of the surface properties of microparticles on the occurrence and distribution of mixed polypeptide coatings and on subsequent cell attachment. By TOF-SIMS images of protein-coated microparticles, they showed that the use of PPG was advantageous resulting in enhanced protein adsorption. Besides, when PPG was used, the replacement of PLGA with the triblock copolymer led to improved stem cell adhesion (Ugur et al., 2020). TOF-SIMS was successfully used in the surface characterization of PLGA with vancomycin incorporated to obtain DDS. The authors studied multilayered mixtures of the antibiotic and PLGA in dimethylsulfoxide (DMSO) solutions. In fact, TOF-SIMS imaging explained that the two chemicals can undertake phase separation when DMSO is used as the solvent. In positive ion mass spectra (Figure 6A) obtained from a PLGA layer (Figure 6A, upper panel) and a mixture of vancomycin and PLGA (Figure 6A, lower panel), both prepared on a Si wafer, diagnostic signals were identified. The ions at *m/z* 100.1131 (Figure 6A, lower panel) were assigned to $C_6H_{14}N^+$ and related to vancomycin. The two ions at *m/z* 100 due to PLGA (Figure 6A, upper panel) were ascribed to $C_4H_4O_3{}^+$ and $C_5H_8O_2{}^+$. The three signals, due to vancomycin ion $C_6H_{14}N^+$ and to PLGA ions $C_4H_4O_3{}^+$ and $C_5H_8O_2{}^+$, were well resolved (Figure 6A, lower panel). In negative ion mass spectra (Figure 6B), basing the calibration on the two PLGA ions $C_6H_7O_4{}^-$ (143) and $C_6H_7O_5{}^-$ (159), the ions at *m/z* 154.9908 and 156.9880 were assigned to vancomycin and specifically to $C_7H_4O_2\ {}^{35}C^-$ and $C_7H_4O_2\ {}^{37}Cl^-$, respectively, whose *m/z* and ion intensity ratio matched the isotopic distribution of $C_7H_4O_2Cl$. Furthermore, the authors showed the applicability of TOF-SIMS in three-dimensional molecular imaging. This technique was powerful in molecular imaging phase-separated vancomycin and PLGA and depth profiling layered PLGA/vancomycin/PLGA structures (Figure 7). The multilayer PLGA/vancomycin/PLGA spin-coated on a Si substrate (Figure 7A) was depth profiled. Several ion species were suitable

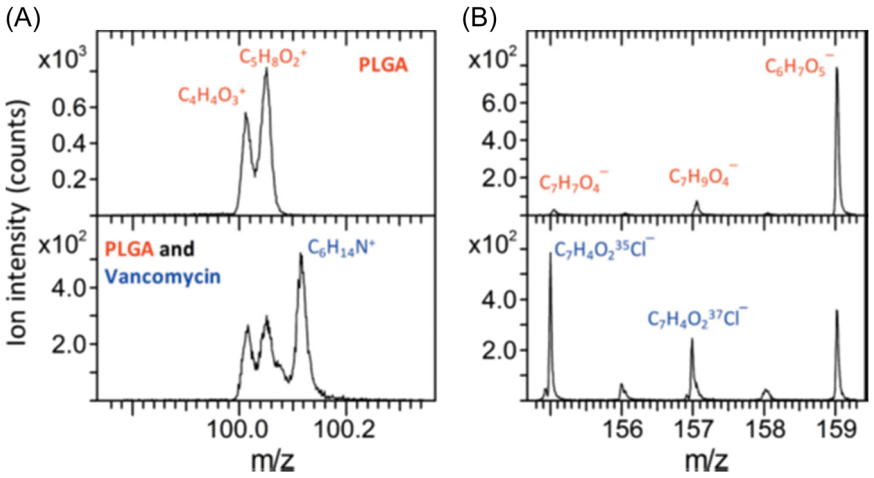

FIGURE 6 Positive (A) and negative (B) secondary ion mass spectra for pure poly(lactide-*co*-glycolide) (PLGA) (upper panels) and their mixture (lower panels), showing the vancomycin diagnostic ions at $C_6H_{14}N$þ, $C_7H_4O_2$ $^{35}Cl^-$, and $C_7H_4O_2$ $^{37}Cl^-$ at *m/z* 100, 155, and 157, respectively. Also shown are PLGA ions $C_4H_4O_3$ þ and $C_5H_8O_2$ þ at *m/z* 100, $C_7H_7O_4^-$ at *m/z* 155, and $C_7H_9O_4^-$ at *m/z* 157. The PLGA ion $C_6H_7O_5^-$ at *m/z* 159 is useful in calibrating the negative ion mass spectrum for the mixture of vancomycin and PLGA to acquire accurate *m/z* for the two vancomycin ions at *m/z* 155 and 157. Reprinted with permission from Du et al. (2018), copyright 2018 (AIP Publishing). [Color figure can be viewed at wileyonlinelibrary.com]

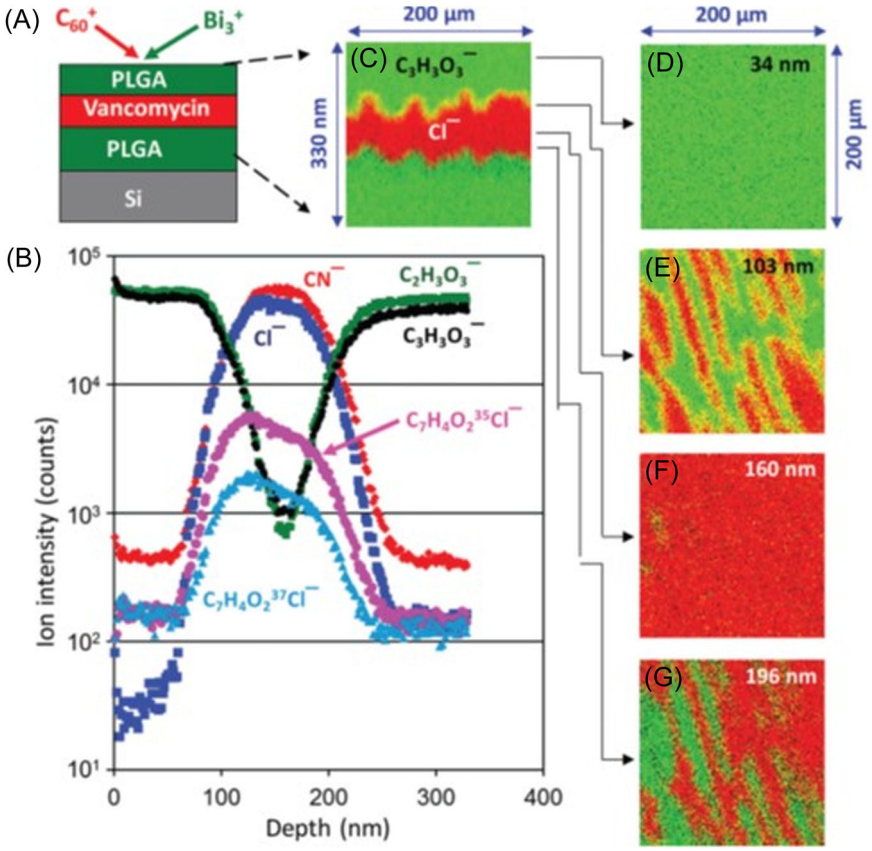

FIGURE 7 Illustration of the poly (lactide-*co*-glycolide) (PLGA)/vancomycin/ PLGA layers prepared on a Si wafer (A) and depth profiles (B) of ions CN^-, Cl^-, $C_7H_4O_2$ $^{35}Cl^-$, and $C_7H_4O_2$ $^{37}Cl^-$ representing vancomycin layer, as well as those of $C_2H_3O_3^-$ and $C_3H_3O_3^-$ representing the PLGA layers. Shown in (C) is a cross-section of the layers expressed by intensities of $C_3H_3O_3^-$ (green in color) and Cl^- (red) for PLGA and vancomycin, respectively, with a probed depth of 330 nm over a rastered area of 200–200 lm^2. The overlapped images of $C_3H_3O_3^-$ and Cl^- (D–G) show distributions of PLGA and vancomycin at probed depths of 34, 103, 160, and 196 nm, respectively. Reprinted with permission from Du et al. (2018), copyright 2018 (AIP Publishing). [Color figure can be viewed at wileyonlinelibrary.com]

for depth profiling the layered structure and depth profiles of Cl^-, CN^-, $C_7H_4O_2$ $^{35}Cl^-$, and $C_7H_4O_2$ $^{37}Cl^-$ for vancomycin and $C_2H_3O_3^-$ and $C_3H_3O_3^-$ for the glycolide and lactide moieties, respectively, of PLGA were selected. The depth profiles of $C_2H_3O_3^-$ and $C_3H_3O_3^-$ (Figure 7B) showed that, at the very center of the vancomycin layer, there were still signals corresponding to these two ions (Du et al., 2018).

3 | DEGRADATION MONITORING OF BIODEGRADABLE POLYMERS BY MS

Plastic materials were invented and designed to resist the action of chemical-physical agents and microorganisms for a long time. Thus, degradation issues have had a central role in their development and in macromolecular chemistry since they can impair the application in particular fields. Polymer degradation is called thermal, thermo-, or photo-oxidative, chemical, thermo-mechanical, biological, and so forth, according to the different process and cause involved (heat, light, microorganisms, or chemicals). Of course, it can be induced by the synergic action of more environmental factors. However, whatever the sources, the degradation mainly gives rise to products with lower MW than the virgin sample and bearing characteristic functional and terminal groups. The new compound originated can be checked by diverse analytical methods, such as NMR, FTIR, and MS, being highly informative and in some cases diagnostic of the degradation pathways. Polymer degradation provides permanent structural changes that in plastic materials are undesirable. Biodegradable polymers are a particular class with an exciting challenge: they must resist to deterioration processes during their usage, then, just after their lifetime, biodegradation is needed. MS can be a valued support in their design and development. In fact, it can provide exhaustive information on macromolecular changes induced by different deterioration processes that can occur during all the lifetimes. Besides, MS methods are helpful to monitor deterioration processes, assess the mechanisms or gain qualitative and quantitative insights on degradation products. MALDI (Rizzarelli & Carroccio, 2009), ESI (Rizzarelli et al., 2019b) and HPLC-ESI-MS (Bernhard et al., 2008; Borrowman et al., 2020; De Hoe et al., 2019; Hajighasemi et al., 2016; Jia et al., 2021, 2023; Loriot et al., 2016; Maksymiak et al., 2013; Muroi et al., 2017; Osaka et al., 2008; Perz et al., 2016; Rankin et al., 2014; Rivas et al., 2017; Sato et al., 2017; Tapia et al., 2019; Wang et al., 2014; Wu et al., 2011), GC-MS (Chrissafis et al., 2011; Jang et al., 2022; Maurer-Jones & Monzo, 2021; Saeaung et al., 2021), Py-GC/MS (Arrieta et al., 2013; Chrissafis et al., 2010; Wattanawong & Aht-Ong, 2021), ICP-MS (Hsieh et al., 2018; Yu et al., 2022) were employed, frequently in combination with other analytical methods. Biodegradable polymer degradation induced by heat (Arrieta et al., 2013; Chrissafis et al., 2010, 2011; Saeaung et al., 2021; Wattanawong & Aht-Ong, 2021), laser or ultraviolet (UV) irradiations (Kumar & Srivastava, 2015; Maurer-Jones & Monzo, 2021; Rizzarelli et al., 2019b), photo- and thermal-oxidation (Maurer-Jones & Monzo, 2021; Rizzarelli & Carroccio, 2009), the relative mechanisms and volatile organic compounds originated from incineration have been studied by GC-MS (Jang et al., 2022; Maurer-Jones & Monzo, 2021; Saeaung et al., 2021), Py-GC/MS (Arrieta et al., 2013; Chrissafis et al., 2010; Wattanawong & Aht-Ong, 2021), TG-GC/MS (Chien & Yang, 2013; Chrissafis et al., 2011), MALDI-MS (Rizzarelli & Carroccio, 2009) and ESI-MS (Rizzarelli et al., 2019b).

ESI-MS by itself (Aminlashgari et al., 2015; Carstens et al., 2008; Hakkarainen et al., 2008; Loh, 2013; Maksymiak et al., 2013; Musioł, Sikorska, Adamus, Janeczek, Kowalczuk, et al., 2016; Musioł, Sikorska, Adamus, Janeczek, Richert, et al., 2016; Musiol et al., 2020; Sikorska et al., 2014; Sikorska et al., 2018; Theiler et al., 2010; Vermet et al., 2017) or the hyphenated HPLC-ESI-MS (Bernhard et al., 2008; Borrowman et al., 2020; De Hoe et al., 2019; Hajighasemi et al., 2016; Jia et al., 2023; Jia et al., 2021; Loriot et al., 2016; Maksymiak et al., 2013; Muroi et al., 2017; Osaka et al., 2008; Perz et al., 2016; Rankin et al., 2014; Rivas et al., 2017; Sato et al., 2017; Tapia et al., 2019; Wang et al., 2014; Wu et al., 2011) have been the most elected techniques in the qualitative and quantitative analysis of hydrolytic, enzymatic, and microbial degradation products of commercial and synthetic biodegradable materials. Polybutylene adipate terephthalate (PBAT) (Figure 2) is widely used in packaging and agricultural fields because of the good mechanical properties. According to its composition, microorganisms in the soil and in compost can degrade it. Commercial biodegradable PBAT is used in agricultural mulching films and degradation, induced by irradiation to mimic the conditions that might be expected for this application, studied, highlithing the formation of cross-linked structures and gel fractions (Maurer-Jones & Monzo, 2021). The biodegradation is mainly assisted by lipase hydrolysis of the ester bonds within the macromolecular chains and produce small molecules. The identification, evolution, and persistence of PBAT biodegradation products have been under scrutiny with the fruitful support of MS, especially HPLC-ESI-MS analysis (De Hoe et al., 2019; Jia et al., 2021; Muroi et al., 2017; Rankin et al., 2014; Zumstein et al., 2018). Interestingly, De Hoe et al. studied the influence of UV-irradiation on the enzymatic hydrolysis product structures of blown, nonstabilized, transparent PBAT films by HPLC-ESI-MS. MS analysis of the enzymatic products of irradiated PBAT films showed the presence of radical-based cross-linking of two terephthalate units, producing benzophenone-like molecules. Moreover, the Authors proved that the addition of photostabilizers to PBAT films reduced the negative effect of UV irradiation on their enzymatic hydrolyzation (De Hoe et al., 2019). HPLC-ESI in negative ion mode, full scan, and multiple reaction

monitoring (MRM), was applied to study the degradation behavior of biodegradable PBAT-based films used for shopping bags or for plastic film mulching on agricultural fields. Pure PBAT films were chosen for the examination by a high-temperature actinomycete isolated from composting environments. Experimental data showed that PBAT was degraded into adipic acid, terephthalic acid, butylene adipate, butylene terephthalate, and butylene adipate-co-terephthalate, originated from hydrolytic cleavage of ester bonds (Rankin et al., 2014). Perz et al. investigated the enzymatic hydrolysis of Ecoflex, a commercial biodegradable and compostable PBAT, together with oligomeric and polymeric model substrates. They selected and compared the specificities of two enzymes of typical compost inhabitants, a fungal and a bacterial cutinase from *Humicola insolens* (HiC) and *Thermobifida cellulosilytica* (Thc_Cut1), respectively. Model substrates were systematically prepared with different chain length of the alcohol and the acid and content of the aromatic fraction. HPLC-ESI-MS analysis, both in positive and negative ion modes, allowed the identification and quantification of the hydrolysis products: terephthalic acid (TA), benzoic acid, adipic acid, mono(4-hydroxybutyl) terephthalate, mono-(2-hydroxyethyl) terephthalate, mono-(6-hydroxyhexyl) terephthalate and bis(4-hydroxybutyl) terephthalate. The experimental data confirmed that the two enzymes hydrolyzed the tested copolyesters. Additionally, they highlighted that Thc_Cut1 hydrolyzed aromatic ester bonds more efficiently than HiC resulting in up to threefold higher concentrations of the monomeric hydrolysis product TA. However, HiC displayed a greater general hydrolytic activity with twofold higher concentration of released molecules (Perz et al., 2016). In a similar way, Borrowman et al. investigated the degradation intermediates derived from the breakdown of a sprayable, synthetic biodegradable poly(ester-urethane-urea) by ultra-HPLC (UHPLC) ESI-MS, both in positive and negative ion modes. Hydrolytic, enzymatic, and in soil degradation experiments were carried out. Monomers and short oligomers, with amino, alcohol, and carboxylic acid moieties, were identified. Remarkably, the most abundant products originated from abiotic degradation (i.e., 6-hydroxy hexanoic acid and its oligomers) were not detected among the compounds derived from soil degradation (Borrowman et al., 2020).

ESI-MS, together with SEC, UV/vis, and ^{1}H NMR spectroscopies, was used to study the UV-induced decomposition oligomers from synthetic light-responsive serinol-based polycarbonate and polyester. ESI-MS allowed establishing that the UV degradation process of serinol-based polyester proceeded via intramolecular cyclization of the functional amine group with the remote ester group, producing a ten-membered cyclic degradation compound. On the contrary, the aliphatic polycarbonates underwent intramolecular cyclization and intermolecular transcarbamation, forming oxazolidinone and 2-aminopropanol terminated oligourethanes (Sun et al., 2019). Sikorska et al. investigated the hydrolytic degradation, in water at 70°C, of nonwoven materials made from PLGA (Sikorska et al., 2014) and of PLA and its blend containing 15 mol% of poly[(R,S)-3-hydroxybutyrate] (Sikorska et al., 2018) by ESI-MS supported by MS/MS, HPLC-UV and ^{1}H NMR. The structures of the PLGA hydrolytic products were established by ESI-MS/MS. Besides, HPLC and ESI-MS analysis identified the lactic and glycolic acids among the water-soluble degradation products. However, data showed that the nonwoven manufacturing method influenced both the release rate of the lactic and glycolic acids and the degradation behavior of the fibers (Sikorska et al., 2014). With the same techniques, the effect of the thickness and method of production of polymeric packaging based on PLA (rigid films and cuboid-bars) on their hydrolytic degradation rate as well as on the pattern of released products was investigated. ESI-MS data, supported by HPLC analyses, allowed establish the chemical structure of water-soluble products as well as the dissimilarities in the degradation products pattern from the PLA-based samples differing in thickness. Lactic and 3-hyroxybutyric acids and their oligomers, oligo-LA, and oligo-HB terminated by -OH and -COOH end-groups were detected. The significant differences in degradation products pattern were predominately observed in the first steps of incubation process and were attributed to an autocatalytic effect (Sikorska et al., 2018). With a similar analytical approach, the same research team carried out studies on the biodegradation behavior of prototype packaging thermoformed from oligo-LA/PHB blends, PLA-extruded, and plain PLA films under industrial composting conditions. Hydrolytic degradation in water at 70°C was performed for reference (Musioł, Sikorska, Adamus, Janeczek, Kowalczuk, et al., 2016; Musioł, Sikorska, Adamus, Janeczek, Richert, et al., 2016). Again, the structures of water-soluble degradation products were identified by NMR and ESI-MS. The results revealed that the biodegradation process was less dependent on the processing of PLA films and more influenced by the degradation conditions (Musioł et al., 2016b).

Both enzymatic and chemical-catalyzed hydrolytic degradation of PCL, used in biomedical applications, have been extensively investigated. Predictably, several lipases accelerate the degradation that preferentially occurs in the amorphous domains. Increasing the amorphous fraction of a biodegradable systems can be used to change the degradation rate according to a new specific application. With the finding of ESI-MS analysis, crosslinking has been shown to decrease the crystallinity thus inducing a higher degradation rate (Theiler et al., 2010). Moreover, in situ cross-linking of PCL

fibres with bis-(ε-caprolactone-4-yl) (BCY) resulted a viable method to prevent the MM decrease during meltspinning. Again, ESI-MS was helpful to establish the influence of in situ crosslinking on the degradation profile of melt-spun PCL fibres with diverse BCY amounts. Noteworthy differences in the degradation products with linear, cyclic, or BCY-related low-MM compounds were distinguished, confirming the impact of crosslinking and processing on the degradation process and water-soluble products (Aminlashgari et al., 2015).

GC/MS (Aparaschivei et al., 2016; Pérez-Lara et al., 2016; Spontón et al., 2013), Py-GC/MS (Arrieta et al., 2014) and MALDI-MS (Bernhard et al., 2008; Dopico-García et al., 2013; Rankin et al., 2014; Rivas et al., 2017; Shi et al., 2015) have been less extensively used to monitor low MW degradation products originated from soil, compost or wastewater. Because of the growing awareness of plastic wastes in the marine environment, biodegradability, mainly studied in the past in soil or compost, has been carried out recently also in wastewater. The structural identification and evolution of degradation products were performed by HPLC-ESI-MS. Interestingly, MALDI-MS imaging (MSI) was used to evidence the hydrolytic reactions and differences on the surface of a PCL–diol solid sample when exposed to different water environments (Rivas et al., 2016; Rivas et al., 2017). Microbial degradation was carried out in aerobic and denitrifying wastewater by a treatment plant. Caprolactone oligomers and PCL chains with a diethylene glycol as terminal group were detected and identified. MALDI-MSI images generated from polymer cuts using the most abundant ions specific of the starting polymer (*m/z* 1155.7, 1269.7, 1383.8, and 1497.9) exhibited important differences in the homogeneity on both intensity and uniformity. Whereas the reference sample (Figure 8A) showed a uniform and intense distribution, the exposed ones (Figure 8B–D) pointed out increasingly heterogeneous spatial patterns with a decreasing intensity following the order sterile -> aerobic -> denitrifying. In the last case (Figure 8D), the disappearance of the peak monitored was almost complete in some parts (deep blue colored areas) (Rivas et al., 2017).

Plastic pollution and contamination in the marine environment, mainly attributed to mishandled plastic waste, yields fragments or microplastics that can have harmful effects on marine organisms with proven transmission along the food chain (van Raamsdonk

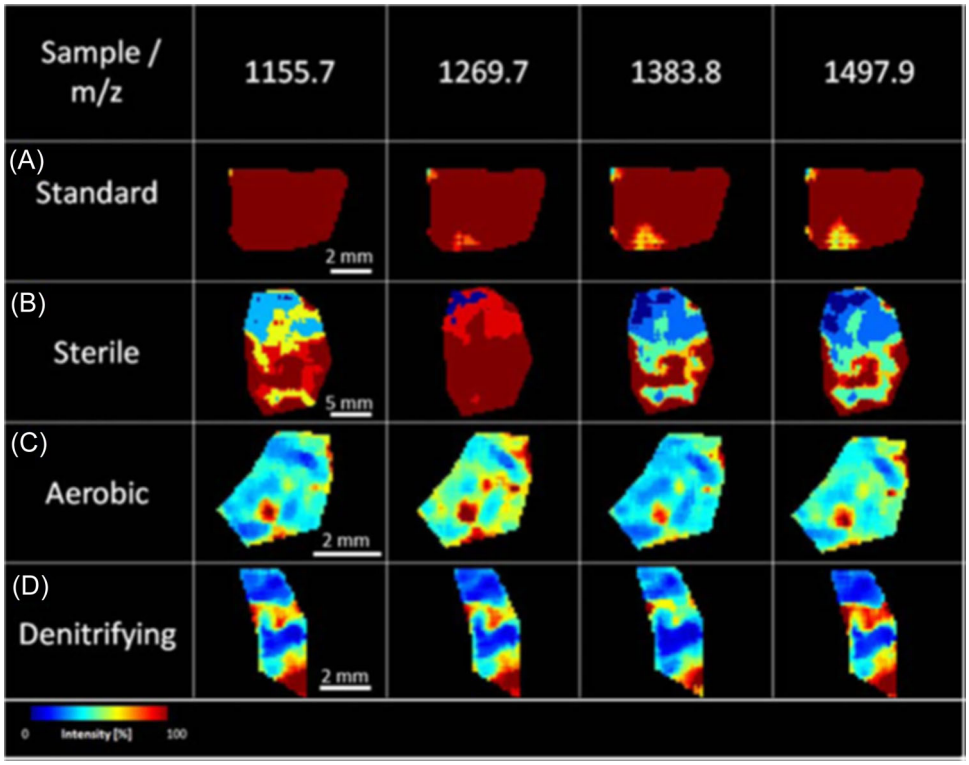

FIGURE 8 Comparison of MALDIToF images corresponding to sections of (A) PCDL standard, (B) control sample kept in sterilized water, (C) sample exposed to aerobic wastewater, and (D) sample exposed to denitrifying wastewater. Images were obtained by data processing with Flex Imaging 4.0 software. Spatial differences among pixels using the different ions are visible across the surface of the samples. Ions shown are sodium adducts $[M + Na]^+$. Reprinted with permission from Rivas et al. (2017), copyright 2017 (Springer). [Color figure can be viewed at wileyonlinelibrary.com]

et al., 2020). In this view, biodegradability tests on microplastics in soil and under marine conditions have gained increased interest. Laboratory procedures have been settled and diverse analytical methods, among wich MS (i.e., GC/MS and HPLC-ESI/MS), applied to check biodegradation and structural information (Cheng et al., 2022; Gunawan et al., 2022; Park et al., 2021). The release of oligomers under marine environmental conditions of bio-based (PLA), microbial (PHBV), and fossil-based polymers (PCL), as substitutes of conventional microbeads (PE, polymethylmetacrylate) for cosmetics, was monitored by HPLC-ESI-MS using both positive and negative ion modes. Under abiotic conditions, the ester hydrolysis of PCL generated monomer, dimer, and trimer of polycaproic acid oligomers. The PHBV microparticles incubated with microorganisms released various dimer/trimer units of HB and HV. In the experimental conditions used, PHBV microparticles were more sensitive to enzymatic cleavage than to abiotic degradation processes (Cheng et al., 2022). Bernhard et al. investigated the aerobic biodegradation in fresh and seawater, using an inoculum from municipal wastewater and artificial seawater, of PEG samples, of different MW. They monitored the fate of degradation products by using by HPLC-ESI and MALDI-MS, both in positive ion mode. Freshwater samples were analyzed without any preparation whereas seawater degradation products had to be treated to remove the salts. The evolution of peak intensity of PEG 970 homologue, for freshwater and seawater media, as a function of the incubation time was set in relation to that with the highest intensity (Figure 9). At the beginning ($t = 0$), the intensity ratios of all homologues show the typical pattern of a polydispersed sample. Then, a shift in the MW

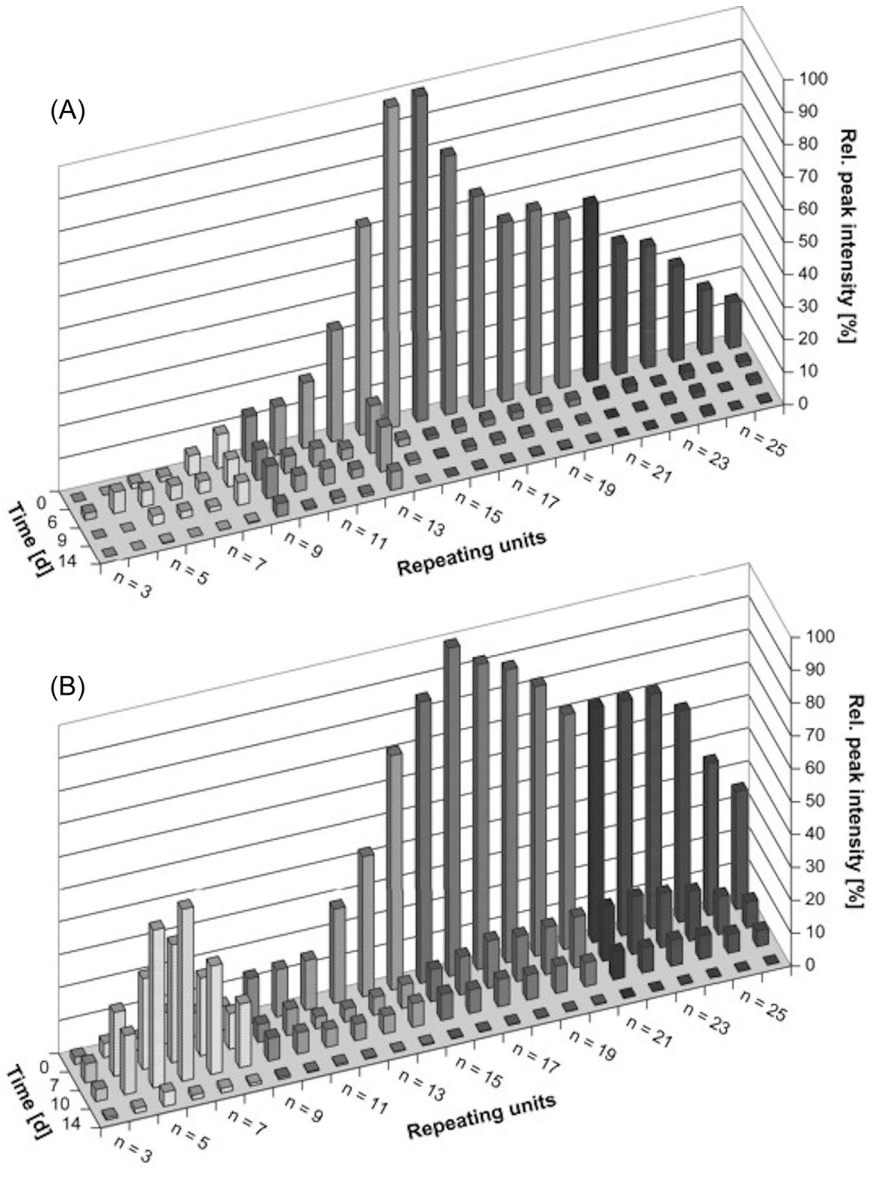

FIGURE 9 Fate of individual homologues during aerobic biodegradation (0–14 d) of polydispersed PEG 970, measured by (D)-ESI-LC–MS. (A) Freshwater media, (B) artificial seawater media. Peak intensities are set in relation to the highest peak intensity detected during all measurements. Reprinted with permission from Bernhard et al. (2008), copyright 2008 (Elsevier).

distribution towards the short-chain homologues is observed for both media. The amount of low MW oligomers increases in both media and decreases again when degradation continues (Figure 9). This approach of course is limited by the different detector responses for the homologues of PEGs. MALDI spectra of PEG 2000 during aerobic biodegradation, in artificial seawater media with marine inoculum, highlighted that the degradation progress after 14 days was limited. A reduction of some PEG homologues in the *m/z* range 1300–1600 was detected but the long-chain PEGs were persistent (Figure 10) (Bernhard et al., 2008).

Thermal and photo-degradation studies of biodegradable polyesters, and polymers as well, are essential for the development of safe materials and select appropriate stabilizers. Thermal degradation of PLA and aliphatic polyesters based on dicarboxylic acids and diols, as well as their related nanocomposites, has been successfully studied by MS (Arrieta et al., 2013; Chrissafis et al., 2010; Chrissafis et al., 2011; Rizzarelli & Carroccio, 2009; Wattanawong & Aht-Ong, 2021). In particular, thermal degradation behavior of synthetic biodegradable poly(propylene azelate) and poly(propylene sebacate) samples was studied to elucidate the degradation mechanisms by TGA, FTIR, and a combination of TG/GC-MS. Aldehydes, alcohols, allyl, diallyl, and carboxylic acids were identified as the main decomposition products. From the structure of decomposition

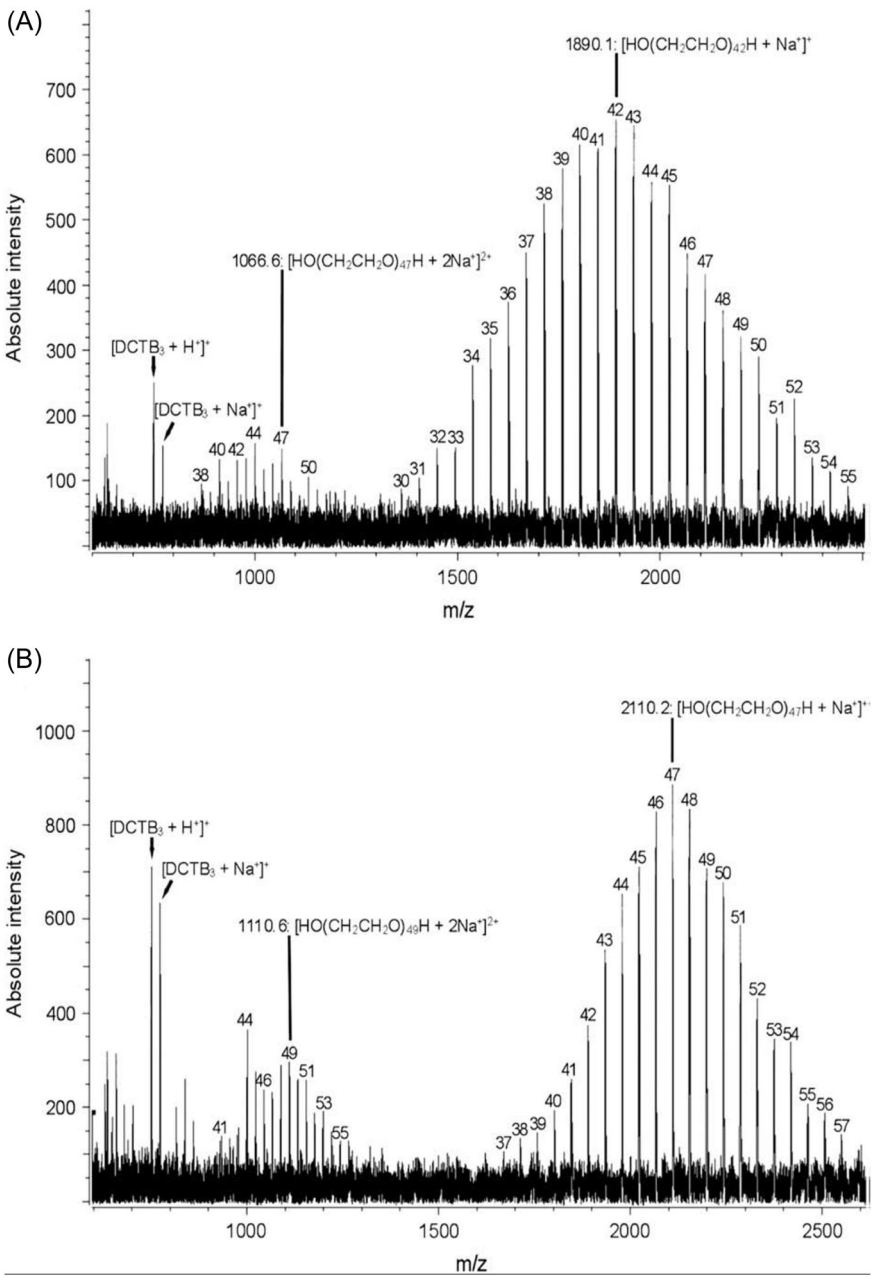

FIGURE 10 Matrix-assisted laser desorption ionization-time of flight mass spectrometry spectra of polydispersed PEG 2000 during aerobic biodegradation in artificial seawater media with marine inoculum, matrix was DCTB. (A) Sample from Day 1, (B) sample from Day 14. Numbers indicate repeating units. Reprinted with permission from Bernhard et al. (2008), copyright 2008 (Elsevier).

compounds, it was established that degradation processes in both polymers took place primarily through a β-H bond scission and secondarily via α–H bond cleveage (Chrissafis et al., 2011). The decomposition products of PBSu and Ag-zeolite PBSu composite films were analyzed by Py-GC/MS to assess their thermal degradation mechanisms. Small molecules such as 1,3-butadiene and tetrahydrofuran, together with cyclic molecules, alkyl, vinyl, and hydroxyl-terminated compounds, were detected for all the samples but with different areas ratio. According to the structures assigned, the β-hydrogen scission was confirmed the main mechanism of thermal degradation of PBSu, similarly to CID fragmentation mechanims (Rizzarelli, 2013). For virgin PBSu, the main degradation products were high molecular weigh compounds such as 3-butenyl 4- hydroxybutyl succinate (allyl product), 3-dibutenyl succinate (diallyl product), all derived from β-hydrogen scission. The cyclisation decomposition reaction from succinic acid end molecules produced the cyclic compounds such as succinic anhydride in agreement with a previous work performed by MALDI analysis (Rizzarelli & Carroccio, 2009). Small amounts of 1,3-butadiene and tetrahydrofuran were observed at low retention time and due to double β-hydrogen scissions of butanediol moiety in the macromolecular chain and dehydration of butanediol end molecules, respectively. The acidity of zeolite influenced the thermal decomposition products of PBSu composites. Ag-zeolites promoted the cracking of PBSu molecules into smaller molecules, while decreased the yield of large molecules (Wattanawong & Aht-Ong, 2021). Exhaustive information on thermo-oxidative degradation mechanisms in synthetic and commercial PBSu were provided by MALDI analysis thanks also to the use of extremely thin polyester films. Structures and end groups of the degradation products identified showed that a α-H abstraction mechanism represented the primary step in PBSu thermal oxidation. A detailed map of the polymer chains originating from the decomposition of the hydroperoxide intermediate by radical rearrangement reactions was depicted. Addidional, semi-quantitative analysis revealed that degradation pathways were time-resolved, showing a different induction period. In commercial PBSu sample, ester and urethane units, related to chain extension, underwent α-H abstraction leading to the formation of additional oligomers, with respect to PBSu, detected in the MALDI spectra (Rizzarelli & Carroccio, 2009). In the literature, MALDI-MS analysis on synthetic biodegradable polymers has frequently detected cyclic or linear ions bearing end groups originated from undesired thermal degradation processes (Raase et al., 2015; Rizzarelli et al., 2015). In some cases, particularly in hyperbranched polyesters, MALDI was not able to distinguish linear and cyclic species by their mass difference, because there was no release of a condensation product, for example, water due to the ring-opening strategy employed (Fischer et al., 2015).

Recently, the laser-induced degradation due to ultrashort laser pulses (ULP) employed to cut extremely thin PLA films was investigated. ULP polymer cutting is a manufacturing technology under scrutiny for its advantages in medical applications. Limited heat transmission to the film portions around the cuts and the consequent precise incisions involve reduced post-processing and endorse ULP cutting appealing for industrial applications. Nonetheless, ULP may induce degradation processes and impair the safe use of the polymer samples. Accordingly, portions of PLA films, ULP cut and uncut, were fully characterized by SEC, DSC, Py-GC/MS, ICP-MS, NMR, and FTIR. PLA oligomers extracted in methanol were analysed by ESI-MS operating both in positive and in negative ion mode. FTIR, ESI-MS, and NMR analysis revealed the formation of olefin end groups originated from a β-H transfer mechanism, which could be due to heat and/or light (Norrish II mechanism). ESI mass spectrum for neat PLA in positive ion mode (Figure 11A) showed two sets of signals, the first due to linear chains bearing 1-dodecanol ester group at one end and the alcohol group at the other (series A), the second relative to cyclic species (series B). Only one series was detected in negative mode (Figure 11B), related to linear chains terminated by -OH and -COO- end groups (series C). The series C wa not detected in positive ion mode because of their lower abundance in comparison with species labelled with A and B. Remarkably, several additional ions were detected both in positive (Figure 11C) and negative (Figure 11D) ESI-MS spectra of the low molecular weight fractions extracted from cut film portions. Sodiated cyclic species (series B) and the linear chains, bearing -OH and olefin end groups (series D), as well as terminated by -OH and -COOH groups (series C), particularly -COOH and -$CH=CH_2$ end groups, were attributed to a photo-induced degradation mechanism (Norrish II type). Remarkably, the detection of oligomers terminated with -OCH_2CH_3 (species F and G), -CHO (species I^-) or -$COCH_2CH_3$ (species L^-) was related to a Norrish I type degradation mechanism that at first induces an homolytic breaking of -CH-CO- bonds creating two radicals giving rise to the different end groups identified (Scheme 1) (Rizzarelli, Piredda, et al., 2019).

Insects used to treat organic waste streams, producing valued protein products, are progressively more exposed to plastic materials assimilating their carbon into organic biomass that is ubiquitous and

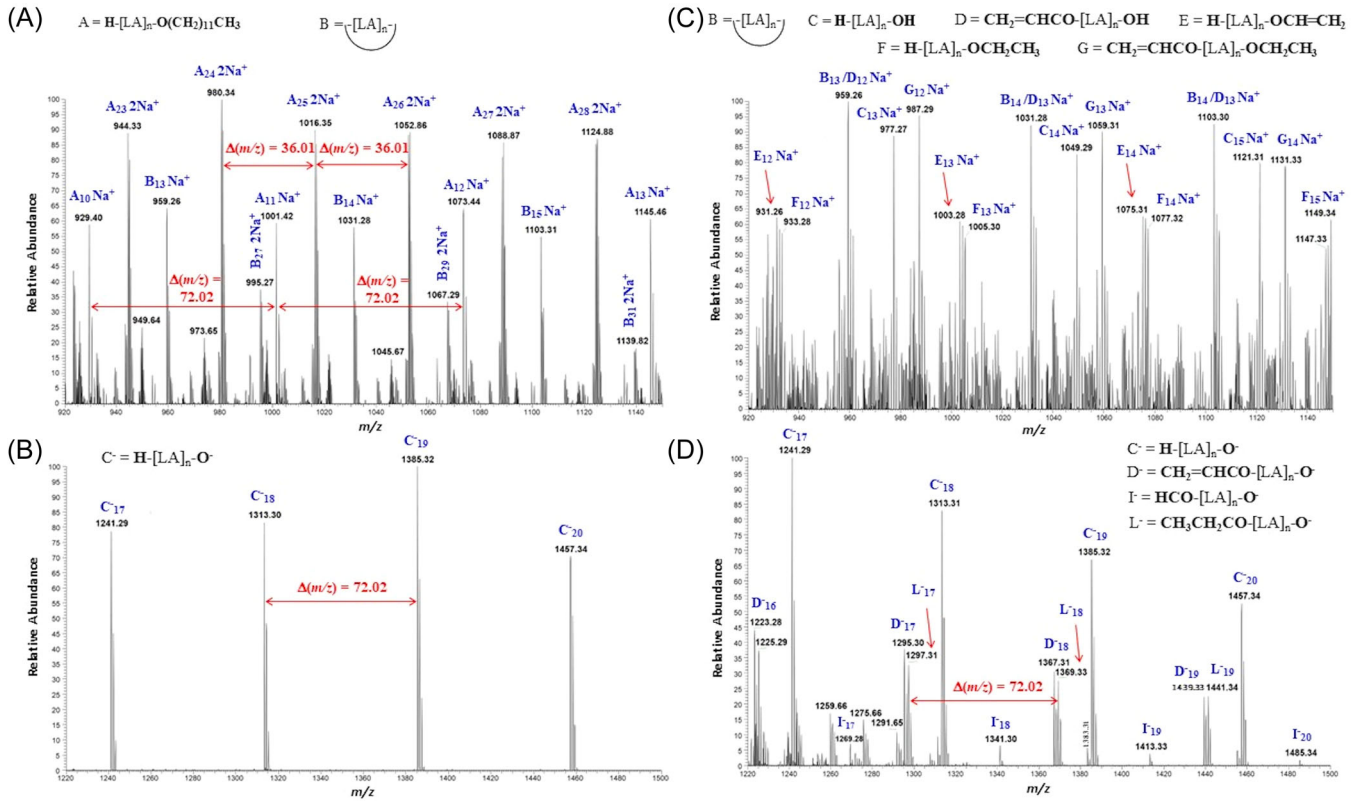

FIGURE 11 Expansion of ESI-MS spectra in (A) positive (+) and (B) negative (−) ion mode of low molecular weight fractions extracted from neat film portions. Expansion of ESI-MS spectra in (C) positive (+) and (D) negative (−) ion mode of the low molecular weight fractions extracted from cut film portions. Adapted and reprinted with permission from Rizzarelli, et al. (2019b) copyright 2019 (Elsevier). [Color figure can be viewed at wileyonlinelibrary.com]

harmful to organisms. Discovering which insects are able of bio-transforming specific plastic types could be helpful in the development of ad hoc insect bio-transformers. One way to explore this interaction concerned the analysis of central carbon metabolism (CCM) metabolites. In this contest, Beale et al. investigated the biochemical impact of traditional (poly(ethylene terephthalate) (PET), PE, PS, expanded PE, PP) and biodegradable plastics (PLA) using three insect models. Black Soldier Fly (BSF), Mealworm (MWO), and Wax Moth (WM) larva were each exposed to the plastic substrates for 5 days to explore any positive metabolic benefits in terms of insect performance and plastic degradation potential. CCM metabolites were analyzed via a targeted multiple reaction monitoring (tMRM) LC-QqQ-MS method. Distinctive expressed routes were observed for each insect model. The Authors found that, when raised on PET, BSF larvae have an elevated pyrimidine metabolism, while the purine metabolism pathway was strongly expressed on other plastics. Moreover, the MWO and WM model insects were metabolically more active on PLA and foam plastic samples (Beale et al., 2022).

4 | ROLE OF MS IN APPLICATION ISSUES OF BIODEGRADABLE POLYMERS

Nowadays, biodegradable polymers are used in wide range of applications from biomedicine to agriculture (Figure 12). As for traditional materials, their usage involves several concerns related to the performance and final target, requirements for human health such as in food contact or the end of life in soil, compost, or other media.

MS has been more and more increasingly supporting investigations concerning application fields of biodegradable polymers, frequently addressed on environmental and human health issues (Biswas et al., 2022; Fojt et al., 2022; Mahmoud et al., 2022; Okoffo et al., 2022; Phothisarattana & Harnkarnsujarit, 2022; Rizzarelli et al., 2011; Savva et al., 2023; Sun et al., 2022; Wang et al., 2022; Wu et al., 2021; Yuan et al., 2021). Studies on additives and their potential migration (Phothisarattana & Harnkarnsujarit, 2022; Savva et al., 2023), on microplastics identification and quantification (Okoffo et al., 2022; Sun et al., 2022; Wang et al., 2022), on the

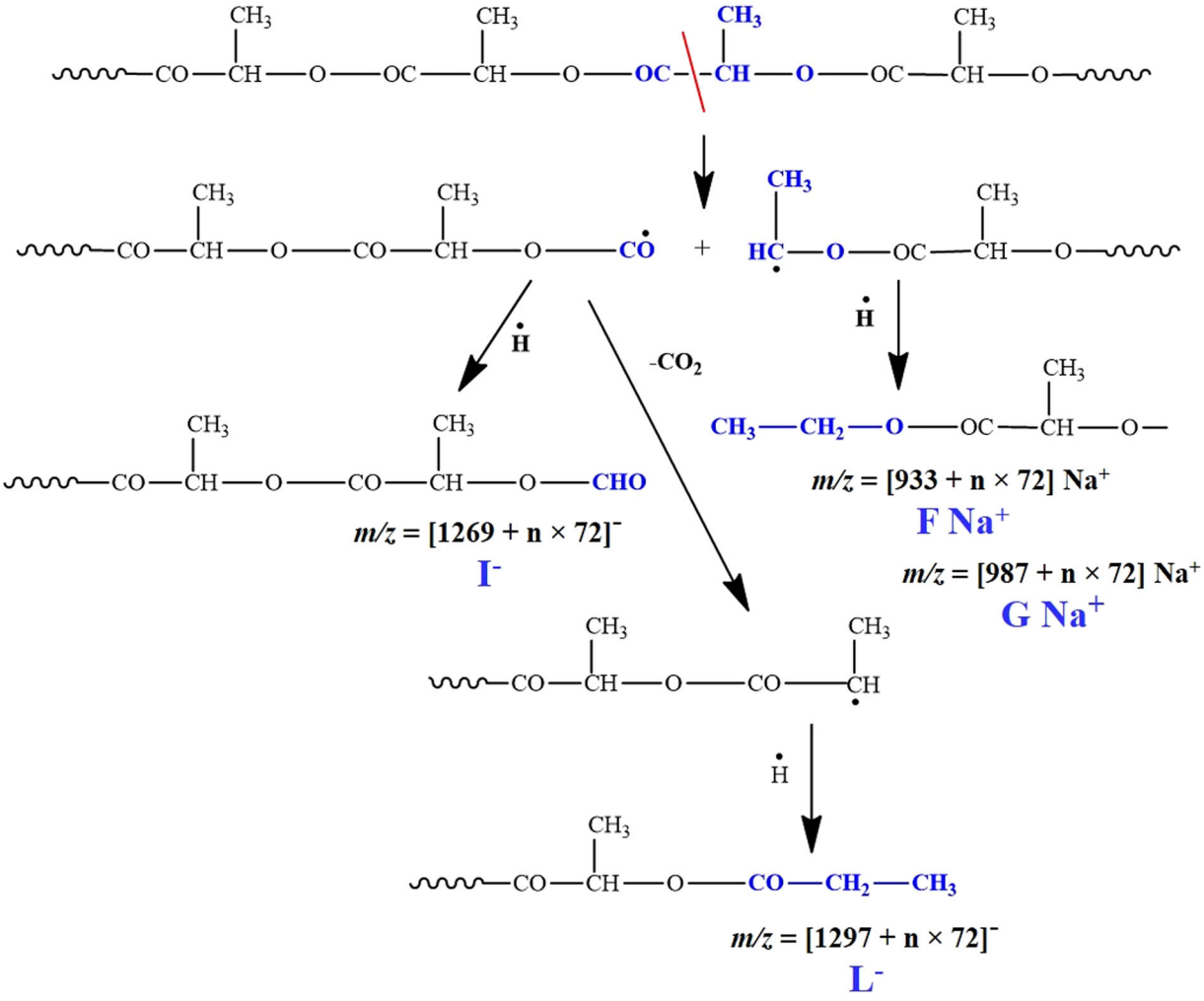

SCHEME 1 Photodecomposition of polylactic acid via the Norrish I reaction. Reprinted with permission from Rizzarelli, Piredda, et al. (2019b), copyright 2019 (Elsevier). [Color figure can be viewed at wileyonlinelibrary.com]

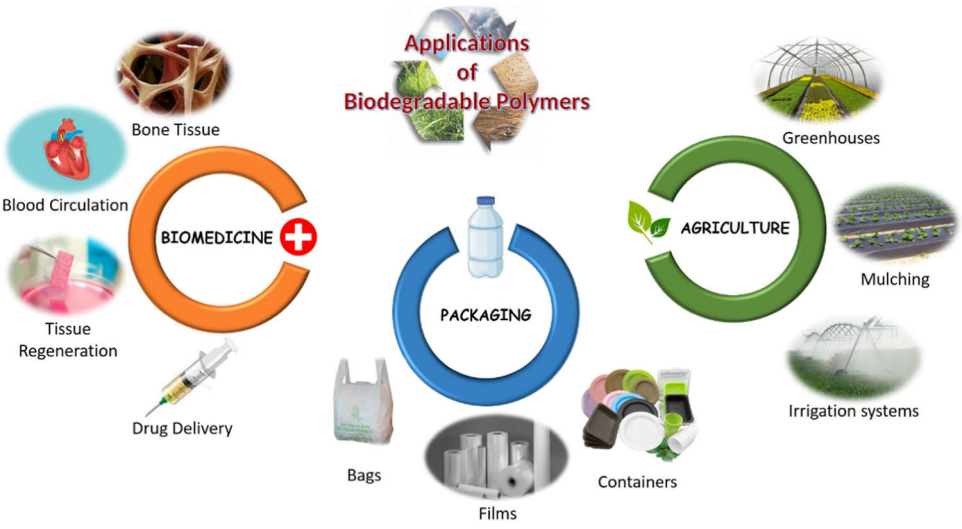

FIGURE 12 Application fields of biodegradable polymers. [Color figure can be viewed at wileyonlinelibrary.com]

PE content in biodegradable polymer blends and carrier bags claimed to be compostable (Rizzarelli et al., 2016), drug release and loading as well as pharmacokinetic (Biswas et al., 2022; Ibarra et al., 2018; Kang et al., 2021; Wu et al., 2021), in some cases combining separation techniques and MS and MS/MS (Biswas et al., 2022; Kang et al., 2021; Yuan et al., 2021), have been carried out.

4.1 | Studies on environmental and human health issues

Biodegradable bioplastics are an appealing alternative to traditional materials. Nevertheless, similarly to traditional plastics, great quantities of plastic additives are used in the formulations of bioplastics to improve their performance and barrier properties. Nowadays, there is a more and more increasing apprehension about causes of chemical exposure. Nonetheless, in bio-based and biodegradable systems there is a limited knowledge about complex additive mixtures. Very recently, Savva et al. carried out by HPLC coupled with high-resolution MS a wide screening of the bioplastics composition of single-use plastic (SUP) items made of PLA and PHB, in comparison with those based on a traditional and fossil-based material, such as high-density PE, being one of the plastic materials with the highest market share. They powdered different types of SUP items (i.e., plates, cups, cutlery, straws, bags, and bottle cap) in the nano-micro range (100 nm–10 μm). The additives were extracted from the materials using three different solvents (methanol, acetone, and toluene) and ultrasonic-assisted solvent extraction. It was not possible to remove the 100% of the additives from the material, but experiments were performed in the same condition to get a comparative fingerprint of primary organics and relative abundances between the different materials. The extracts were analyzed by a QExactive-hybrid quadrupole Orbitrap mass analyzer equipped with a heated ESI source, both in positive and negative ion mode. About two hundreds of additives were tentatively recognized in the bioplastics SUP items. In particular, an average of 123 and 121 plastic additives were found in PLA and PHB items, respectively. Among the additives, plasticizers were the most abundant and the phthalates group was the most found, with 63 plastic additives established by standards and quantified (Savva et al., 2023).

Undoubtedly, biodegradable polymers are promising alternatives for conventional plastics, but they recently have been received attention for the potential negative impact in soil ecosystems. In fact, some evidence showed that microplastics (MPs) can modify the physical properties of soil (i.e., pH, evaporation, and aggregation), microbial communities and function, and enzymatic activities (Yang et al., 2021). Dissolved organic matter (DOM) is a relevant constituent of soil carbon providing substances involved in physical-chemical and biological processes in soil. Carbon is dominant in MPs, consequently they may potentially contribute to the soil carbon and change its cycling processes (Rillig et al., 2021). Interestingly, Sun et al. estimated the effects of biodegradable PLA and PBSu MPs at a concentration of 1% (w/w) on chemical composition and properties of DOM in two soil types, a black soil (BS) and a yellow soil (YS). They carried out a comparative study on PE and PS MPs. They used fluorescence excitation-emission matrix spectroscopy and FT-ICR-MS, with an ESI ion source and combined with solid-phase extraction procedures. FT-ICR-MS provided a detailed molecular-level DOM properties in the diverse MPs treatments. MPs addition significantly increased the number of DOM molecules in BS soil. The identified formula numbers of DOM were 1432 in control and 3563, 3498, 2666, and 3329 in MPs treatments for PBSu, PLA, PE, and PS, respectively. On the contrary, for the DOM in YS soil, the modification of MPs reduced the molecular numbers. In fact, the identified formula number of DOM in the control was 4906, while just 2642 molecules were detected in PBS buffer-treated samples. PBSu substantially enhanced the soil-dissolved organic carbon and the relative intensities of protein-like components. The FT-ICR-MS showed that more labile-active DOM molecules were preferentially found in biodegradable MPs experiments, and this result was related to the polymer degradation. The PE and PS MPs changed the molecular compositions of the soil DOM (Sun et al., 2022).

There is also growing concern regarding the potential environmental pollution and release of harmful chemicals (particularly additives) from MPs, including those from biodegradable items. In fact, MPs originated from biodegradable plastics are mistrusting the safety of this promising materials. Py-GC/MS has been displayed to be an appropriate tool for the concurrent identification and mass quantification of numerous synthetic polymers in different environmental samples. Okoffo et al. developed and validated an analytical method coupling pressurized liquid extraction and Py-GC/MS combined with thermochemolysis to identify and quantify at once five micro-bioplastics (i.e., PLA, PHAs, PBSu, PCL, and PBAT) in environmental samples (wastewater, biosolids, marine sediments, and drinking/stormwater samples), irrespective of particle size, shape, and a prior optical separation. The interpretation of the pyrograms was based on an in-house database and the literature data. The limits of quantification for the target micro-bioplastics ranged between 0.02 and 0.05 mg/g. PLA and PBAT were

regularly detected in wastewater, biosolids, and sediment samples (concentrations 0.07 ÷ 0.18 mg/g). The developed analytical method could be potentially extended in assessing the biodegradation of bioplastics in environmental samples by quantifying the induced changes in the microbioplastics concentration (Okoffo et al., 2022). For the same purpose, Wang et al. developed a method based on alkali-assisted thermal depolymerization and LC-MS/MS analysis, specifically to quantify PLA MPs. MPs were efficiently depolymerized to lactic acid and detected by LC-MS/MS with a limit of quantification of 18.7 ng/g. They did not need previous separation or extraction from the environmental samples. Using this method, PLA MPs were detected in all the sediment samples of a reservoir at a range of 53.5–491 ng/g dw, and the concentrations decreased with the sediment depth (Wang et al., 2022).

In biodegradable plastic food packaging, metal oxides, among which titanium dioxide (TiO_2) and zinc oxide (ZnO) nanoparticles (NPs), enhanced mechanical, thermal and barrier properties as well as functional performance, such as antimicrobial activity against various microorganisms. However, applications of nano-TiO_2 and nano-ZnO in food contact substances must fulfil safe migration limits. Migration of NPs is a mass transfer phenomenon of components from packaging into foods. International authorities establish through regulations the use of metal oxides in food contact materials to control migration levels of substances from the packaging as a safety issue. In 2021, the European Food Safety Authority stated that TiO_2 can no longer be considered safe when used as a food additive. Thus, determining the potential migration behavior is fundamental for the commercial application of biodegradable polymers. Phothisarattana and Harnkarnsujarit studied the effects of TiO_2 and ZnO nanofillers (1%–5%) on bioplastic packaging microstructural changes for infrared absorption, thermal stability and overall and specific migration behavior in distilled water, 10% ethanol and 3% acetic acid. NPs were compounded with thermoplastic starch (TPS) and then blended with PBAT to be processed via blown-film extrusion. ICP-MS was used to monitor metal oxides release, predictably dependent on the simulant nature. Films with ZnO showed higher migration levels, particularly in acid simulant due to high dissolution of ZnO particles. Release of TiO_2 had a maximum at 3%–4% of NPs content followed by a sharp drop at higher TiO_2 percentage. Overall, nanocomposites films containing ZnO showed higher migration levels than the TiO_2 ones, indicating that the latter was more inert. Anyway, migration levels of both NPs incorporated in PBAT/TPS blown films were affected by the matrix structure alteration due to simulant penetrations, interaction and adhesion forces between metals and polymers and favorable dissolution of the metal into simulants (Phothisarattana & Harnkarnsujarit, 2022). PE in complex biodegradable polymer blends and carrier bags claimed to be compostable was checked by Py-GC/MS and TGA. Polymer blends based on PLA, PBAT, native starch (NS), and calcium carbonate ($CaCO_3$), with known amount of PE (0%–10%), prepared by melt mixing, were analyzed by a two steps Py-GC/MS optimized method (Figure 13). In the first step (400°C, Figure 13A), pyrolysis products from thermal breaking of PLA, NS, and PBAT were detected. In the second one (500°C, Figure 13B), triplet peaks characteristic for PE, due to α,ω-dienes, α-alkenes, and n-alkanes, were detected (Figures 13C,D). TGA was used to quantify the amount of PE in the blends. Furthermore, the analytical strategy was employed in the analyses of commercial carrier bags claimed to be compostable. The determination of the composition of the biodegradable carrier bags is significant to fulfill the compostability requirements established in the standard specification EN 13432-2000. In fact, according to this standard, "each significant organic constituent of the packaging material must be biodegradable." "Significant" means any constituent present in more than 1% of dry weight of that material. This implies that the maximum allowed concentration of PE that can be found in a compostable carrier bag is 1%. In two commercial carrier bags, the Py-GC/MS at 500°C provided pyrograms that were a fingerprint for PE with triplets corresponding to linear chains of α,ω-dienes, α-alkenes, and n-alkanes. Then, by TGA analysis a component with a degradation temperature of about 455°C, corresponding to that of PE, was detected. The relative weight loss % of the two carrier bags were estimated at 7.6% and 14%. The results showed that the combination of TGA and Py-GC/MS can be applied with relevant practical and legal implications (Rizzarelli et al., 2016).

Biomass resources are increasingly employed for manufacturing plastic products in the view of reducing the depletion of the fossil ones. Indeed, wholly or partly biobased, fossil-based, and/or natural polymers and additives constitute the current plastic items in the market. Laboratory procedures and standard methods for the measurement of the biobased carbon content in monomers, polymers, and plastic items and products, based on ratio of carbon isotopes, ^{12}C, ^{13}C, and ^{14}C have been developed. Nowadays, the knowledge of the biobased content in plastic items is essential to assess their environmental impact and meet legislative requirements. Investigations on biomass carbon ratios of several materials have been carried out by AMS (Flores et al., 2009; Funabashi et al., 2010; Tachibana et al., 2009).

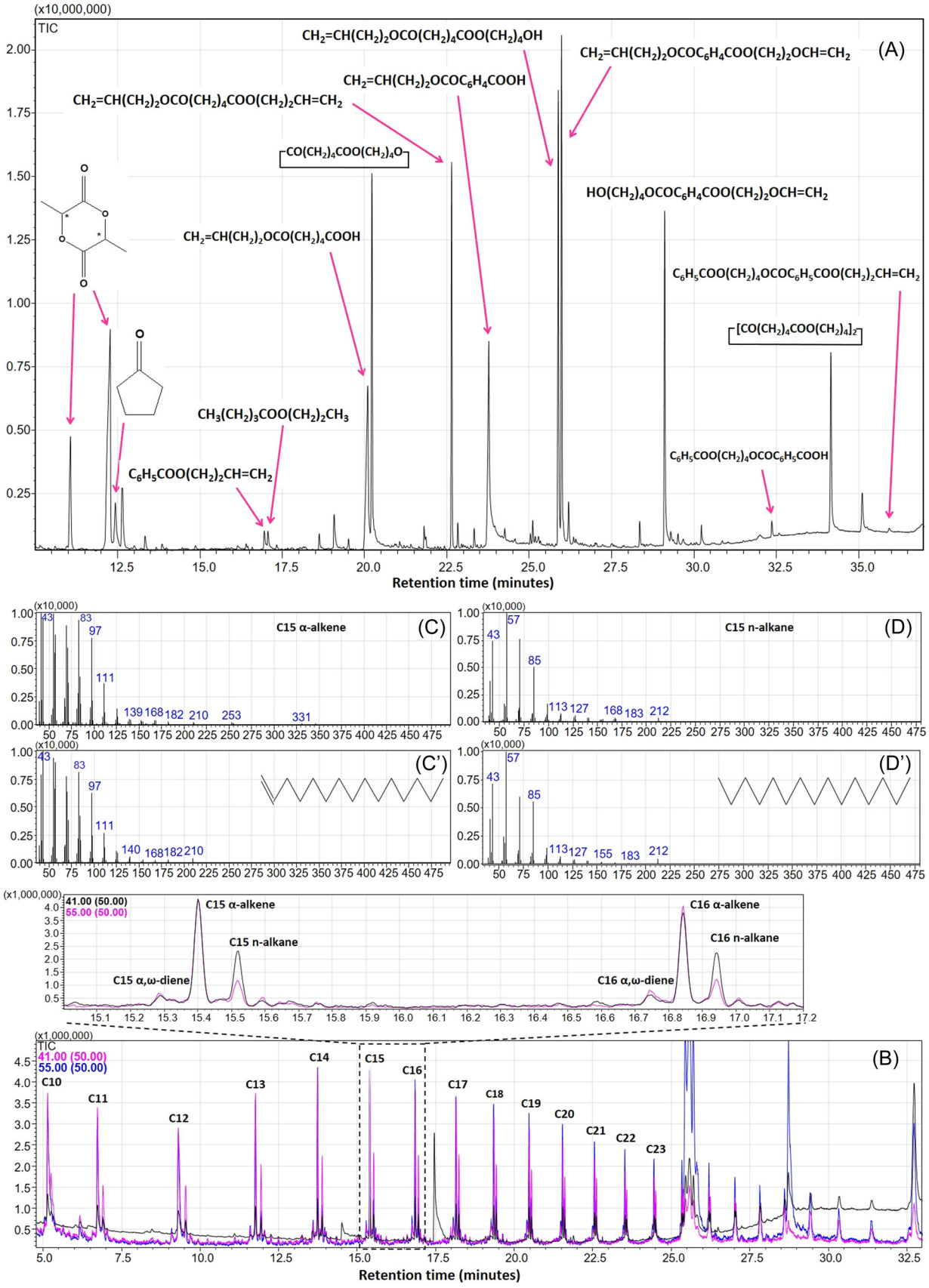

FIGURE 13 (A) Total ion current (TIC) trace of pyrolysis products of BPE10 at 400°C. (B) TIC and single ion current (SIC) traces at *m/z* 41 and 55 of the degradation products of BPE10 at 500°C. (C, D) Experimental mass spectra and (C′ and D′) from the library of degradation products of BPE10 at 500°C (RT 15.4 and 15.5 min). Adapted and reprinted with permission from Rizzarelli et al. (2016), copyright 2016 (Elsevier). [Color figure can be viewed at wileyonlinelibrary.com]

Funabashi et al. analyzed the biomass carbon ratio of PLA or PBSu and their composites with inorganic and biobased $CaCO_3$. Determination of biomass carbon ratio was based on the ratio of ^{14}C to ^{12}C in the samples using AMS. Furthermore, the consequence of pretreatment (oxidation temperature and reaction by acid) on the biomass-carbon ratio was investigated. Biomass carbon ratios (BCR) of PLA and biobased $CaCO_3$ were nearly 100%, while those of PBSu and nonbiobased $CaCO_3$ were more or less 0%. BCR of PLA/inorganic $CaCO_3$ and PBSu/biobased $CaCO_3$ composites, after pretreatment (oxidation reaction at 980°C), were in agreement with the expected values. Studying the effects of pretreatment for biomass carbon ratio measurements by AMS, the Authors highlighted that $CaCO_3$ in composite samples can be separated from polymers by pretreatment of reaction by phosphoric acid (H_3PO_4) (Funabashi et al., 2010). In a similar way, the same research group evaluated by AMS the biomass carbon ratios of polymer composites based on fossil-based PBSu as matrix and corn starch (CS) or cellulose filler (CF) with a small amount of furfural (FR) from biomass. They found that PBSu with 40 wt% of CS or CF had a BCR of 31% and 36%, respectively. The AMS data were compared with the carbon composition obtained using NMR analysis that confirmed almost the BCR measured by AMS (Flores et al., 2009). More recently, Berto et al. explored the suitability characterization of carbon stable isotopes ($\delta^{13}C$) of traditional and biodegradable plastic items (carrier bags and bottles for drinking water) by elemental analyser/IRMS. The $\delta^{13}C$ values determined in different food packaging reflect the biobased origin of biodegrdable materials. On the contrary, the recycled samples showed a $\delta^{13}C$ signature between plant- and fossil-derived polymers. Additionally, preliminary abiotic and biotic degradation processes in plastic materials, recovered on beaches and in seawater, showed less negative $\delta^{13}C$ values (Berto et al., 2017).

4.2 | Drug release and pharmacokinetic studies

Some biodegradable materials, named "bioresorbable polymers," can be easily absorbed by the body via hydrolytic or enzymatic processes. Among the marketed bioresorbable polymers, PLA, PLLA, poly(D-lactide), poly(DL-lactide), poly(glycolide) (PGA), PLGA, PCL, PEG and their derivatives have been, and still are, widely studied with the support of MS (Rizzarelli et al., 2020) and MS/MS (Rizzarelli & Rapisarda, 2023). Their chemical–physical properties and adjustable degradation rates have made them fitting for several applications, that is, as orthopedic, drug delivery, and cardiology. Several research have been focused on drug release and pharmacokinetic, with attention on the connected degradation rate, by MS coupled with LC and supported frequently by MS/MS (Ahmad et al., 2019; Alam et al., 2014; Alshetaili et al., 2019; Benhabbour et al., 2019; Chen, Pederson, et al., 2010; Dahmana et al., 2020; Fernández et al., 2022; Graves et al., 2015; Han et al., 2020; Ibrahim et al., 2022; Kang et al., 2021; Makarov et al., 2014; Mita et al., 2009; Moeller et al., 2012; Ren et al., 2022; Sanders et al., 2012; Shi et al., 2019; Tappa et al., 2017; Wu et al., 2019; Zhao et al., 2019). Several investigations by LC/MS and MS/MS have been focused on biodegradable DDS (i.e., microspheres, microcapsules, micelles or nanoparticles, implants), particularly to determine drug loading or concentrations (Ahmad et al., 2019; Alshetaili et al., 2019; Benhabbour et al., 2019; Ibrahim et al., 2022; Kang et al., 2021; Phan et al., 2018; Shi et al., 2019; Tang & Singh, 2010; Wu et al., 2019) and track drugs or hormone release and fate, both in vitro and in vivo (Alam et al., 2014; Chen, Pederson, et al., 2010; Dahmana et al., 2020; Han et al., 2020; Ren et al., 2022). Recently, for the high sensitivity, accuracy, and precision, analytical strategies based on UHPLC coupled with MS/MS have been developed, with appealing interest for pharmacokinetic study. The analytical approaches allowed monitoring DDS fate and pharmacokinetic features after administration (Ahmad et al., 2019; Alshetaili et al., 2019; Han et al., 2020; Shi et al., 2019; Tang & Singh, 2010; Wu et al., 2019) and were able to check the fate of pharmaceutical polymeric excipients (Shi et al., 2019). Several studies on PLGA and PEG copolymers and conjugates by LC-MS have been reported in the literature (Ahmad et al., 2019; Alam et al., 2014; Alshetaili et al., 2019; Benhabbour et al., 2019; Chen, Pederson, et al., 2010; Graves et al., 2015; Han et al., 2020; Kang et al., 2021; Ren et al., 2022; Sanders et al., 2012;Shi et al., 2019; Wu et al., 2019; Zhao et al., 2019). Controlled drug release microspheres based on three different biodegradable polymers (PLGA 7525 A, PLA, PLGA 5050 A) loaded with finasteride, used against alopecia, were estimated for subcutaneous long-acting injectable formulations (LAIF). Morphology, surface structure, and particle size were evaluated by scanning electron microscopy and laser-light particle size analysis. Drug loading was determined by HPLC, while plasma finasteride concentrations were monitored by LC-MS/MS. Mass spectra were recorded on ESI and positive ion mode, using MRM. PLGA 7525 A provided a suitable drug concentration level for 1 month without burst release and was selected for the finasteride LAIF because the termination of finasteride release met the target period

of 1 month (Kang et al., 2021). Two different PLGA polymers, one acid and one ester terminated, and one PLGA/PEG diblock copolymer were investigated as potential biodegradable polymeric nanoparticles of fenretinide (anticancer drug) with the purpose of enhancing its apparent low water solubility and intestinal absorptivity. UPLC/MS and UV detection were used for the quantitative determination of fenretinide. Interestingly, an influence of terminal groups of PLGA NPS was observed, with the acid-terminated ones performing the best drug release and the ester ended the best cell permeability. Moreover, the PLGA/PEG NPS showed a better drug release than the ester-terminated PLGA and the poorest cell permeation. However, all three biodegradable formulations accomplished better than the fenretinide alone in both drug release and cell permeation tests (Graves et al., 2015). Recently, a new LC-MS/MS method for the direct quantitation of D-α-Tocopheryl PEG 1000 succinate (TPGS) in biological matrices has been developed. TPGS is a biodegradable amphiphilic polymer derived from the esterification of vitamin E with PEG 1000. It is US Food and Drug Administration-approved and widely used in nanocarrier DDS. The simultaneous quantitation of TPGS and its metabolite, PEG1000, produced by its hydrolysis, was challeng by LC-MS/MS and MRM since both molecules are polydisperse. In fact, this resulted in multiple charges, different adduct patterns, and consequently complex ESI mass spectra (Figure 14) (Ren et al., 2022). However, the several precursor ions were further fragmented by in-source CID at a higher declustering potential to a limited number of TPGS/PEG1000 specific fragment ions tested as surrogate ions of TPGS/PEG1000 to quantify all polymers in the biological sample (Figure 15). MRM transitions (*m/z* 557.4−99.0 and 221.3–89.1) produced by the surrogate ions *m/z* 557.4 and 221.3 showed the best signal-to-noise ratio for quantitation of TPGS and PEG1000, respectively. Optimization of experimental conditions allowed to investigate the pharmacokinetics, tissue distribution, and excretion of TPGS and PEG1000 in rat after oral and intravenous dosing. After oral administration, neither TPGS nor PEG1000 were found in plasma showing that TPGS had very low bioavailability. After intravenous injection of TPGS, PEG1000 and TPGS were detected (Figure 16) (Ren et al., 2022).

Fernández et al. investigated a potentially efficient treatment of prostate cancer through the conjugation of a known and highly active chemotherapeutic drug (Paclitaxel, PTX) to the sidechains of a pH-susceptible biodegradable polyacetal polymer. Polymer conjugate (tert-Ser-PTX) aimed to increase stability in circulation and prevent side effects and was compared with PTX alone. Determination of total drug loading and free drug content in the tert-Ser-PTX, drug release in simple and complex media, stability in serum, and quantification of PTX and impurity (7-epi-PTX) in tissue samples were all carried out by LC-MS/MS analyses. Experimental data showed a sustained release of PTX provided by tert-Ser-PTX conjugate over 2 weeks in a pH-responsive manner and suggested the application of DDS as a sound treatment for prostate cancer (Fernández et al., 2022).

Recently, also ICP-MS has been more and more employed to evaluate the loading efficiency and pharmacokinetic in biodegradable DDS, especially nanoparticles, encapsulating specific drugs containing metals (Chen et al., 2021; Ibarra et al., 2018; Pathak & Dhar, 2015; Shi et al., 2015; Wang et al., 2012; Wu et al., 2021; Xiao et al., 2011, 2012; Zhang et al., 2014). Preliminary digestion treatments are usually needed to determine drug loading in the biodegradable polymeric systems. On the contrary, drug release is monitored in buffer solution, with PBS replaced with CH_3COONH_4 buffer to avoid ion suppression in ICP-MS analysis. Interestingly, Xiao et al. monitored the drug release by HPLC coupled with ICP-MS

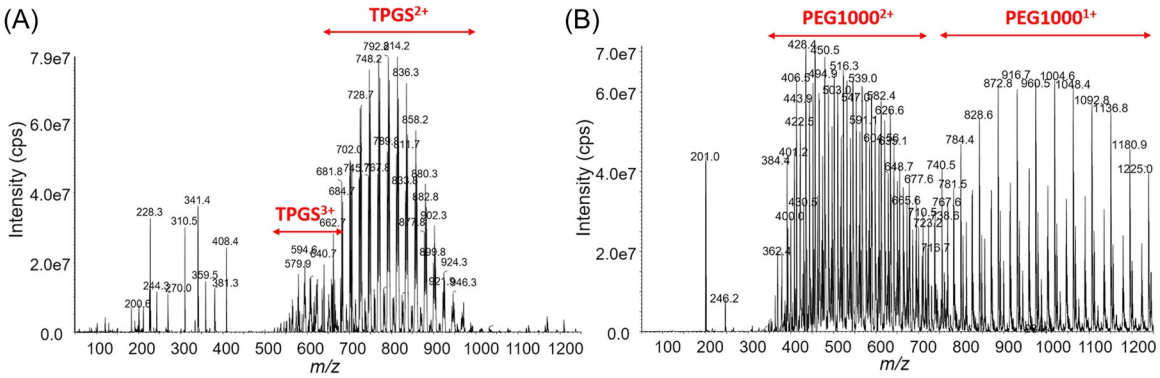

FIGURE 14 Q1 full scan of (A) TPGS and (B) PEG1000 at DP 50 V. Reprinted with permission from Ren et al. (2022), copyright 2022 (Elsevier). [Color figure can be viewed at wileyonlinelibrary.com]

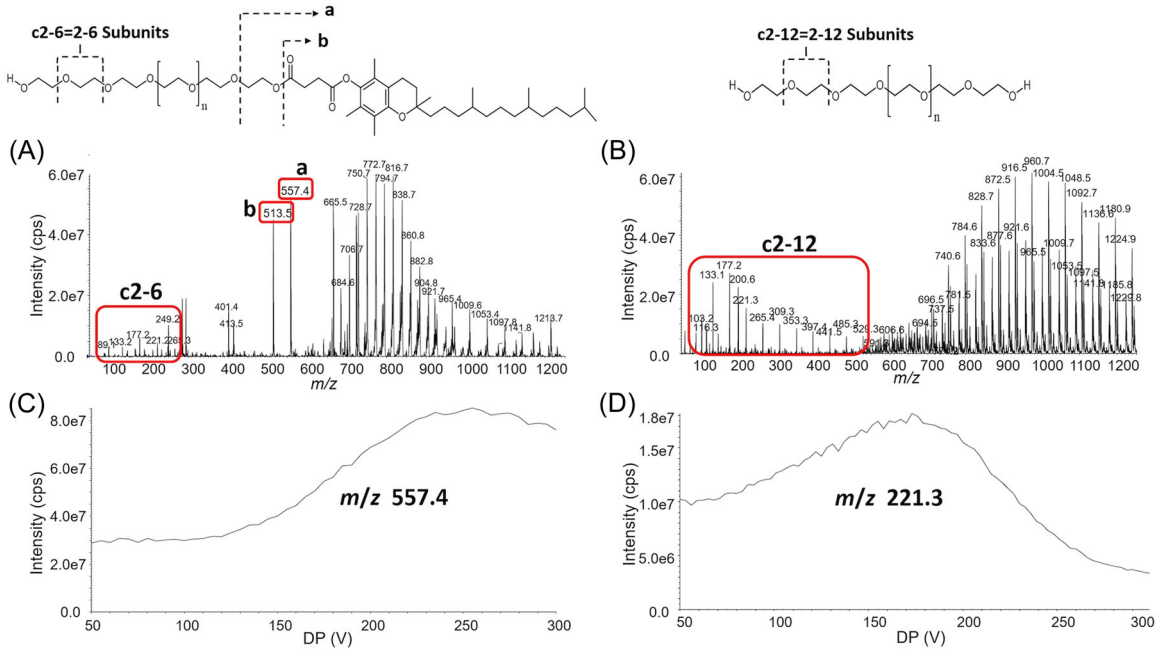

FIGURE 15 Q1 full scan of (A) TPGS and (B) PEG1000 at DP 200 V, tocopheryl PEG 1000 succinate fragment ions and PEG1000 fragment ions (red circle) produced by DP 200 V; Optimizing DP of (C) TPGS-specific fragment ion (*m/z* 557.4) and (D) PEG1000-specific fragment ion (*m/z* 221.3). Reprinted with permission from Ren et al. (2022), copyright 2022 (Elsevier). [Color figure can be viewed at wileyonlinelibrary.com]

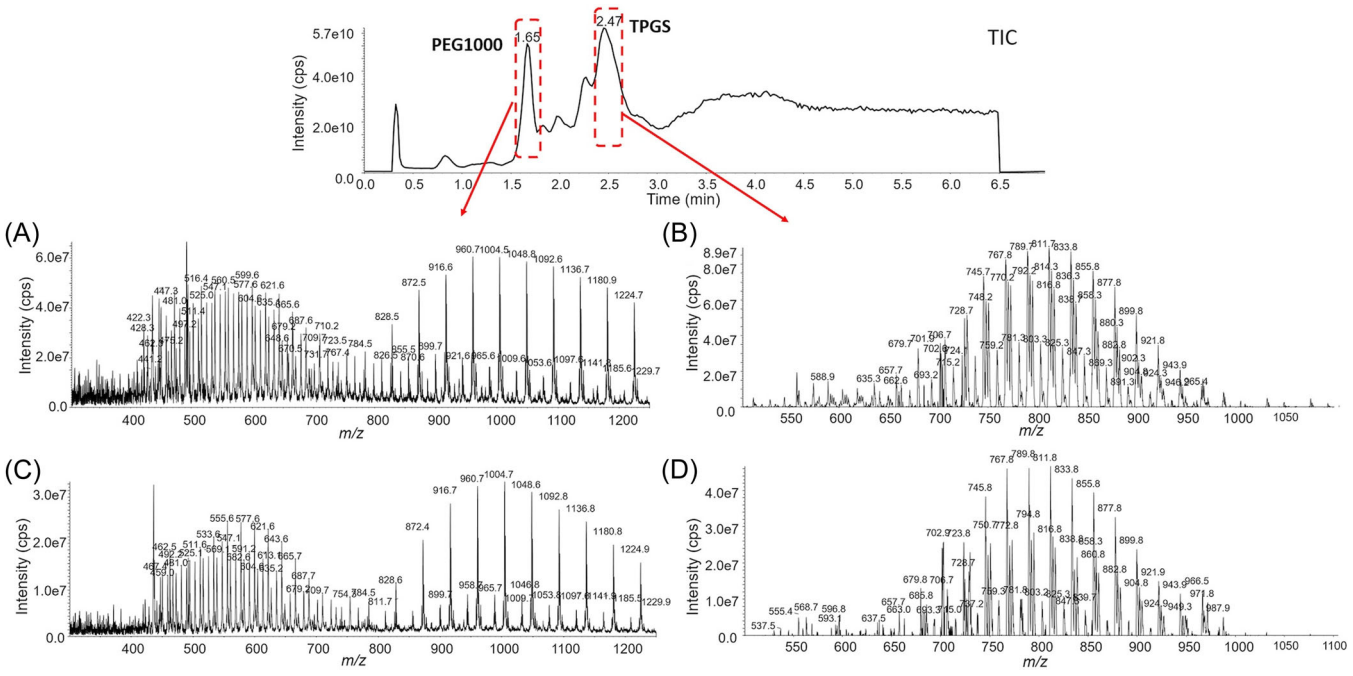

FIGURE 16 Mass spectra of chromatographic peaks corresponding to PEG1000 and tocopheryl PEG 1000 succinate (TPGS) in (A, B) reference standards and (C, D) a plasma sample collected from a rat 1 h after intravenous injection of TPGS. Reprinted with permission from Ren et al. (2022), copyright 2022 (Elsevier). [Color figure can be viewed at wileyonlinelibrary.com]

analysis of Pt species released in simulated medium from biodegradable micelles of methoxy poly(ethylene glycol)-block-poly(L-lactide-co-2-methyl-2-carboxyl-propylene carbonate/Pt) bearing pendant COOH groups (Xiao et al., 2012) and a Pt(IV) complex covalently conjugated to the amphiphilic tri-block copolymer, methoxy poly(ethylene glycol)-*block*-poly(caprolactone)-*block*-poly(L-lysine), containing pendant amino groups (Xiao et al., 2011). The outlet of

the LC column was directly connected to the sample introduction system of ICP-MS and model compounds were used to assign the detected chromatographic peaks. The results allowed to conclude that the Pt-carboxylate and amide coordination bonds were more susceptible to hydrolysis than the polymeric backbones and to depict the hydrolysis and release pathways of the biodegradable platinum DDS (Xiao et al., 2011, 2012). Recently, ICP-MS has been used to assess the loading efficiency in PLGA NPs encapsulating self-synthesized thiol B cage (BC-EG-SH), gadolinium (Gd) atoms, and 20 nm citrate-coated gold nanoparticles (AuNPs) (PLGA-Gd/B-AuNPs), investigating the in vivo pharmacokinetics and micro-distribution in tumor. The Authors aimed to develop a novel magnetic resonance imaging (MRI)-detectable boron (B)-containing nanoassemblies and evaluate their potential for boron neutron capture therapy (BNCT). BNCT is a cellular-level selective radiation therapy and is considered an attractive treatment strategy against cancers. B and Gd concentrations in PLGA NPs as well as in cells, tumor, and muscle were determined by ICP-MS. The results showed that BC-EG-SH was the most optimal B compound for encapsulation among three different molecules as its encapsulation efficiency could be enhanced by the addition of AuNPs, reaching approximately 30%. Moreover, the diagnostic ability of Gd was not affected by the PLGA-loaded AuNPs, paving the way for future studies regarding the noninvasive imaging of the distribution of NPs in patients (Wu et al., 2021).

A limited number of studies on biodegradable DDS have been carried out by GC-MS/MS (Brochhausen et al., 2009), MALDI and MALDI-MSI (Tang & Singh, 2010; Wei, Yu, et al., 2021) and TOF-SIMS (Burns & Gardella, 2008). In particular, GC-MS/MS was used in drug release to determine the residual prostaglandin E2 content in biodegradable PLGA microspheres (Brochhausen et al., 2009). MALDI

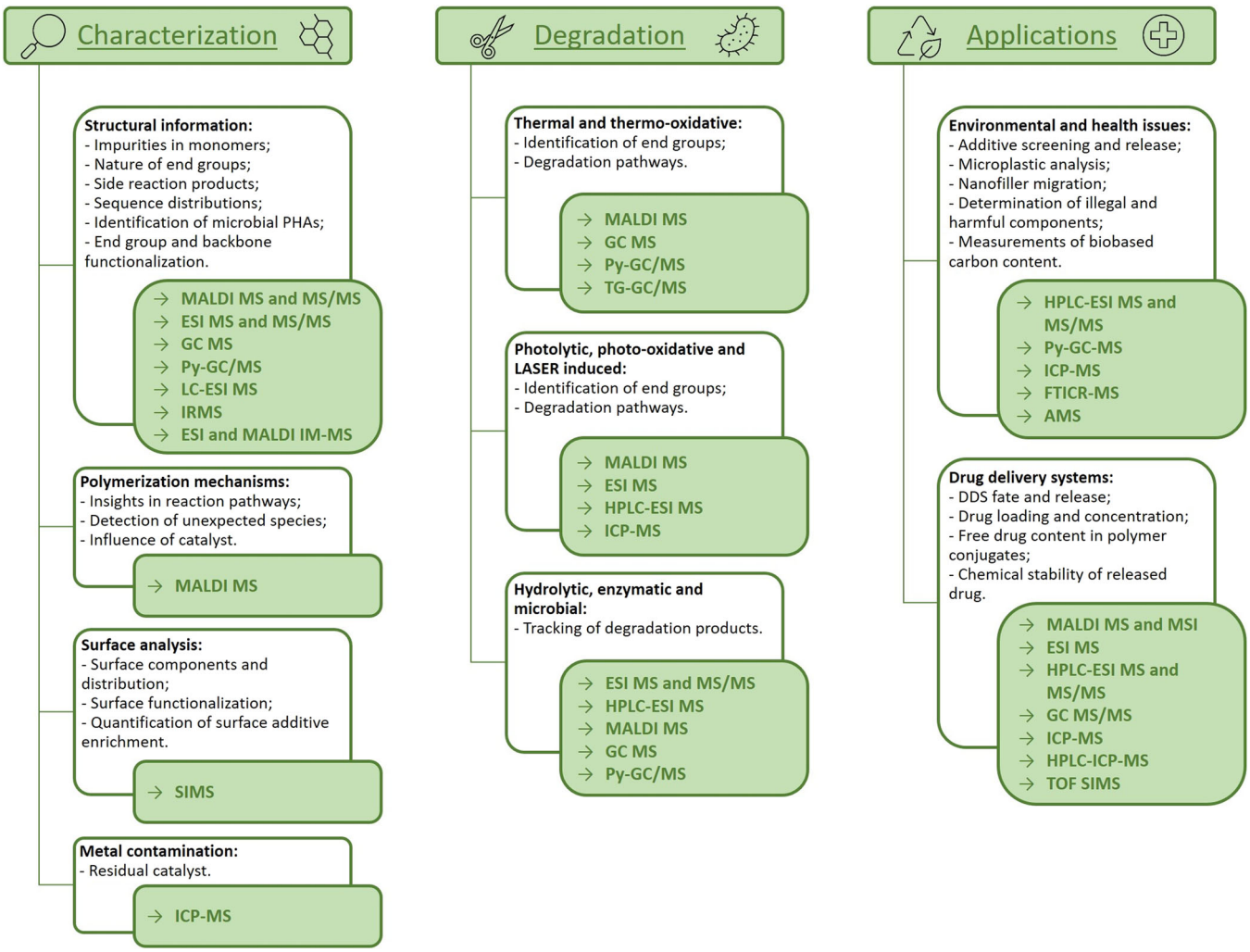

FIGURE 17 Overview on the information provided by mass spectrometry in the characterization, degradation, and applications of synthetic and microbial biodegradable polymers. [Color figure can be viewed at wileyonlinelibrary.com]

was employed in the investigation on mPEG-PLGAmPEG-based delivery system for long-term controlled release of salmon calcitonin (sCT) after single subcutaneous injection. sCT is the most frequently used calcitonin, exploited for many years in the treatment of metabolic bone diseases, such as osteoporosis. The chemical stability of released sCT was evaluated by MALDI-TOF and compared to sCT control, incubated in PBS at 37°C. At high incubation time, ions related to a degradation product were detected. However, the peak due to the sCT appeared as the major in the spectra, pointing out that most of the sCT retained the chemical integrity (Tang & Singh, 2010).

5 | CONCLUSIONS

In the last 15 years, several MS techniques have been successfully applied in the structural characterization, in the degradation tracking and to get insights on the applications of biodegradable polymeric systems. MS analysis requires the conversion of the analyte molecules to gas-phase ions, and their subsequent separation and detection according to their mass-to-charge ratio. Accordingly, the sample must be capable of forming stable gas-phase ions, which precludes the analysis of saturated and very large or cross-linked polymers. Additionally, mixtures and polymeric blends may not be characterized properly because of potential differences in ionization and detection efficiencies of the different constituents. Despite that, valuable information ranging from the synthesis to the end-of-life options have been acquired on biodegradable polymeric systems, both microbial and synthetic. Soft ionization methods, such as MALDI and ESI-MS, by themselves, supported or hyphenated with other techniques, as well as GC/MS and Py-GC/MS, provided evidence on impurity in monomers, repetitive units and end group structures, polymerization mechanism, successful synthesis and side reaction products, identification of microbial PHAs, surface functionalization and behavior, residual catalyst, degradation products and pathways, environmental and health issues as well as on DDS (Figure 17). Surface analysis of biodegradable polymers by SIMS supported information about the chemical structure of the surface components and distribution, surface functionalization, and contamination, which can prejudice the surface properties in many processes. ICP-MS was thoroughly applied in checking metal contamination due to residual catalyst, to monitor drug delivery or establish drug loading and nanofiller migration. In cases where the characterization of the polymer architecture was complex, such as for isomeric structures, multidimensional MS techniques was successfully employed providing unequivocal identification. Moreover, MS techniques have also been helpful in investigating the degradation rate and drug release profile of bioresorbable DDS. Different kind of MS investigations concern environmental and health features related to applications of biodegradable in different fields. Analysis on additives, microplastics, nanofiller migration, illegal usage of polyethylene in compostable carrier bags, and determination of biobased carbon content represent relevant example of the helpful application implications in which MS methods and analytical strategies have been decisive. Nevertheless, in most cases, more techniques are combined to determine details in complex biodegradable polymeric systems, to overcome drawbacks, discriminate isobaric species, and to get significant information on specific applications.

Though there are several papers on the utilization of MS in the field of biodegradable polymers, synthetic and microbial, it is expected that advances in analytical techniques will act as an engine and have a greater attention in the future as they might provide answers and more understanding on the fate of biodegradable items also in real conditions, solving controversies and supporting legislative choices to safeguard the environment. In the meantime, we wish that this review would be valuable in supporting the choice of the appropriate MS technique in future studies or generating new application ideas, helpful in the development of biodegradable materials.

AUTHOR CONTRIBUTIONS

Paola Rizzarelli: Conceptualization; data curation; funding acquisition; project administration; resources; supervision; writing—original draft; writing—review and editing. **Melania Leanza**: Investigation; writing—original draft; writing—review and editing. **Marco Rapisarda**: Investigation; writing—original draft; writing—review and editing.

ACKNOWLEDGMENTS

This research was partially funded by PO FESR 2014–2020. Action 1.1.5, project "New therapeutic strategies in ophthalmology: bacterial, viral and microbial infections—NUSTEO", CUP: G68I18000700007—application code 08CT2120090065.

ORCID

Paola Rizzarelli http://orcid.org/0000-0002-6727-4335

REFERENCES

Adamus G. 2009. Molecular level structure of (R,S)-3-hydroxybutyrate/(R,S)-3-hydroxy-$_4$–ethoxybutyrate copolyesters with dissimilar architecture. *Macromolecules 42*, 4547–4557.

Ahmad N, Ahmad R, Alam MA, Ahmad FJ, Amir M, Pottoo FH, Sarafroz M, Jafar M, Umar K. 2019. Daunorubicin oral bioavailability enhancement by surface-coated natural biodegradable macromolecule chitosan-based polymeric nanoparticles. *International Journal of Biological Macromolecules 128*, 825–8838.

Alalwiat A, Tang W, Gerişlioğlu S, Becker ML, Wesdemiotis C. 2017. Mass spectrometry and ion mobility characterization of bioactive peptide-synthetic polymer conjugates. *Analytical Chemistry*. *89*, 1170–1177.

Alam N, Khare V, Dubey R, Saneja A, Kushwaha M, Singh G, Sharma N, Chandan B, Gupta PN. 2014. Biodegradable polymeric system for cisplatin delivery: Development, in vitro characterization and investigation of toxicity profile. *Materials Science and Engineering C 38*(1), 85–93.

Ali I, Jamil N. 2014. Enhanced biosynthesis of poly(3-hydroxybutyrate) from potato starch by bacillus cereus strain 64-ins in a laboratory-scale fermenter. *Preparative Biochemistry and Biotechnology 44*(8), 822–833.

Allen AD, Anderson WA, Ayorinde FO, Eribo BE. 2010. Biosynthesis and characterization of copolymer poly(3HB-co-3HV) from saponified Jatropha curcas oil by Pseudomonas oleovorans. *Journal of Industrial Microbiology and Biotechnology 37*(8), 849–856.

Alsafadi D, Ibrahim MI, Alamry KA, Hussein MA, Mansour A. 2020. Utilizing the crop waste of date palm fruit to biosynthesize polyhydroxyalkanoate bioplastics with favorable properties. *Science of the Total Environment 737*, 139716.

Alshetaili AS, Ansari MJ, Anwer MK, Ganaie MA, Iqbal M, Alshahrani SM, Alalaiwe AS, Alsulays BB, Alshehri S, Sultan AS. 2019. Enhanced oral bioavailability of ibrutinib encapsulated poly (lactic-co-glycolic acid) nanoparticles: Pharmacokinetic evaluation in rats. *Current Pharmaceutical Analysis 15*(6), 661–668.

Aminlashgari N, Pal J, Sanwari S, Nandan B, Srivastava RK, Hakkarainen M. 2015. Degradation product profiles of melt-spun in situ cross-linked poly(ε-caprolactone) fibers. *Materials Chemistry and Physics*. *156*, 82–88.

Aparaschivei D, Todea A, Păuşescu I, Badea V, Medeleanu M, Şişu E, Puiu M, Chiriţă-Emandi A, Peter F. 2016. Synthesis, characterization, and enzymatic degradation of copolymers of ε-caprolactone and hydroxy-fatty acids. *Pure and Applied Chemistry 88*(12), 1191–1201.

Arrieta MP, López J, Rayón E, Jiménez A. 2014. Disintegrability under composting conditions of plasticized PLA–PHB blends. *Polymer Degradation and Stability 108*, 307–318.

Arrieta MP, Parres F, Lopez J, Jimenez A. 2013. Development of a novel pyrolysis-gas chromatography/mass spectrometry method for the analysis of poly(lactic acid) thermal degradation products. *The Journal of Analytical and Applied Pyrolysis 101*, 150–155.

Arshad A, Ashraf B, Ali I, Jamil N. 2017. Biosynthesis of polyhydroxyalkanoates from styrene by Enterobacter spp. isolated from polluted environment. *Frontiers in Biology 12*(3), 210–218.

Ashby RD, Solaiman DKY, Nuñez A, Strahan GD, Johnston DB. 2017. Burkholderia sacchari DSM 17165: A source of compositionally-tunable block-copolymeric short-chain poly (hydroxyalkanoates) from xylose and levulinic acid. *Bioresource Technology 253*, 333–342.

Astolfi ML, Marconi E, Lorini L, Valentino F, Silva F, Ferreira BS, Canepari S, Majone M. 2020. Elemental concentration and migratability in bioplastics derived from organic waste. *Chemosphere*, *259*, 127472.

Bakkali-Hassani C, Hooker JP, Voorter P-J, Rubens M, Cameron NR, Junkers T. 2022. One-pot multifunctional polyesters by continuous flow organocatalysed ring-opening polymerisation for targeted and tunable materials design. *Polymer Chemistry 13*(10), 1387–1393.

Bansal KK, Özliseli E, Saraogi GK, Rosenholm JM. 2020. Assessment of intracellular delivery potential of novel sustainable poly(δ-decalactone)-based micelles. *Pharmaceutics 12*(8), 726.

Barrère C, Selmi W, Hubert-Roux M, Coupin T, Assumani B, Afonso C, Giusti P. 2014. Rapid analysis of polyester and polyethylene blends by ion mobility-mass spectrometry. *Polymer Chemistry 5*(11), 3576–3582.

Beale DJ, Shah RM, Marcora A, Hulthen A, Karpe AV, Pham K, Wijffels G, Paull C. 2022. Is there any biological insight (or respite) for insects exposed to plastics? Measuring the impact on an insects central carbon metabolism when exposed to a plastic feed substrate. *Science of the Total Environment 831*, 154840.

Bege N, Steinmüller SO, Kalinowski M, Reul R, Klaus S, Petersen H, Curdy C, Janek J, Kissel T. 2012. Drug-eluting stents based on Poly(ethylene carbonate): Optimization of the stent coating process. *European Journal of Pharmaceutics and Biopharmaceutics 80*(3), 562–570.

Benhabbour SR, Kovarova M, Jones C, Copeland DJ, Shrivastava R, Swanson MD, Sykes C, Ho PT, Cottrell ML, Sridharan A, Fix SM, Thayer O, Long JM, Hazuda DJ, Dayton PA, Mumper RJ, Kashuba ADM, Victor Garcia J. 2019. Ultra-long-acting tunable biodegradable and removable controlled-release implants for drug delivery. *Nature Communications 10*(1), 4324.

Bernhard M, Eubeler JP, Zok S, Knepper TP. 2008. Aerobic biodegradation of polyethylene glycols of different molecular weights in wastewater and seawater. *Water Research 42*(19), 4791–4801.

Berthod A, Crank JA, Rundlett KL, Armstrong DW. 2009. A second-generation ionic liquid matrix-assisted laser desorption/ionization matrix for effective mass spectrometric analysis of biodegradable polymers. *Rapid Communications in Mass Spectrometry 23*(21), 3409–3422.

Berto D, Rampazzo F, Gion C, Noventa S, Ronchi F, Traldi U, Giorgi G, Cicero AM, Giovanardi O. 2017. Preliminary study to characterize plastic polymers using elemental analyser/isotope ratio mass spectrometry (EA/IRMS). *Chemosphere 176*, 47–56.

Bhati R, Samantaray S, Sharma L, Mallick N. 2010. Poly-β-hydroxybutyrate accumulation in cyanobacteria under photo-autotrophy. *Biotechnology Journal 5*(11), 1181–1185.

Biernacki M, Marzec M, Roick T, Pätz R, Baronian K, Bode R, Kunze G. 2017. Enhancement of poly(3-hydroxybutyrate-co-3-hydroxyvalerate) accumulation in Arxula adeninivorans by stabilization of production. *Microbial Cell Factories 16*(1), 144.

Biswas E, Banerjee KK, Karmakar S, Karmakar S, Pal TK. 2022. Preparation and evaluation of eprosartan mesylate-loaded PLGA nanostructures. *Research Journal of Pharmacy and Technology 15*(1), 103–112.

Blaj D-A, Balan-Porcarasu M, Petre BA, Harabagiu V, Peptu C. 2021. MALDI mass spectrometry monitoring of cyclodextrin-oligolactide derivatives synthesis. *Polymer 233*, 124186.

Blanquer S, Tailhades J, Darcos V, Amblard M, Martinez J, Nottelet B, Coudane J. 2010. Easy synthesis and ring-opening polymerization of 5-Z-amino-δ- valerolactone: New degradable amino-functionalized (Co)polyesters. *Journal of Polymer Science, Part A: Polymer Chemistry 48*(24), 5891–5898.

Borrowman CK, Bücking M, Göckener B, Adhikari R, Saito K, Patti AF. 2020. LC-MS analysis of the degradation products of a sprayable, biodegradable poly(ester-urethane-urea). *Polymer Degradation and Stability 178*, 109218. https://doi.org/10.1016/j.polymdegradstab.2020.109218

Brochhausen C, Zehbe R, Watzer B, Halstenberg S, Gabler F, Schubert H, Kirkpatrick CJ. 2009. Immobilization and controlled release of prostaglandin E2 from poly-L-lactide-co-glycolide microspheres. *Journal of Biomedical Materials Research - Part A 91*(2), 454–462.

Burns SA, Gardella Jr. JA. 2008. Quantitative ToF-SIMS studies of protein drug release from biodegradable polymer drug delivery membranes. *Applied Surface Science 255*(4), 1170–1173.

Carstens MG, Van Nostrum CF, Verrijk R, De Leede LGJ, Crommelin DJA, Hennink WE. 2008. A mechanistic study on the chemical and enzymatic degradation of PEG-Oligo(ε-caprolactone) micelles. *Journal of Pharmaceutical Sciences 97*(1), 506–518.

Casettari L, Castagnino E, Stolnik S, Lewis A, Howdle SM, Illum L. 2011. Surface characterisation of bioadhesive PLGA/chitosan microparticles produced by supercritical fluid technology. *Pharmaceutical Research 28*(7), 1668–1682.

Charles L, Chendo C, Poyer S. 2020. Ion mobility spectrometry–mass spectrometry coupling for synthetic polymers. *Rapid Communications in Mass Spectrometry 34*(S2), e8624.

Chen M, Dong M, Havelund R, Regina VR, Meyer RL, Besenbacher F, Kingshott P. 2010. Thermo-responsive core-sheath electrospun nanofibers from poly (N−isopropylacrylamide)/polycaprolactone blends. *Chemistry of Materials 22*(14), 4214–4221.

Chen H, Liu Z, Wei B, Huang J, You X, Zhang J, Yuan Z, Tang Z, Guo Z, Wu J. 2021. Redox responsive nanoparticle encapsulating black phosphorus quantum dots for cancer theranostics. *Bioactive Materials 6*(3), 655–665.

Chen S, Pederson D, Oak M, Singh J. 2010. In vivo absorption of steroidal hormones from smart polymer-based delivery systems. *Journal of Pharmaceutical Sciences 99*(8), 3381–3388.

Chen S-C, Zhang F-H, Huang K-L, Tian F, Zhang Z-H, Zhou R, Feng X-J, Zhou X, He M-Y, Gu J, Chen Q, Wu C-D. 2020. The crucial roles of guest water in a biocompatible coordination network in the catalytic ring-opening polymerization of cyclic esters: A new mechanistic perspective. *Chemical Science 11*(12), 3345–3354.

Chendo C, Phan TNT, Rollet M, Gigmes D, Charles L. 2018. Adduction of ammonium to polylactides to modify their dissociation behavior in collision-induced dissociation. *Rapid Communications in Mass Spectrometry 32*(5), 423–430.

Cheng J, Eyheraguibel B, Jacquin J, Pujo-Pay M, Conan P, Barbe V, Hoypierres J, Deligey G, Halle AT, Bruzaud S, Ghiglione J-F, Meistertzheim A-L. 2022. Biodegradability under marine conditions of bio-based and petroleum-based polymers as substitutes of conventional microparticles. *Polymer Degradation and Stability 206*, 110159.

Chien YC, Yang SH. 2013. Investigation of the combustion kinetics and polycyclic aromatic hydrocarbon emissions from polycaprolactone combustion. *Environmental Technology (United Kingdom) 34*(2), 149–155.

Chrissafis K, Paraskevopoulos KM, Bikiaris D. 2010. Thermal degradation kinetics and decomposition mechanism of two new aliphatic biodegradable polyesters poly(propylene glutarate) and poly(propylene suberate). *Thermochimica Acta 505*(1–2), 59–68.

Chrissafis K, Paraskevopoulos KM, Papageorgiou GZ, Bikiaris DN. 2011. Thermal decomposition of poly(propylene sebacate) and poly(propylene azelate) biodegradable polyesters: Evaluation of mechanisms using TGA, FTIR and GC/MS. *Journal of Analytical and Applied Pyrolysis 92*(1), 123–130.

Cicogna F, Coiai S, Rizzarelli P, Carroccio S, Gambarotti C, Domenichelli I, Yang C, Dintcheva NTz, Filippone G, Pinzino C, Passaglia E. 2014. Functionalization of aliphatic polyesters by nitroxide radical coupling. *Polymer Chemistry 5*(19), 5656–5667.

Crecelius AC, Baumgaertel A, Schubert U.S. 2009. Tandem mass spectrometry of synthetic polymers. *Journal of Mass Spectrometry 44*, 1277–1286.

Crotty S, Gerişlioğlu S, Endres KJ, Wesdemiotis C, Schubert US. 2016. Polymer architectures via mass spectrometry and hyphenated techniques: A review. *Analytica Chimica Acta 932*, 1–21.

Dahmana N, Kowalczuk L, Gabriel D, Behar-Cohen F, Gurny R, Kalia YN. 2020. Ocular biodistribution of spironolactone after a single intravitreal injection of a biodegradable sustained-release polymer in rats. *Molecular Pharmaceutics 17*(1), 59–69.

De Hoe GX, Zumstein MT, Getzinger GJ, Rüegsegger I, Kohler H-PE, Maurer-Jones MA, Sander M, Hillmyer MA, McNeill K. 2019. Photochemical transformation of poly(butylene adipate-co-terephthalate) and its effects on enzymatic hydrolyzability. *Environmental Science and Technology 53*(5), 2472–2481.

Den Berghe HV, Garric X, Vert M, Coudane J. 2011. New amoxicillin-poly(lactic acid)-based conjugates: Synthesis and in vitro release of amoxicillin. *Polymer International 60*(3), 398–404.

Dintcheva NT, Arrigo R, Baiamonte M, Rizzarelli P, Curcuruto G. 2017. Concentration-dependent anti-/pro-oxidant activity of natural phenolic compounds in bio-polyesters. *Polymer Degradation and Stability 142*, 21–28.

Dopico-García S, Ares-Pernas A, Otero-Canabal J, Castro-López M, López-Vilariño JM, González-Rodríguez V, Abad-López MJ. 2013. Insight into industrial PLA aging process by complementary use of rheology, HPLC, and MALDI. *Polymers for Advanced Technologies 24*(8), 723–731.

Doumbia AS, Vezin H, Ferreira M, Campagne C, Devaux E. 2015. Studies of polylactide/zinc oxide nanocomposites: Influence of surface treatment on zinc oxide antibacterial activities in

textile nanocomposites. *Journal of Applied Polymer Science 132*(17), 41776.

Dria RD, Goudy BA, Moga KA, Corbin PS. 2012. Synthesis and characterization of multi-armed calixarene- and resorcinarene-core polylactide star polymers. *Polymer Chemistry 3*(8), 2070–2081.

Du L, Yang X, Li W, Li H, Feng S, Zeng R, Yu B, Xiao L, Liu Y, Tu M, Nie H-Y. 2018. Time-of-flight secondary ion mass spectrometry analyses of vancomycin. *Biointerphases 13*(3), 03B401.

Duale K, Latos P, Chrobok A, Domiński A, Maksymiak MM, Adamus G, Kowalczuk M. 2021. Towards advances in molecular understanding of boric acid biocatalyzed ring-opening (Co)polymerization of δ-valerolactone in the presence of ethylene glycol as an initiator. *Molecules 26*(16), 4859.

Duale K, Zięba M, Chaber P, Di Fouque DJ, Memboeuf A, Peptu C, Radecka I, Kowalczuk M, Adamus G. 2018. Molecular level structure of biodegradable poly(delta-valerolactone) obtained in the presence of boric acid. *Molecules 23*(8), 2034.

Ekere I, Johnston B, Tchuenbou-Magaia F, Townrow D, Wojciechowski S, Marek A, Zawadiak J, Duale K, Zięba M, Sikorska W, Adamus G, Goslar T, Kowalczuk M, Radecka I. 2022. Bioconversion process of polyethylene from Waste Tetra Pak® packaging to polyhydroxyalkanoates. *Polymers 14*(14), 2840.

Elain A, Le Fellic M, Corre Y-M, Le Grand A, Le Tilly V, Audic J-L, Bruzaud S. 2015. Rapid and qualitative fluorescence-based method for the assessment of PHA production in marine bacteria during batch culture. *World Journal of Microbiology and Biotechnology 31*(10), 1555–1563.

El-Kadi SM, Elbagory M, El-Zawawy HAH, El-Shaer HFA, Shoukry AA, El-Nahrawy S, Omara AE-D, Ali DFI. 2021. Biosynthesis of poly-ß-hydroxybutyrate (Phb) from different bacterial strains grown on alternative cheap carbon sources. *Polymers 13*(21), 3801.

Ezati N, Abdouss M, Rouhani M, Kerr PG, Kowsari E. 2022. Novel serotonin decorated molecularly imprinted polymer nanoparticles based on biodegradable materials; a potential self-targeted delivery system for Irinotecan. *Reactive and Functional Polymers 181*, 105437.

Feng Q, Tong R. 2017. Controlled photoredox ring-opening polymerization of O-carboxyanhydrides. *Journal of the American Chemical Society 139*(17), 6177–6182.

Fernández Y, Movellan J, Foradada L, Giménez V, García-Aranda N, Mancilla S, Armiñán A, Borgos SE, Hyldbakk A, Bogdanska A, Gobbo OL, Prina-Mello A, Ponti J, Calzolai L, Zagorodko O, Gallon E, Niño-Pariente A, Paul A, Schwartz Jr. S, Abasolo I, Vicent MJ. 2022. In vivo antitumor and antimetastatic efficacy of a polyacetal-based paclitaxel conjugate for prostate cancer yherapy. *Advanced Healthcare Materials 11*(7), 2101544.

Fischer AM, Schüll C, Frey H. 2015. Hyperbranched poly(glycolide) copolymers with glycerol branching points via ring-opening copolymerization. *Polymer 72*, 436–446.

Flores ED, Funabashi M, Kunioka M. 2009. Mechanical properties and biomass carbon ratios of poly(butylene succinate) composites filled with starch and cellulose filler using furfural as plastlcizer. *Journal of Applied Polymer Science*, *112*(6), 3410–3417.

Fojt J, Romanekova I, Prochazkova P, David J, Brtnický M, Kučerik J. 2022. A simple method for quantification of polyhydroxybutyrate and polylactic acid micro-bioplastics in soils by evolved gas analysis. *Molecules 27*, 1898.

Fouquet TNJ, Pizzala H, Rollet M, Crozet D, Giusti P, Charles L. 2020. Mass spectrometry-based analytical strategy for comprehensive molecular characterization of biodegradable poly(lactic-co-glycolic acid) copolymers. *Journal of the American Society for Mass Spectrometry 31*(7), 1554–1562.

Funabashi M, Ninomiya F, Flores ED, Kunioka M. 2010. Biomass carbon ratio of polymer composites measured by accelerator mass spectrometry. *Journal of Polymers and the Environment 18*(2), 85–93.

Ge L, Amy Tan G-Y, Wang L, Chen C-L, Li L, Ngin Tan S, Wang J-Y. 2016. Determination of monomeric composition in polyhydroxyalkanoates by liquid chromatography coupled with on-line mass spectrometry and off-line nuclear magnetic resonance. *Talanta 146*, 107–113.

Gerislioglu S, Adams SR, Wesdemiotis C. 2018. Characterization of singly and multiply PEGylated insulin isomers by reversed-phase ultra-performance liquid chromatography interfaced with ion mobility mass spectrometry. *Analytica Chimica Acta 1004*, 58–66.

Gorrasi G, Meduri A, Rizzarelli P, Carroccio S, Curcuruto G, Pellecchia C, Pappalardo D. 2016. Preparation of poly (glycolide-co-lactide)s through a green process: Analysis of structural, thermal, and barrier properties. *Reactive and Functional Polymers 109*, 70–78.

Graves RA, Ledet GA, Glotser EY, Mitchner DM, Bostanian LA, Mandal TK. 2015. Formulation and evaluation of bio-degradable nanoparticles for the oral delivery of fenretinide. *European Journal of Pharmaceutical Sciences 76*, 1–9.

Gümüştaş S, Balcan M, Kinal A. 2022. Investigation of initiator metal efficiency in the ring-opening polymerization of lactones: An experimental and computational study. *Polymer International 71*(7), 912–920. https://doi.org/10.1002/pi.6361

Gunawan NR, Tessman M, Zhen D, Johnson L, Evans P, Clements SM, Pomeroy RS, Burkart MD, Simkovsky R, Mayfield SP. 2022. Biodegradation of renewable polyurethane foams in marine environments occurs through depolymerization by marine microorganisms. *Science of the Total Environment 850*, 158761.

Hagagy N, Saddiq AA, Tag HM, Selim S, AbdElgawad H, Martínez-Espinosa RM. 2022. Characterization of polyhydroxybutyrate, PHB, synthesized by newly isolated Haloarchaea Halolamina spp. *Molecules 27*(21), 7366.

Hajighasemi M, Nocek BP, Tchigvintsev A, Brown G, Flick R, Xu X, Cui H, Hai T, Joachimiak A, Golyshin PN, Savchenko A, Edwards EA, Yakunin AF. 2016. Biochemical and structural insights into enzymatic depolymerization of polylactic acid and other polyesters by microbial carboxylesterases. *Biomacromolecules 17*(6), 2027–2039.

Hakkarainen M, Adamus G, Hoglund A, Kowalczuk M, Albertsson A-C. 2008. ESI-MS reveals the influence of hydrophilicity and architecture on the water-soluble degradation product patterns of biodegradable homo- and copolyesters of 1,5-dioxepan-2-one and ε-caprolactone. *Macromolecules 41*(10), 3547–3554.

Hamdy SM, Danial AW, Gad El-Rab SMF, Shoreit AAM, Hesham AE-L. 2022. Production and optimization of bioplastic (Polyhydroxybutyrate) from Bacillus cereus strain SH-02 using response surface methodology. *BMC Microbiology 22*(1), 183.

Han FY, Liu Y, Kumar V, Xu W, Yang G, Zhao C-X, Woodruff TM, Whittaker AK, Smith MT. 2020. Sustained-release ketamine-loaded nanoparticles fabricated by sequential nanoprecipitation. *International Journal of Pharmaceutics 581*, 119291.

He M, Cheng Y, Liang Y, Xia M, Leng X, Wang Y, Wei Z, Zhang W, Li Y. 2020. Amino acid complexes with tin as a new class of catalysts with high reactivity and low toxicity towards biocompatible aliphatic polyesters. *Polymer Journal 52*(6), 567–574.

Hsieh YK, Chang C-T, Jen I-H, Pu F-C, Shen S-H, Wan D, Wang J. 2018. Use of gold nanoparticles to investigate the drug embedding and releasing performance in biodegradable poly(glycerol sebacate). *ACS Applied Nano Materials 1*(9), 4474–4482.

Ibarra J, Encinas D, Blanco M, Barbosa S, Taboada P, Juárez J, Valdez MA. 2018. Co-encapsulation of magnetic nanoparticles and cisplatin within biocompatible polymers as multifunctional nanoplatforms: Synthesis, characterization, and in vitro assays. *Materials Research Express*, *5*(1), 015023.

Ibrahim MI, Alsafadi D, Safi E, Alenazi E, Aboulsoud M, Hussein MA, Alamry KA. 2022. Biosynthesized poly(3-hydroxybutyrate-co-3-hydroxyvalerate) as biocompatible microcapsules with extended-release for busulfan and montelukast. *International Journal of Biological Macromolecules 213*, 728–737.

Impallomeni G, Ballistreri A, Carnemolla GM, Franco D, Guglielmino SPP. 2015. Matrix-assisted laser desorption/ionization time-of-flight vs. fast-atom bombardment and electrospray ionization mass spectrometry in the structural characterization of bacterial poly(3-hydroxyalkanoates). *Rapid Communications in Mass Spectrometry 29*(9), 811–820.

Impallomeni G, Ballistreri A, Carnemolla GM, Guglielmino SPP, Nicolò MS, Cambria MG. 2011. Synthesis and characterization of poly(3-hydroxyalkanoates) from Brassica carinata oil with high content of erucic acid and from very long chain fatty acids. *International Journal of Biological Macromolecules 48*(1), 137–145.

Impallomeni G, Ballistreri A, Carnemolla GM, Rizzo MG, Nicolò MS, Guglielmino SPP. 2018. Biosynthesis and structural characterization of polyhydroxyalkanoates produced by Pseudomonas aeruginosa ATCC 27853 from long odd-chain fatty acids. *International Journal of Biological Macromolecules 108*, 608–614.

Impallomeni G, Carnemolla GM, Puzzo G, Ballistreri A, Martino L, Scandola M. 2013. Characterization of biodegradable poly(3-hydroxybutyrate-co-butyleneadipate) copolymers obtained from their homopolymers by microwave-assisted transesterification. *Polymer 54*(1), 65–74.

Impallomeni G, Mineo PG, Vento F, Ballistreri A. 2021. Novel pranoprofen-poly(ε-caprolactone) conjugates: Microwave-assisted synthesis and structural characterization. *Polymer International 70*(5), 604–611.

Jang M, Yang H, Park S-A, Sung HK, Koo JM, Hwang SY, Jeon H, Oh DX, Park J. 2022. Analysis of volatile organic compounds produced during incineration of non-degradable and biodegradable plastics. *Chemosphere 303*, 134946.

Jia H, Zhang M, Weng Y, Zhao Y, Li C, Kanwal A. 2021. Degradation of poly(butylene adipate-co-terephthalate) by Stenotrophomonas sp. YCJ1 isolated from farmland soil. *Journal of Environmental Sciences (China) 103*, 50–58.

Jia X, Zhao K, Zhao J, Lin C, Zhang H, Chen L, Chen J, Fang Y. 2023. Degradation of poly(butylene adipate-co-terephthalate) films by Thermobifida fusca FXJ-1 isolated from compost. *Journal of Hazardous Materials 441*, 129958.

Johnston B, Jiang G, Hill D, Adamus G, Kwiecień I, Zięba M, Sikorska W, Green M, Kowalczuk M, Radecka I. 2017. The molecular-level characterization of biodegradable polymers originated from polyethylene using non-oxygenated polyethylene wax as a carbon source for polyhydroxyalkanoate production. *Bioengineering 4*(3), 73.

Johnston B, Radecka I, Chiellini E, Barsi D, Ilieva VI, Sikorska W, Musiol M, Zięba M, Chaber P, Marek AA. 2019. Mass spectrometry reveals molecular structure of polyhydroxyalkanoates attained by bioconversion of oxidized polypropylene waste fragments. *Polymers 11*, 1580–1600.

Johnston B, Radecka I, Hill D, Chiellini E, Ilieva VI, Sikorska W, Musioł M, Zięba M, Marek AA, Keddie D, Mendrek B, Darbar S, Adamus G, Kowalczuk M. 2018. The microbial production of polyhydroxyalkanoates from waste polystyrene fragments attained using oxidative degradation. *Polymers 10*(9), 957.

Jyoti P, Patil N, Masakapalli SK. 2021. Insights into the polyhydroxybutyrate biosynthesis in Ralstonia solanacearum using parallel 13C tracers and comparative genome analysis. *ACS Chemical Biology 16*(7), 1215–1222.

Kang DW, Ryu CH, Kim JH, Choi G-W, Kim S, Chon CH, Cho H-Y. 2021. Pharmacokinetic-pharmacodynamic modeling approach for dose prediction of the optimal long-acting injectable formulation of finasteride. *International Journal of Pharmaceutics 601*, 120527.

Ke W, Zha Z, Mukerabigwi JF, Chen W, Wang Y, He C, Ge Z. 2017. Matrix metalloproteinase-responsive multifunctional peptide-linked amphiphilic block copolymers for intelligent systemic anticancer drug delivery. *Bioconjugate Chemistry 28*(8), 2190–2198.

Kolmas J, Sobczak M, Olędzka E, Nałęcz-Jawecki G, Dębek C. 2014. Synthesis, characterization and in vitro evaluation of new composite bisphosphonate delivery systems. *International Journal of Molecular Sciences 15*(9), 16831–16847.

Kowalczuk M. 2016. New vistas in mass spectrometry for sequence analysis of natural and synthetic biodegradable macromolecules. *Chimica Oggi/Chemistry Today 34*(2), 12–15.

Kowalczuk M, Adamus G. 2016. Mass spectrometry for the elucidation of the subtle molecular structure of biodegradable polymers and their degradation products. *Mass Spectrometry Reviews 35*(1), 188–198.

Kumar P, Srivastava R. 2015. IR 820 stabilized multifunctional polycaprolactone glycol chitosan composite nanoparticles for cancer therapy. *RSC Advances 5*(69), 56162–56170.

Kwiecień I, Adamus G, Kowalczuk M. 2012. Electrospray ionisation mass spectrometry molecular-level structural characterisation of novel phenoxycarboxylic acid–oligo(3-hydroxybutyrate)

conjugates with potential agricultural applications. *Rapid Communication in Mass Spectrometry 26*, 2673–2682.

Kwiecień I, Bałakier T, Jurczak J, Kowalczuk M, Adamus G. 2015. Molecular architecture of novel potentially bioactive (co)oli-1151 goesters containing pesticide moieties established by electrospray ionization multistage mass spectrometry. *Rapid Communications in Mass Spectrometry 29*, 533–544.

Kwiecień I, Radecka I, Kwiecień M, Adamus G. 2016. Synthesis and structural characterization of bioactive PHA and γ-PGA oligomers for potential applications as a delivery system. *Materials 9*(5), 307.

Landim LB, Miranda Jr. EO, de Araújo NA, Pinto JC, Cabral-Albuquerque ECM, Cunha S, Fialho RL. 2019. Solvent-free mechanochemical polymerization of urea-succinic acid and urea-succinic acid-glycerol mixtures. *Journal of Cleaner Production 238*, 117742.

Lee J-W, Jeong ED, Cho EJ, Gardella Jr. JA, Hicks Jr. W, Hard R, Bright FV. 2008. Surface-phase separation of PEO-containing biodegradable PLLA blends and block copolymers. *Applied Surface Science 255*(5 PART 1), 2360–2364.

Liang S-Y, Wan S-C, Ho Y-P, Horng Y-T, Soo P-C, Peng W-P. 2022. Rapid quantification of polyhydroxybutyrate polymer from single bacterial cells with mass spectrometry. *Analytical Chemistry 94*(34), 11734–11738.

Lis-Cieplak A, Charuk F, Sobczak M, Zgadzaj A, Drobniewska A, Szeleszczuk Ł, Oledzka E. 2020. Development and evaluation of matrices composed of β-cyclodextrin and biodegradable polyesters in the controlled delivery of pindolol. *Pharmaceutics 12*(6), 500.

Liu G, Kong X, Wan H, Narine S. 2008. Production of 9-hydroxynonanoic acid from methyl oleate and conversion into lactone monomers for the synthesis of biodegradable polylactones. *Biomacromolecules 9*(3), 949–953.

Liu J, Tao L, Xu J, Jia Z, Boyer C, Davis TP. 2009. RAFT controlled synthesis of six-armed biodegradable star polymeric architectures via a 'core-first' methodology. *Polymer*, *50*(19), 4455–4463.

Lochee Y, Jhurry D, Bhaw-Luximon A, Kalangos A. 2010. Biodegradable poly(ester-ether)s: Ring-opening polymerization of D,L-3-methyl-1,4-dioxan-2-one using various initiator systems. *Polymer International 59*(9), 1310–1318.

Loh XJ. 2013. The effect of pH on the hydrolytic degradation of poly (ε-caprolactone)-block-poly(ethylene glycol) copolymers. *Journal of Applied Polymer Science 127*(3), 2046–2056.

Loriot M, Linossier I, Vallée-Réhel K, Fay F. 2016. Syntheses, characterization, and hydrolytic degradation of P(ε-caprolactone-co-δ-valerolactone) copolymers: Influence of molecular weight. *Journal of Applied Polymer Science 133*(7), 43007.

Mahato RP, Kumar S, Singh P. 2021. Optimization of growth conditions to produce sustainable polyhydroxyalkanoate bioplastic by Pseudomonas aeruginosa EO1. *Frontiers in Microbiology 12*, 711588.

Mahmoud LAM, Telford R, Livesey TC, Katsikogianni M, Kelly AL, Terry LR, Ting VP, Nayak S. 2022. Zirconium-based MOFs and their biodegradable polymer composites for controlled and sustainable delivery of herbicides. *ACS Applied Bio Materials 5*(8), 3972–3981.

Makarov C, Cohen V, Raz-Pasteur A, Gotman I. 2014. In vitro elution of vancomycin from biodegradable osteoconductive calcium phosphate-polycaprolactone composite beads for treatment of osteomyelitis. *European Journal of Pharmaceutical Sciences 62*, 49–56.

Maksymiak M, Bałakier T, Jurczak J, Kowalczuk M, Adamus G. 2016. Bioactive (co)oligoesters with antioxidant properties-synthesis and structural characterization at the molecular level. *RSC Advances 6*(62), 57751–57761.

Maksymiak M, Debowska R, Jelonek K, Kowalczuk M, Adamus G. 2013. Structural characterization of biocompatible lipoic acid-oligo-(3-hydroxybutyrate) conjugates by electrospray ionization mass spectrometry. *Rapid Communications in Mass Spectrometry 27*(7), 773–783.

Maurer-Jones MA, Monzo EM. 2021. Quantifying photochemical transformations of poly(butylene adipate-co-terephthalate) films. *ACS Applied Polymer Materials 3*(2), 1003–1011.

Mita M, Mita A, Sarantopoulos J, Takimoto CH, Rowinsky EK, Romero O, Angiuli P, Allievi C, Eisenfeld A, Verschraegen CF. 2009. Phase I study of paclitaxel poliglumex administered weekly for patients with advanced solid malignancies. *Cancer Chemotherapy and Pharmacology 64*(2), 287–295.

Moeller S, Kegler R, Sternberg K, Mundkowski RG. 2012. Influence of sirolimus-loaded nanoparticles on physiological functions of native human polymorphonuclear neutrophils. *Nanomedicine: Nanotechnology, Biology, and Medicine 8*(8), 1293–1300.

Mohiti-Asli M, Pourdeyhimi B, Loboa EG. 2014. Novel, silver-ion-releasing nanofibrous scaffolds exhibit excellent antibacterial efficacy without the use of silver nanoparticles. *Acta Biomaterialia 10*(5), 2096–2104.

Montaudo G, Samperi F, Montaudo MS. 2006. Characterization of synthetic polymers by MALDI-MS. *Progress in Polymer Science 31*(3), 277–357.

Mostafa YS, Alrumman SA, Alamri SA, Otaif KA, Mostafa MS, Alfaify AM. 2020. Bioplastic (poly-3-hydroxybutyrate) production by the marine bacterium Pseudodonghicola xiamenensis through date syrup valorization and structural assessment of the biopolymer. *Scientific Reports 10*(1), 8815.

Mukherjee C, Varghese D, Krishna JS, Boominathan T, Rakeshkumar R, Dineshkumar S, Brahmananda Rao CVS, Sivaramakrishna A. 2023 Recent advances in biodegradable polymers–properties, applications and future prospects. *European Polymer Journal 192*, 112068.

Muroi F, Tachibana Y, Soulenthone P, Yamamoto K, Mizuno T, Sakurai T, Kobayashi Y, Kasuya K-I. 2017. Characterization of a poly(butylene adipate-co-terephthalate) hydrolase from the aerobic mesophilic bacterium Bacillus pumilus. *Polymer Degradation and Stability 137*, 11–22.

Musioł M, Jurczyk S, Sobota M, Klim M, Sikorska W, Zieba M, Janeczek H, Rydz J, Kurcok P, Johnston B, Radecka, I. 2020. (Bio)degradable polymeric materials for sustainable future-part 3: Degradation studies of the PHA/wood flour-based composites and preliminary tests of antimicrobial activity. *Materials 13*(9), 2200.

Musioł M, Sikorska W, Adamus G, Janeczek H, Kowalczuk M, Rydz J. 2016. (Bio)degradable polymers as a potential material for food packaging: Studies on the (bio)degradation process of PLA/(R,S)-PHB rigid foils under industrial composting

conditions. *European Food Research and Technology 242*(6), 815–823.

Musioł M, Sikorska W, Adamus G, Janeczek H, Richert J, Malinowski R, Jiang G, Kowalczuk M. 2016. Forensic engineering of advanced polymeric materials. Part III—Biodegradation of thermoformed rigid PLA packaging under industrial composting conditions. *Waste Management 52*, 69–76.

Ogaki R, Green FM, Li S, Vert M, Alexander MR, Gilmore IS, Davies MC. 2008. A comparison of the static SIMS and G-SIMS spectra of biodegradable homo-polyesters. *Surface and Interface Analysis 40*(8), 1202–1208.

Ojha N, Das N. 2018. A statistical approach to optimize the production of Polyhydroxyalkanoates from Wickerhamomyces anomalus VIT-NN01 using response surface methodology. *International Journal of Biological Macromolecules 107*, 2157–2170.

Okoffo ED, Chan CM, Rauert C, Kaserzon S, Thomas KV. 2022. Identification and quantification of micro-bioplastics in environmental samples by pyrolysis-gas chromatography-mass spectrometry. *Environmental Science and Technology 56*(19), 13774–13785.

Oledzka E, Sokolowski K, Sobczak M, Kolodziejski W. 2011. α-Amino acids as initiators of ε-caprolactone and L,L-lactide polymerization. *Polymer International 60*(5), 787–793.

Osaka I, Yoshimoto A, Watanabe M, Takama M, Murakami M, Kawasaki H, Arakawa R. 2008. Quantitative determination of cyclic polylactic acid oligomers in serum by direct injection liquid chromatography-tandem mass spectrometry. *Journal of Chromatography B: Analytical Technologies in the Biomedical and Life Sciences 870*(2), 247–250.

Park SL, Cho JY, Kim SH, Bhatia SK, Gurav R, Park S-H, Park K, Yang Y-H. 2021. Isolation of Microbulbifer sp. Sol66 with high polyhydroxyalkanoate-degrading activity from the marine environment. *Polymers 13*(23), 4257.

Parwe SP, Chaudhari PN, Mohite KK, Selukar BS, Nande SS, Garnaik B. 2014. Synthesis of ciprofloxacin-conjugated poly (L-lactic acid) polymer for nanofiber fabrication and antibacterial evaluation. *International Journal of Nanomedicine 9*(1), 1463–1477.

Pathak RK, Dhar S. 2015. A nanoparticle cocktail: Temporal release of predefined drug combinations. *Journal of the American Chemical Society 137*(26), 8324–8327.

Pedrón S, Peinado C, Bosch P, Anseth KS. 2010. Synthesis and characterization of degradable bioconjugated hydrogels with hyperbranched multifunctional cross-linkers. *Acta Biomaterialia 6*(11), 4189–4198.

Pelosi C, Duce C, Wurm FR, Tinè MR. 2021. Effect of polymer hydrophilicity and molar mass on the properties of the protein in protein-polymer conjugates: The case of PPEylated myoglobin. *Biomacromolecules 22*(5), 1932–1943.

Peptu C, Blaj D-A, Balan-Porcarasu M, Rydz J. 2022. Cyclodextrin-oligocaprolactone derivatives—Synthesis and advanced structural characterization by MALDI mass spectrometry. *Polymers 14*(7), 1436.

Peptu C, van den Brink OF., Harabagiu V, Simionescu BC, Kowalczuk M, Silberring J. 2012. Molecular level differentiation between end-capped and intramolecular azofunctional oligo (e-caprolactone) positional isomers through liquid chromatography multistage mass spectrometry. *The Journal of Polymer Science Part A: Polymer Chemistry 50*, 2421–2431.

Peptu C, Danchenko M, Škultéty L, Mosnáček J. 2018. Structural architectural features of cyclodextrin oligoesters revealed by fragmentation mass spectrometry analysis. *Molecules 23*(9), 2259.

Pérez-Lara LF, Vargas-Suárez M, Lõpez-Castillo NN, Cruz-Gõmez MJ, Loza-Tavera H. 2016. Preliminary study on the biodegradation of adipate/phthalate polyester polyurethanes of commercial-type by Alicycliphilus sp. BQ8. *Journal of Applied Polymer Science 133*(6), 42992.

Perz V, Bleymaier K, Sinkel C, Kueper U, Bonnekessel M, Ribitsch D, Guebitz GM. 2016. Substrate specificities of cutinases on aliphatic-aromatic polyesters and on their model substrates. *New Biotechnology 33*(2), 295–304.

Phan CM, Walther H, Smith RW, Riederer D, Lau C, Osborn Lorenz K, Subbaraman LN, Jones L. 2018. Determination of the release of PEG and HPMC from nelfilcon. A daily disposable contact lenses using a novel in vitro eye model. *J Biomater Sci Polym Ed. 29*, 2124–2136.

Phothisarattana D, Harnkarnsujarit N. 2022. Migration, aggregations and thermal degradation behaviors of TiO_2 and ZnO incorporated PBAT/TPS nanocomposite blown films. *Food Packaging and Shelf Life 33*, 100901.

Pignatello R, Impallomeni G, Pistarà V, Cupri S, Graziano ACE, Cardile V, Ballistreri A. 2015. New amphiphilic derivatives of poly(ethylene glycol) (PEG) as surface modifiers of colloidal drug carriers. III. Lipoamino acid conjugates with carboxy- and amino-PEG5000 polymers. *Materials Science and Engineering C 46*, 470–481.

Pignatello R, Pantò V, Impallomeni G, Carnemolla GM, Carbone C, Puglisi G. 2013. New amphiphilic conjugates of amino-poly (ethylene glycols) with lipoamino acids as surface modifiers of colloidal drug carriers. *Macromolecular Chemistry and Physics 214*(1), 46–55.

Prian K, Aloui I, Legros V, Buchmann W. 2019. Study of the gas-phase decomposition of multiply lithiated polycaprolactone, polytetrahydrofurane and their copolymer by two different activation methods: Collision-induced dissociation and electron transfer dissociation. *Analytica Chimica Acta 1048*, 85–95.

Qin M, Gong J, Zeng G, Song B, Cao W, Shen M, Chen Z. 2022. The role of microplastics in altering arsenic fractionation and microbial community structures in arsenic-contaminated riverine sediments. *Journal of Hazardous Materials 433*, 128801.

Raase JM, Reichert K-H, Schomäcker R. 2015. Direct condensation of lactic acid in the presence or absence of supported zirconium sulfate. *Journal of Applied Polymer Science 132*(36), 42444.

Radecka I, Irorere V, Jiang G, Hill D, Williams C, Adamus G, Kwiecień M, Marek AA, Zawadiak J, Johnston B, Kowalczuk M. 2016. Oxidized polyethylene wax as a potential carbon source for PHA production. *Materials 9*(5), 367.

Rankin K, Lee H, Tseng PJ, Mabury SA. 2014. Investigating the biodegradability of a fluorotelomer-based acrylate polymer in a soil-plant microcosm by indirect and direct analysis. *Environmental Science and Technology 48*(21), 12783–12790.

Ren T, Li R, Zhao L, Fawcett JP, Sun D, Gu J. 2022. Biological fate and interaction with cytochromes P450 of the nanocarrier

material, D-α-tocopheryl polyethylene glycol 1000 succinate. *Acta Pharmaceutica Sinica B 12*(7), 3156–3166.

Rillig MC, Leifheit E, Lehmann J. 2021. Microplastic effects on carbon cycling processes in soils. *PLoS Biology 19*, e3001130.

Rivas D, Ginebreda A, Pérez S, Quero C, Barceló D. 2016. MALDI-TOF MS Imaging evidences spatial differences in the degradation of solid polycaprolactone diol in water under aerobic and denitrifying conditions. *Science of the Total Environment 566–567*, 27–33.

Rivas D, Zonja B, Eichhorn P, Ginebreda A, Pérez S, Barceló D. 2017. Using MALDI-TOF MS imaging and LC-HRMS for the investigation of the degradation of polycaprolactone diol exposed to different wastewater treatments. *Analytical and Bioanalytical Chemistry 409*(23), 5401–5411.

Rizzarelli P. 2013. Matrix-assisted laser desorption ionization time-of-flight/time-of-flight tandem mass spectra of biodegradable polybutylenesuccinate. *Rapid Communications in Mass Spectrometry 27*(19), 2213–2225.

Rizzarelli P, Carroccio S. 2015. Recent trends in the structural characterization and degradation of biodegradable polymers by modern mass spectrometry in biodegradable polymers. 1: *Advancement in Biodegradation Study and Applications*. Nova Publisher. 77–134.

Rizzarelli P, Carroccio S. 2014. Modern mass spectrometry in the characterization and degradation of biodegradable polymers. *Analytica Chimica Acta 808*, 18–43.

Rizzarelli P, Carroccio S. 2009. Thermo-oxidative processes in biodegradable poly(butylene succinate). *Polymer Degradation and Stability 94*(10), 1825–1838.

Rizzarelli P, Cirica M, Pastorelli G, Puglisi C, Valenti G. 2015. Aliphatic poly(ester amide)s from sebacic acid and aminoalcohols of different chain length: Synthesis, characterization and soil burial degradation. *Polymer Degradation and Stability 121*, 90–99.

Rizzarelli P, La Carta S, Mirabella EF, Rapisarda M, Impallomeni G. 2022. Sequencing biodegradable and potentially biobased polyesteramide of sebacic acid and 3-amino-1-propanol by MALDI-TOF-TOF tandem mass spectrometry. *Polymers 14*(8), 1500.

Rizzarelli P, La Carta S, Rapisarda M, Valenti G. 2019. Analytical methods in resorbable polymer development and degradation tracking. in Materials for Biomedical Engineering: Absorbable Polymers, Elsevier, 351–408.

Rizzarelli P, Piredda G, La Carta S, Mirabella EF, Valenti G, Bernet R, Impallomeni G. 2019. Characterization and laser-induced degradation of a medical grade polylactide. *Polymer Degradation and Stability 169*, 108991.

Rizzarelli P, Puglisi C. 2008. Structural characterization of synthetic poly(ester amide) from sebacic acid and 4-amino-1-butanol by matrix-assisted laser desorption ionization time-of-flight/time-of-flight tandem mass spectrometry. *Rapid Communications in Mass Spectrometry 22*(6), 739–754.

Rizzarelli P, Rapisarda M. 2021. Tandem mass spectrometry in the analysis of biodegradable polymers. in Mass Spectrometry: Theory and Applications, Nova Publisher, 127–181.

Rizzarelli P, Rapisarda M. 2023. Matrix-assisted laser desorption and electrospray ionization tandem mass spectrometry of microbial and synthetic biodegradable polymers. *Polymers 15*, 2356.

Rizzarelli P, Rapisarda M, Perna S, Mirabella EF, La Carta S, Puglisi C, Valenti G. 2016. Determination of polyethylene in biodegradable polymer blends and in compostable carrier bags by Py-GC/MS and TGA. *Journal of Analytical and Applied Pyrolysis 117*, 72–81.

Rizzarelli P, Rapisarda M, Valenti G. 2020. Mass spectrometry in bioresorbable polymer development, degradation and drug-release tracking. *Rapid Communications in Mass Spectrometry 34*(S2), e8697.

Rizzarelli P, Zampino D, Ferreri L, Impallomeni G. 2011. Direct electrospray ionization mass spectrometry quantitative analysis of sebacic and terephthalic acids in biodegradable polymers. *Analytical Chemistry 83*(3), 654–660.

Saeaung K, Phusunti N, Phetwarotai W, Assabumrungrat S, Cheirsilp B. 2021. Catalytic pyrolysis of petroleum-based and biodegradable plastic waste to obtain high-value chemicals. *Waste Management 127*, 101–111.

Safaei Nikouei N, Lavasanifar A. 2011. Characterization of the thermo- and pH-responsive assembly of triblock copolymers based on poly(ethylene glycol) and functionalized poly(ε-caprolactone). *Acta Biomaterialia 7*(10), 3708–3718.

Saito T, Takojima K, Oyama T, Hatanaka S, Konno T, Yamamoto T, Tajima K, Isono T, Satoh T. 2019. Trimethyl glycine as an environmentally benign and biocompatible organocatalyst for ring-opening polymerization of cyclic carbonate. *ACS Sustainable Chemistry and Engineering 7*(9), 8868–8875.

Salazar A, Yepes M, Correa G, Mora A. 2014. Polyhydroxyalkanoate production from unexplored sugar substrates [Producción de polihidroxialcanoatos a partir de sustratos azucarados inexplorados]. *DYNA (Colombia) 81*(185), 73–77.

Sallam S, Dolog I, Paik BA, Jia X, Kiick KL, Wesdemiotis C. 2018. Sequence and conformational analysis of peptide-polymer bioconjugates by multidimensional mass spectrometry. *Biomacromolecules 19*, 1498–1507.

Sallam S, Luo Y, Becker ML, Wesdemiotis C. 2017. Multidimensional mass spectrometry characterization of isomeric biodegradable polyesters. *European Journal of Mass Spectrometry 23*(6), 402–410.

Sanders WG, Hogrebe PC, Grainger DW, Cheung AK, Terry CM. 2012. A biodegradable perivascular wrap for controlled, local and directed drug delivery. *Journal of Controlled Release 161*(1), 81–89.

Santra S, Shaw Z, Narayanam R, Jain V, Banerjee T. 2020. Selective O-alkylation of 2,2′-bis(hydroxymethyl)propionic acid to synthesize biodegradable polymers for drug delivery applications. *ACS Applied Polymer Materials*, *2*(8), 3465–3473.

Sato H, Nakamura S, Fouquet T, Ohmura T, Kotani M, Naito Y. 2020. Molecular characterization of polyethylene oxide based oligomers by surface-assisted laser desorption/ionization mass spectrometry using a through-hole alumina membrane as active substrate. *Rapid Communications in Mass Spectrometry 34*(5), e8597.

Sato S, Saika A, Shinozaki Y, Watanabe T, Suzuki K, Sameshima-Yamashita Y, Fukuoka T, Habe H, Morita T, Kitamoto H. 2017. Degradation profiles of biodegradable plastic films by biodegradable plastic-degrading enzymes from the yeast Pseudozyma antarctica and the fungus Paraphoma sp. B47-9. *Polymer Degradation and Stability 141*, 26–32.

Savva K, Borrell X, Moreno T, Pérez-Pomeda I, Barata C, Llorca M, Farré M. 2023. Cytotoxicity assessment and suspected screening of plastic additives in bioplastics of single-use household items. *Chemosphere 313*, 137494.

Scherger M, Räder HJ, Nuhn L. 2021. Self-immolative RAFT-polymer end group modification. *Macromolecular Rapid Communications 42*(8), 2000752.

Scionti V, Wesdemiotis C. 2012. Electron transfer dissociation versus collisionally activated dissociation of cationized biodegradable polyesters. *Journal of Mass Spectrometry 47*(11), 1442–1449.

Serrano CA, Zhang Y, Yang J, Schug KA. 2011. Matrix-assisted laser desorption/ionization mass spectrometric analysis of aliphatic biodegradable photoluminescent polymers using new ionic liquid matrices. *Rapid Communications in Mass Spectrometry 25*(9), 1152–1158.

Serrano-Ruiz H, Martin-Closas L, Pelacho A.M. 2021. Biodegradable plastic mulches: Impact on the agricultural biotic environment. *Science of the Total Environment750*, 141228.

Shen Y, Zhang J, Zhao Z, Zhao N, Liu F, Li Z. 2019. Preparation of amphiphilic poly(ethylene glycol)-b-poly(γ-butyrolactone) diblock copolymer via ring-opening polymerization catalyzed by a cyclic trimeric phosphazene base or alkali alkoxide. *Biomacromolecules 20*(1), 141–148.

Shi M, Jiang H, Yin L, Liu Y, Xu M. 2019. Development of an UPLC-MS/MS method coupled with in-source CID for quantitative analysis of PEG-PLA copolymer and its application to a pharmacokinetic study in rats. *Journal of Chromatography B: Analytical Technologies in the Biomedical and Life Sciences 1125*, 121716.

Shi C, Yu H, Sun D, Ma L, Tang Z, Xiao Q, Chen X. 2015. Cisplatin-loaded polymeric nanoparticles: Characterization and potential exploitation for the treatment of non-small cell lung carcinoma. *Acta Biomaterialia 18*, 68–76.

Shiravand F, Ascione L, Persico P, Carfagna C, Brocks T, Maria Odila Hilário Cioffi, Puglisi C, Samperi F, Ambrogi V. 2016. A novel hybrid linear–hyperbranched poly(butylene adipate) copolymer as an epoxy resin modifier with toughening effect. *Polymer International 65*, 308–319.

Sikorska W, Adamus G, Dobrzynski P, Libera M, Rychter P, Krucinska I, Komisarczyk A, Cristea M, Kowalczuk M. 2014. Forensic engineering of advanced polymeric materials—Part II: The effect of the solvent-free non-woven fabrics formation method on the release rate of lactic and glycolic acids from the tin-free poly(lactide-co-glycolide) nonwovens. *Polymer Degradation and Stability 110*, 518–528.

Sikorska W, Musioł M, Rydz J, Zięba M, Rychter P, Lewicka K, Šiškova A, Mosnáčková K, Kowalczuk M, Adamus G. 2018. Prediction studies of environment-friendly biodegradable polymeric packaging based on PLA. Influence of specimens' thickness on the hydrolytic degradation profile. *Waste Management 78*, 938–947.

Sobczak M. 2012. Enzyme-catalyzed ring-opening polymerization of cyclic esters in the presence of poly(ethylene glycol). *Journal of Applied Polymer Science 125*(5), 3602–3609.

Spontón M, Casis N, Mazo P, Raud B, Simonetta A, Ríos L, Estenoz D. 2013. Biodegradation study by Pseudomonas sp. of flexible polyurethane foams derived from castor oil. *International Biodeterioration and Biodegradation 85*, 85–94.

Sriramani M, Senbagam D, Senthilkumar B, Anbarasu K, Amutha R. 2022. Optimization of PHB production utilizing agro-waste as a sustainable substrate by the native isolate Bacillus cereus. *Research Journal of Biotechnology 17*(8), 32–41.

Srisawat P, Higuchi-Takeuchi M, Honda R, Shirai T, Kondo A, Hoshino Y, Numata K. 2022. Engineered nanogel particles enhance the photoautotrophic biosynthesis of polyhydroxyalkanoate in marine photosynthetic bacteria. *ACS Sustainable Chemistry and Engineering 10*(13), 4133–4142.

Sriyapai T, Chuarung T, Kimbara K, Samosorn S, Sriyapai P. 2022. Production and optimization of polyhydroxyalkanoates (PHAs) from Paraburkholderia sp. PFN 29 under submerged fermentation. *Electronic Journal of Biotechnology 56*, 1–11.

Steinbach T, Wurm FR. 2016. Degradable polyphosphoester-protein conjugates: "pPEylation" of proteins. *Biomacromolecules 17*(10), 3338–3346.

Sun J, Jung D, Schoppa T, Anderski J, Picker M-T, Ren Y, Mulac D, Stein N, Langer K, Kuckling D. 2019. Light-responsive serinol-based polycarbonate and polyester as degradable scaffolds. *ACS Applied Bio Materials 2*(7), 3038–3051.

Sun Y, Li X, Li X, Wang J. 2022. Deciphering the fingerprint of dissolved organic matter in the soil amended with biodegradable and conventional microplastics based on optical and molecular signatures. *Environmental Science and Technology 56*(22), 15746–15759.

Susithra K, Narayanan KB, Ramesh U, Raja CE, Premkumar G, Varatharaju G, Vijayakumar A, Kannan M, Rajarathinam K. 2021. Statistical optimization of poly-β-hydroxybutyrate biosynthesis using the spent mushroom substrate by Bacillus tequilensis PSR-2. *Waste and Biomass Valorization 12*(12), 6709–6725.

Tachibana Y, Maeda T, Ito O, Maeda Y, Kunioka M. 2009. Utilization of a biodegradable mulch sheet produced from poly(lactic acid)/Ecoflex®/modified starch in Mandarin orange groves. *International Journal of Molecular Sciences 10*(8), 3599–3615.

Takizawa K, Nulwala H, Hu J, Yoshinaga K, Hawker CJ. 2008. Molecularly defined (L)-lactic acid oligomers and polymers: Synthesis and characterization. *Journal of Polymer Science, Part A: Polymer Chemistry 46*(18), 5977–5990.

Talelli M, Vicent MJ. 2014. Reduction sensitive poly(l-glutamic acid) (PGA)-protein conjugates designed for polymer masked-unmasked protein therapy. *Biomacromolecules 15*(11), 4168–4177.

Tang D, Noordover BAJ, Sablong RJ, Koning CE. 2011. Metal-free synthesis of novel biobased dihydroxyl-terminated aliphatic polyesters as building blocks for thermoplastic polyurethanes. *Journal of Polymer Science, Part A: Polymer Chemistry 49*(13), 2959–2968.

Tang Y, Singh J. 2010. Thermosensitive drug delivery system of salmon calcitonin: In vitro release, in vivo absorption, bioactivity and therapeutic efficacies. *Pharmaceutical Research 27*(2), 272–284.

Tapia JB, Haines J, Yapor JP, Reynolds MM. 2019. Identification of the degradation products of a crosslinked polyester using LC-MS. *Polymer Degradation and Stability 168*, 108948.

Tappa K, Jammalamadaka U, Ballard DH, Bruno T, Israel MR, Vemula H, Meacham JM, Mills DK, Woodard PK, Weisman JA. 2017. Medication eluting devices for the field

of OBGYN (MEDOBGYN): 3D printed biodegradable hormone eluting constructs, a proof of concept study. *PLoS ONE 12*(8), e0182929.

Ten Breteler MR, Feijen J, Dijkstra PJ, Signori F. 2013. Synthesis and thermal properties of hetero-bifunctional PLA oligomers and their stereocomplexes. *Reactive and Functional Polymers 73*(1), 30–38.

Theerasilp M, Chalermpanapun P, Sunintaboon P, Sungkarat W, Nasongkla N. 2018. Glucose-installed biodegradable polymeric micelles for cancer-targeted drug delivery system: Synthesis, characterization and in vitro evaluation. *Journal of Materials Science: Materials in Medicine 29*(12), 177.

Theiler S, Teske M, Keul H, Sternberg K, Möller M. 2010. Synthesis, characterization and in vitro degradation of 3D-microstructured poly(ε-caprolactone) resins. *Polymer Chemistry. 1*, 1215–1225.

Ugur D, Sottile V, Montero-Menei CN, Boury F, Zelzer M. 2020. Relating polymeric microparticle formulation to prevalence or distribution of fibronectin and poly-d-lysine to support mesenchymal stem cell growth. *Biointerphases 15*(4), 041008.

van Raamsdonk LWD, van der Zande M, Koelmans AA, Hoogenboom RLAP, Peters RJB, Groot MJ, Peijnenburg AACM, Weesepoel YJA. 2020. Current insights into monitoring, bioaccumulation, and potential health effects of microplastics present in the food chain. *Foods 9*(1), 72.

Van Royen P, Boschmans B, Dos Santos A, Schacht E, Dubruel P, Cornelissen R, Beenaerts L, Van Vaeck L. 2011. Static secondary ion mass spectrometry for the surface characterisation of individual nanofibres of polycaprolactone functionalised with an antibacterial additive. *Analytical and Bioanalytical Chemistry 399*(3), 1163–1172.

Vermet G, Degoutin S, Chai F, Maton M, Flores C, Neut C, Danjou PE, Martel B, Blanchemain N. 2017. Cyclodextrin-modified PLLA parietal reinforcement implant with prolonged antibacterial activity. *Acta Biomaterialia 53*, 222–232.

Wang C, Yu J, Lu Y, Hua D, Wang X, Zou X. 2021. Biodegradable microplastics (BMPs): A new cause for concern? *Environmental Science and Pollution Research 28*, 66511–66518.

Wang L, Peng Y, Xu Y, Zhang J, Zhang T, Yan M, Sun H. 2022. An in situ depolymerization and liquid chromatography-tandem mass spectrometry method for quantifying polylactic acid microplastics in environmental samples. *Environmental Science and Technology 56*(18), 13029–13035.

Wang R, Hu X, Wu S, Xiao H, Cai H, Xie Z, Huang Y, Jing X. 2012. Biological characterization of folate-decorated biodegradable polymer-platinum(II) complex micelles. *Molecular Pharmaceutics 9*(11), 3200–3208.

Wang X, Zachman AL, Chun YW, Shen F-W, Hwang Y-S, Sung H-J. 2014. Polymeric stent materials dysregulate macrophage and endothelial cell functions: Implications for coronary artery stent. *International Journal of Cardiology 174*(3), 688–695.

Wattanawong N, Aht-Ong D. 2021. Antibacterial activity, thermal behavior, mechanical properties and biodegradability of silver zeolite/poly(butylene succinate) composite films. *Polymer Degradation and Stability 183*, 109459.

Wei X-F, Bohlén M, Lindblad C, Hedenqvist M, Hakonen A. 2021. Microplastics generated from a biodegradable plastic in freshwater and seawater. *Water Research 198*, 117123.

Wei D, Yu Y, Huang Y, Jiang Y, Zhao Y, Nie Z, Wang F, Ma W, Yu Z, Huang Y, Zhang X-D, Liu Z-Q, Zhang X, Xiao H. 2021. A near-infrared-II polymer with tandem fluorophores demonstrates superior biodegradability for simultaneous drug tracking and treatment efficacy feedback. *ACS Nano 15*(3), 5428–5438.

Wei R-J, Zhang X-H, Zhang Y-Y, Du B-Y, Fan Z-Q, Qi G-R. 2014. Functional poly(carbonate-co-ether) synthesis from glycidyl methacrylate/CO_2 copolymerization catalyzed by Zn-Co(iii) double metal cyanide complex catalyst. *RSC Advances 4*(7), 3188–3194.

Weidner SM, Falkenhagen J, Knop K, Thünemann A. 2009. Structure and end-group analysis of complex hexanediol-neopentylglycol-adipic acid copolyesters by matrix-assisted laser desorption/ionization collision-induced dissociation tandem mass spectrometry. *Rapid Communications in Mass Spectrometry 23*, 2768–2774.

Wesdemiotis C. 2017. Multidimensional mass spectrometry of synthetic polymers and advanced materials. *Angewandte Chemie International Edition 56*, 1452–1464.

Wesdemiotis C, Solak N, Polce MJ, Dabney DE, Chaicharoen K, Katzenmeyer BC. 2011. Fragmentation pathways of polymer ions. *Mass Spectrometry Reviews 30*, 523–559.

Wesdemiotis C, Williams-Pavlantos KN, Keating AR, McGee AS, Bochenek C. 2023. Mass spectrometry of polymers: A tutorial review. *Mass Spectrometry Reviews*, 1–50.

Wu C-Y, Hsieh H-H, Chang T-Y, Lin J-J, Wu C-C, Hsu M-H, Lin M-C, Peng S-L. 2021. Development of mri-detectable boron-containing gold nanoparticle-encapsulated biodegradable polymeric matrix for boron neutron capture therapy (Bnct). *International Journal of Molecular Sciences 22*(15), 8050.

Wu Q, Liu D, Zhang X, Wang D, DongYe M, Chen W, Lin D, Zhu F, Chen W, Lin H. 2019. Development and effects of tacrolimus-loaded nanoparticles on the inhibition of corneal allograft rejection. *Drug Delivery 26*(1), 290–299.

Wu R, Zhang J-F, Fan Y, Stoute D, Lallier T, Xu X. 2011. Reactive electrospinning and biodegradation of cross-linked methacrylated polycarbonate nanofibers. *Biomedical Materials 6*(3), 035004.

Xiao H, Qi R, Liu S, Hu X, Duan T, Zheng Y, Huang Y, Jing X. 2011. Biodegradable polymer-cisplatin(IV) conjugate as a pro-drug of cisplatin(II). *Biomaterials 32*(30), 7732–7739.

Xiao H, Zhou D, Liu S, Zheng Y, Huang Y, Jing X. 2012. A complex of cyclohexane-1,2-diaminoplatinum with an amphiphilic biodegradable polymer with pendant carboxyl groups. *Acta Biomaterialia 8*(5), 1859–1868.

Yang H, Feng K, Song Y, Huang W, Jiang Q, Xue X, Jiang L, Jiang B, Zhang G. 2022. Anionic hybrid copolymerization of cyclic and vinyl monomers without transesterification. *Macromolecular Chemistry and Physics 224*(3), 2200301.

Yang L, Zhang Y, Kang S, Wang Z, Wu C. 2021. Microplastics in soil: A review on methods, occurrence, sources, and potential risk. *Science of the Total Environment. 780*, 146546.

Yi X, Batrakova E, Banks WA, Vinogradov S, Kabanov AV. 2008. Protein conjugation with amphiphilic block copolymers for enhanced cellular delivery. *Bioconjugate Chemistry 19*(5), 1071–1077.

Yu L, Chang GT, Zhang H, Ding JD. 2008. Injectable block copolymer hydrogels for sustained release of a PEGylated drug. *International Journal of Pharmaceutics 348*(1–2), 95–106.

Yu Y, Sintim HY, Astner AF, Hayes DG, Bary A, Zelenyuk A, Qafoku O, Kovarik L, Flury M. 2022. Enhanced transport of TiO_2 in unsaturated sand and soil after release from biodegradable plastic during composting. *Environmental Science and Technology 56*(4), 2398–2406.

Yuan Y, Hungerford NL, Gauthier E, Ouwerkerk D, Yong KWL, Fletcher MT, Laycock B. 2021. Extraction and determination of the Pimelea toxin simplexin in complex plant-polymer biocomposites using ultrahigh-performance liquid chromatography coupled with quadrupole Orbitrap mass spectrometry. *Analytical and Bioanalytical Chemistry 413*(20), 5121–5133.

Zhang G, Zhang R, Wen X, Li L, Li C. 2008. Micelles based on biodegradable poly(L-glutamic acid)-b-polylactide with paramagnetic Gd ions chelated to the shell layer as a potential nanoscale MRI-Visible delivery system. *Biomacromolecules 9*(1), 36–42.

Zhang Q, Vakili MR, Li X-F, Lavasanifar A, Le XC. 2014. Polymeric micelles for GSH-triggered delivery of arsenic species to cancer cells. *Biomaterials 35*(25), 7088–7100.

Zhao C, Liu A, Santamaria CM, Shomorony A, Ji T, Wei T, Gordon A, Elofsson H, Mehta M, Yang R, Kohane DS. 2019. Polymer-tetrodotoxin conjugates to induce prolonged duration local anesthesia with minimal toxicity. *Nature Communications 10*(1), 2566.

Zhu Y, Sheng R, Luo T, Li H, Sun J, Chen S, Sun W, Cao A. 2011. Honeycomb-structured films by multifunctional amphiphilic biodegradable copolymers: Surface morphology control and biomedical application as scaffolds for cell growth. *ACS Applied Materials and Interfaces 3*(7), 2487–2495.

Żółtowska K, Sobczak M, Olędzka E. 2015. Novel zinc-catalytic systems for ring-opening polymerization of ε-caprolactone. *Molecules 20*(2), 2816–2827.

Zorn G, Simonovsky FI, Ratner BD, Castner DG. 2022. XPS and ToF-SIMS characterization of new biodegradable poly(peptide-urethane-urea) block copolymers. *Advanced Healthcare Materials 11*(9), 2100894.

Zumstein MT, Schintlmeister A, Nelson TF, Baumgartner R, Woebken D, Wagner M, Kohler H-PE, McNeill K, Sander M. 2018. Biodegradation of synthetic polymers in soils: Tracking carbon into CO_2 and microbial biomass. *Science Advances 4*(7), eaas9024.

AUTHOR BIOGRAPHIES

Paola Rizzarelli was born in Catania, Italy. She received her PhD in Chemical Sciences from Catania University under the supervision of Professor Giorgio Montaudo. Currently, she is a senior researcher at the Institute for Polymers, Composites, and Biomaterials (IPCB) of the Italian Research Council in Catania. Her research interests have been centred on sustainability and environmental issues caused by the extended use of plastics and their waste management. Her current research is focused on the design, synthesis, characterization, and applications of biodegradable polymeric systems, as well as to the development of analytical methods, by using also mass spectrometric techniques.

Melania Leanza earned a master degree in Organic and Bioorganic Chemistry in January 2021 at the University of Catania (Italy) and conducted research on valorization of agri-food waste focusing on extraction and characterization of polyphenols as natural antioxidants. She joined Dr. Paola Rizzarelli research group at the National Research Council (CNR) Institute of Polymers, Composites and Biomaterials (IPCB), Catania in 2021 as a research collaborator. Her research focuses on synthesis and characterization of biodegradable polymers and development of alternative packaging for pharmaceutical industry.

Marco Rapisarda earned a master degree in Chemistry in July 2009 at the University of Catania (Italy). Since 2014, his research has focused on the characterization and degradation of polymeric materials, in particular for applications in the field of packaging and related to environmental sustainability and disposal. His activities concern the development of analytical methods, study of biodegradable and bioplastic polymeric blends, evaluation of the mechanical properties of biodegradable and traditional films used in primary and secondary packaging, characterization and degradation of commercial and synthetic polymeric materials, degradation and biodegradation tests.

How to cite this article: Rizzarelli P, Leanza M, Rapisarda M. Investigations into the characterization, degradation, and applications of biodegradable polymers by mass spectrometry. *Mass Spectrometry Reviews*, (2023),1–42.
https://doi.org/10.1002/mas.21869